THREE-DIMENSIONAL ANALYSIS OF COLOUR DOPPLER ULTRASOUND
IMAGES: THE RELATIONSHIP OF VASCULAR FLOW TO OVARIAN STRUCTURES
AND THEIR FUNCTION IN BUFFALO COWS AND BEEF CALVES

A Thesis Submitted to the
College of Graduate and Postdoctoral Studies in
Partial Fulfillment of the Requirements
For the Degree of Master of Science in the
Department of Veterinary Biomedical Sciences
University of Saskatchewan
Saskatoon, Saskatchewan, Canada

By
Serena L. Caunce

**PERMISSION TO USE**


NAME OF AUTHOR:          Serena L. Caunce

                        Department of Veterinary Biomedical Sciences

DEGREE:                 Master of Science


In presenting this thesis in partial fulfillment of the requirements for a Master degree from the University of Saskatchewan, I agree that the Libraries of this University may make it freely available for inspection. I further agree that permission for copying of this thesis in any manner, in whole or in part, for scholarly purposes may be granted by the professor or professors who supervised my thesis work, or, in their absence, by the Head of the Department or the Dean of the College in which my thesis work was done. It is understood that any copying or publication or use of this thesis or parts thereof for financial gain shall not be allowed without my written permission. It is also understood that due recognition shall be given to me and to the University of Saskatchewan in any scholarly use which may be made of any material in my thesis.

Requests for permission to copy or to make other use of material in this thesis in whole or part should be addressed to:


       Head of the Department of Veterinary Biomedical Sciences

       Western College of Veterinary Medicine

       52 Campus Drive

       University of Saskatchewan

       Saskatoon, Saskatchewan

       S7N 5B4

# ABSTRACT

The main objective of this thesis was to develop a three-dimensional method to assess ovarian structures and relate their vascularity to their function (i.e. hormone production, oocyte quality, ovulatory capacity, etc.). This novel method uses video segments recorded after free-hand movement of the routine linear-array transducer, obtained vascularity index values are independent of speed of transducer movement, and the method does not require a-priori operator selection of images, i.e. is an objective method.

In Study 1, colour Doppler ultrasonography was used to assess the ovaries of water buffalo (*Bubalus bubalis*) who were induced to ovulate using a gonadotropin releasing hormone analogue. Ultrasonographic examinations were performed daily to assess ovulation and subsequent corpus luteum (CL) development. Recorded cineloops were exported from the ultrasound machine and analyzed on a personal computer equipped with imaging software from two sources, Fiji (ImageJ) and Imaris. Fiji was used to perform conventional two-dimensional image analysis and Imaris was used to develop a new three-dimensional analysis method that does not require operator selection of images (i.e. objective method). Verification of the three-dimensional method was performed using two-dimensional data. Buffalo that did not ovulate within 24 hours of artificial insemination (40h from time of gonadotrophin releasing hormone analogue treatment) (n=3) tended to have lower change in vascular flow (P=0.06) to their preovulatory follicles when compared to those that ovulated (n=13) using the three-dimensional analysis method.

In Study 2, power Doppler ultrasonography was used to assess the ovaries of 4-month-old prepubertal beef heifers (*Bos taurus*) who were superstimulated using two follicle stimulating hormone (FSH) protocols. Ultrasonographic scans were performed on the day of luteinizing hormone (LH) treatment, the day of oocyte collection, and the third and seventh day following follicular aspiration. The three-dimensional method developed in Study 1 was used to calculate vascularity indices for the four time points. Ovarian vascularity was then related to the expansion of the cumulus-oocyte-complexes that were retrieved, as well as the subsequent luteal tissue that developed following follicle aspiration. Luteal vascularity index measured at three days following follicular aspiration were related to the rise in plasma progesterone concentration over time (from 24 h following LH to day seven after aspiration) (r=0.65, P<0.01). Prepubertal calves

demonstrated an increase in ovarian vascularity index under the influence of exogenous LH that was similar to adult animals. Additionally, an increased duration of superstimulation (seven days instead of four) was important for calves in the development of luteal tissue on day seven, luteal vascularity and progesterone production.

In conclusion, three-dimensional image analysis of colour Doppler ultrasound images was superior to two-dimensional in detecting follicles that did not ovulate. This method using power Doppler ultrasound images was also applied to prepubertal calves undergoing superstimulation and found that luteal vascular flow was related to progesterone production following follicular aspiration.

# ACKNOWLEDGEMENTS

This thesis would not have come together without the encouragement and guidance from my supervisor Dr. Jaswant Singh. Dr. Jaswant was one of my professors in first year veterinary medicine. I entered the world of research under Jaswant's guidance as a summer research student, after encouragement from Dr. Palomino. Dr. Jaswant is the most patient supervisor a 'budding' researcher could ever ask for. Despite all my mishaps, Jaswant encouraged me to explore graduate studies. After discussion with my mentors, including Dr. Doug Whiteside, I decided to pursue a Master of Science degree, in conjunction with my Doctor of Veterinary Medicine.

I want to thank Drs. Gregg Adams, Dinesh Dadarwal, Fernanda Dias, and Manuel Palomino who passed on valuable knowledge that was pertinent to my research. Thank-you to the graduate chairs, Drs. Karen Machin and Ali Honaramooz, and department head, Dr. Gillian Muir, for giving me direction when I needed it. As well to the WCVM office of the Associate Dean of Research, acting and past, Drs. Liz Snead and Baljit Singh, for their support both in words and as a source of funding. To GADVASU, specifically, Drs. Parkash Brar and Shahbaz Dhindsa for their hospitality and support while in India. Many thanks to my colleagues in the RRL, especially to Dr. Ana Rita Krause, because without her, our gym trips and our Tim Hortons, my sanity would have been lost.

Thank-you to my friends from the WCVM class of 2016 and beyond, for supporting me while doing this dual degree. I appreciated the French treats when I could not attend a conference in France, and for those who have edited parts of this thesis, despite the grueling course load that is veterinary medicine. To my good friend Will who introduced me to BJJ, an avenue for releasing steam, and for commiserating during our graduate studies. To my Mynx Family for the years of balancing my 'work' life and reminding me that life is better upside-down.

Finally, I need to thank my family. I have been in school for too many years, and I could not have made it through without their love and support. To my mother, Yukari, who now uses 'Google Scholar it' as a frequent term. To my father, Carl, who cannot understand all the words of my research work, but will read it anyway. To my sister Tanya, who has become my best friend, and to my two adorable nieces, Mikayla and Danyka, who give me something to look forward to at the end.

iv

# TABLE OF CONTENTS

**LIST OF FIGURES**

ix

# LIST OF ABBREVIATIONS

2D = two-dimensional
3D = three-dimensional
μg = microgram
AI = artificial insemination
CL = corpus luteum
COC = cumulus-oocyte-complex
d = day
D3 = day 3
D5 = day 5
D7 = day 7
eCG = equine chorionic gonadotrophin
FGF = fibroblast growth factor
FSH = follicle stimulating hormone
GnRH = gonadotropin-releasing hormone
h = hour
hCG = human chorionic gonadotropin
HCl = hydrochloric acid
kg = kilogram
LH = luteinizing hormone
LutV = luteal vascularity index
mg = milligram
mL = millilitre
mm = millimetre
OC = oocyte collection
OvV = ovarian vascularity index
P4 = progesterone
PBS = phosphate buffered saline
PGF = prostaglandin F2α
pLH = porcine luteinizing hormone
SEM = standard error of the mean
USP = United States Pharmacopeia
VEGF = vascular endothelial growth factor

# CHAPTER 1: INTRODUCTION AND LITERATURE REVIEW

A general understanding of the use of Doppler ultrasonography in reproduction is required prior to its use in research. The following chapter serves as an introduction to colour Doppler ultrasonography and some basic principles of physics. The estrous cycle of cattle and buffalo are mentioned in brief with the inclusion of how Doppler ultrasonography is used to assess ovarian structures. The current research and the limitations of Doppler ultrasonographic image analysis are reviewed. This literature review forms the basis of the subsequent chapters in which a novel volumetric and objective method is developed and applied in water buffalo and beef cattle.

## 1.1 Colour Doppler Ultrasonography

Ultrasonography has been used as a tool in the characterization of the female reproductive tract of domestic animals [1, 2]. This technique has grown in popularity in the dairy practice since the early 1980's [1], specifically in the areas of pregnancy diagnosis and fetal sex determination [3, 4]. Ultrasound can also be used to detect ovulation [4] and, in conjunction with manipulation of the estrous cycle, it eliminates the need for estrus detection during artificial insemination protocols [5, 6].

Colour Doppler ultrasonography has been used in both veterinary and human medical fields for assessment of internal female genitalia for diagnostic and therapeutic purposes [1, 7-12]. It is integral to have an understanding of the basic theory behind Doppler imaging prior to its application in research, as not all of the colour flow that is overlaid on the grey-scale image represents blood flow, some of which is artefactual. Doppler ultrasonography is currently available in three forms on the modern day ultrasound machine: colour, power and spectral [7]. Colour and power modes will predominate this discussion, with a brief mention of the limitations of spectral Doppler with regards to the vasculature of ovarian structures.

## 1.1.1 What is Colour Doppler Ultrasonography?

Doppler ultrasonography functions using the Doppler shift phenomenon [1, 7, 10, 13] whereby ultrasound waves that are emitted from a transducer travel in a waveform of known frequency. When the waveform hits a target that is moving towards the transducer, the reflected wave returns to the transducer at a higher frequency, known as a positive Doppler shift [10].

Similarly, the sound wave that hits an object that is moving away from the transducer is returned at a lower frequency, or negative shift.

Colour Doppler ultrasonography is the most popular and widely used mode of Doppler imaging [1, 7, 14]. The ultrasound beam contacts blood cells that are travelling in a vessel, either towards or away from the transducer, and the returning sound wave is projected on the ultrasound machine, creating a colour map based on the velocity and direction of the blood flow [7]. The blood flow that moves towards the transducer will show up on the screen in shades of red, while blood flow away from the transducer is in shades of blue [13]. This technology can demonstrate differences in vascular flow by a colour change or a change in direction due to turbulent flow, as well as venous versus arterial blood flow [7].

However, just as brightness mode ultrasonography has forms of artefacts, colour Doppler mode has disturbances in the colour mapping that can construe the observer's interpretation of the image [7]. These disturbances include: "colour aliasing", "blooming", and "flash artefact". "Colour aliasing" is an artefact that is visualized as flow that is going in the opposite direction, thereby making the vessels appear turbulent when, in reality, laminar flow exists. This can be minimized by increasing the number of ultrasound wave forms sent and received per second (pulse-repetition frequency) or by increasing the velocity range [7]. "Blooming" is the over-representation of the colour flow outside of a vessel and can be reduced by decreasing the colour gain [7]. "Flash artefacts" are attributed to moving structures that are not the vessels of interest, usually due to movement of the animal or movement of the surrounding intestines while scanning [7]. Researchers must be aware of these artefacts when using colour Doppler ultrasonography in order to determine the most accurate settings dependent on their organ of interest.

Power Doppler ultrasonography is a specialized form of colour Doppler that uses the intensity of the signal to produce the colour mapping over-laid on the grey-scale image [13, 15] irrespective of the direction of blood flow. Ultrasonographic machines that are equipped with a power mode may be able to detect lower flowing velocities due to an increase in sensitivity [7, 15, 16]. Power Doppler is advantageous for several reasons including: a reduction in noise, a lower effect of aliasing, and independence from the insonation angle, which is the angle of the blood flow relative to the direction of the sound waves [15]. However, in the author's opinion, each individual ultrasound machine differs in the quality of the technological development of

their colour and power Doppler features. Additionally, power Doppler may not be able to detect smaller capillaries in the center of a corpus luteum [17]. Current research in cattle is employing either colour or power Doppler ultrasonography [14, 18, 19]. While power Doppler mode is not currently available on ultrasound machines that are used for portable cow-side ultrasonographic management in beef or dairy industries in North America, the use of power Doppler in reproductive research of large animals may increase with increases in technology.

Spectral Doppler mode allows an operator to gain information on the velocity of blood flow in a specific vessel [1, 7, 13]. For this mode, a 'gate' is placed over the vessel while in brightness mode, and activation of spectral mode provides the viewer with the wave form of blood flow where the peak systolic, end diastolic and time-averaged maximum velocity can then be computed by the software installed on the ultrasound machine [7]. The major limitation of this technique is that these measures are dependent on the angle of insonation which is not possible to detect in small capillaries or tortuous vessels, therefore it is not possible to obtain accurate measures of blood velocity using spectral Doppler or to calculate blood volume in certain tissues like the corpus luteum (CL) [20]. Additionally, the sample gate has a minimum size to which it can be adjusted (i.e. 1 mm), depending on the machine, therefore artefacts can occur if the vessel is smaller than the sample gate [7, 13]. To address this limitation, two relative indices have been utilized on the ovarian arteries that do not rely on the insonation angle: resistance index and pulsatility index [1, 7]. Resistance index (RI) is a measure of the ratio of the difference between peak systolic velocity and the end diastolic velocity divided over the peak systolic velocity. Simply put, it is the resistance to blood flow in the downstream vessel; the lower the resistance, the greater the blood flow. Pulsatility index (PI) takes into consideration the time-averaged maximum velocity within a vessel, in addition to peak systolic and end diastolic velocity. PI relies on the pulse of an artery, and therefore is best reserved for vessels with non-continuous blood flow during diastole. Where necessary, resistance index or pulsatility index will be mentioned in the remainder of this review, however the focus will be on colour and power Doppler modes.


**1.1.2 Using Colour Doppler to Assess Vascularity**

Colour Doppler ultrasonography was first used in human assisted reproductive cycles to assess ovarian blood flow prior to *in vitro* production of embryos in the 1990's [11, 12, 21].

More recent studies showed that women with undiagnosed infertility are more likely to have decreased uterine and ovarian arterial blood flow during the luteal phase, as measured by pulsatility index [22]. Additionally, when there was little detectable blood flow within the stroma of the ovary, women had poor oocyte recovery, lower ovarian volume, fewer large (>14 mm) follicles and poor embryo production *in vitro* [23]. This is despite equivalence in age, body weight, and duration of infertility.

After its advancement in human reproductive research, colour Doppler was applied to large domestic animal reproductive research [1, 24], in particular to cattle by assessing the anatomy and physiology of ovarian structures: follicles and corpora lutea [9, 10, 25, 26]. While its application in clinical practice is currently limited, either due to cost or convenience, colour Doppler ultrasonography of the CL in cattle has been used to predict pregnancy success in recipients for embryo transfer, providing evidence that its use would be cost saving for the producer [27]. Additionally, the vascularity of the ovulatory follicle was used to predict the progesterone production and vascularity of the CL that formed following ovulation [14].

Thus, despite a delay in the use of Doppler ultrasonography in the reproductive management of livestock, when accessible, it continues to produce new information for reproductive research in veterinary and human medicine. The following review focuses predominantly on how colour Doppler ultrasonography is used to gain information on the function of ovarian structures in cattle and buffalo that would otherwise be overlooked in brightness mode alone. Where relevant, a comparison of information from other species is included.

## 1.2 Colour Doppler Ultrasonography for Assessment of Ovarian Dynamics in Cattle and Water Buffalo

Colour Doppler ultrasonography and its applications in cattle reproductive medicine has been previously reviewed [1, 4, 10, 17, 28-30]. In water buffalo (*Bubalus bubalis*), the research is less extensive, but has been gaining popularity through recent years in India, Italy and Brazil [31-35]. While ultrasonography in brightness mode has been performed in calves [36], colour Doppler ultrasonography has yet to be explored. The following sections will serve as background information to two studies that extend the knowledge of colour Doppler ultrasound data in three-dimensions for cattle and buffalo.

4

Vascularity by colour and power Doppler can be measured in several methods, which can be grouped as either subjective or objective [19, 20, 30, 37]. The least labour intensive is having a trained operator estimate the percentage of coloured regions surrounding the region of interest, here the follicles or corpora lutea [19]. The advantage of a subjective method is that it can be performed in real-time while scanning the animal, therefore is most practical for on-farm or cow-side reproductive management. Subjective visual grading of vascularity of the CL has been compared with objective measurements using trained personnel, and has shown adequate relationships between the two methods [18]. However, several disadvantages may arise with subjective grading, including observer bias in research, especially when comparing several treatment groups, the inability to accurately assess small changes in blood flow over time, and its difficulty in conceptualizing the three-dimensional structures from a two-dimensional moving image on the ultrasound screen. Alternatively, objective measurements can be made by exporting the images to be analyzed on an external computer using software (ImageJ, Adobe Photoshop, VOCAL, etc.), or by using spectral Doppler settings that are built into the ultrasound machine, which have their own limitations, as mentioned above. Analysis on an external computer can be performed by selecting the coloured regions and quantifying the regions either by pixels or metric measurements ($mm^2$) of the area [18, 31]. Other methods have also been adopted using a percentage of the circumference or area of interest that is occupied by coloured regions [7, 14]. By increasing the number of images that an observer selects (example from three images to five images), this may allow the researcher to have a better representation of the tissue of interest [18]. Finally, an exploration of three-dimensional ultrasound is becoming more available [20, 38].

## 1.2.1 Changes in Ovarian Vascularity during the Normal Estrous Cycle

Vascularity surrounding the ovarian follicle is likely important for transportation of nutrients, oxygen, and hormones to the growing follicle [39]. Development of the vasculature surrounding bovine follicles begins at the secondary stage (200-400μm in diameter), when theca interna cells and several layers of granulosa cells are present [40]. As found using scanning electron microscopy, this microvasculature consists of two layers: the outer plexus and the inner plexus. The inner plexus is thought to be important in theca interna cell differentiation, selection of a dominant follicle, ovulation of cumulus-oocyte complexes, and the development of the CL

[40]. The outer plexus connects stromal capillaries within the ovary, with the theca externa providing support (nutritional and hormonal) as antral follicles grow [40]. Systemic and local blood pressure and capillary characteristics, however, are not static, and therefore are difficult to analyze using scanning electron microscopy. This vasculature can be evaluated *in vivo* using ultrasonography. Indeed, the technology has been used to detect the blood flow within the bovine ovary [1, 4]. The use of colour Doppler ultrasonography in ovaries of cattle started over ten years ago by a group in Japan that assessed the changes in vascularity through the early and mid-cycle CL [1, 9]. The remainder of this section will discuss pertinent information on the vascularity surrounding follicles, while luteal vascularity will be discussed in a later section.

Ovarian follicular dynamics in cattle (*Bos taurus*) were first assessed using ultrasonography in B-mode (brightness modality) in the 1980's [41], with colour Doppler coming into play twenty years later [1, 9]. The sound waves emitted from the ultrasound transducer travel through the fluid-filled follicles, being non-echogenic or anechoic, and appear as black circular to ovoid structures on the image screen [3]. Using real-time ultrasonography, it was discovered that cattle showed a wave-like pattern of follicular growth that supported a "two-wave" hypothesis [42-44]. Similarly, interovulatory intervals in water buffalo showed one to three waves of follicular growth, with the two wave pattern predominating [45, 46]. Serial ultrasonography, or the ability to observe the ovaries throughout the estrous cycle, has assisted researchers in the development of protocols for stimulating the ovary to grow new follicles, i.e. induction of a new wave of follicles [47, 48]. Wave emergence has traditionally been indicative of the appearance of several follicles of 3-4 mm in diameter [49], with the first wave of follicles appearing just before ovulation of the previous cycle [43]. In two-wave cycles, the second (ovulatory) wave emerges around day 10 following ovulation, while in three-wave interovulatory intervals show the emergence of the third (ovulatory) wave at day 16 [43]. Water buffalo show similar wave emergence, with the first wave appearing one day following ovulation [46]. Two-wave cycles have their second wave emerging at 10.8 days, and three-wave cycles show emergence of their second (anovulatory) wave at 9.8 days [46]. Buffalo with three-wave cycles show a third wave at 16.8 days [46]. Although, new technologies with greater resolution (e.g. ultrasound biomicroscopy) or frequent examinations are beginning to question whether wave emergence is the appearance of several 3-4 mm follicles [50-52], the studies within this thesis will follow the traditional definition of wave emergence as ultrasonography using 5 to 7.5 MHz is more

6

clinically relevant. The frequency of the waves emitted from the transducer is important for depth of penetration and resolution of individual structures, with ovarian structures gaining better resolution at 7.5 MHz compared with 5 MHz [3]. With serial observations using the transrectal approach, we are able to follow follicles from wave emergence to ovulation and the growth of the subsequent CL.

Follicles undergo three phases: growth, static, and regression or ovulation [44]. During the growing phase of follicles in cattle, one follicle is indicated to be the dominant follicle, a process called selection or deviation, and this is usually determined by a difference in diameter where the dominant follicle is larger than all other subordinate follicles [44, 53]. During selection, the dominant follicle acquires greater number of luteinizing hormone (LH) receptors that allows it to grow during decline and nadir in follicle stimulating hormone (FSH) concentration [44, 49, 54-56]. Vascularity will increase for only one of the follicles during selection, where the dominant follicle is more vascular than subordinate follicles. Estradiol and inhibin are also increased in production from the dominant follicle, which suppresses the growth of the subordinate follicles [44]. In mares, this increase in vascularity has been shown to precede an increase in diameter [57]. Additionally, in cattle, small follicles that had detectable blood flow to their periphery remained larger than follicles with diminished blood flow [58]. Selection of the dominant follicle appears to be associated with a reduction in the mRNA expression of the soluble forms of the receptors for vascular endothelial growth factors 1 and 2 (sVEGFR1 and sVEGFR2) [39], therefore allowing greater VEGF binding to membrane VEGF receptors thus increasing the production of new vasculature. Furthermore, while the granulosa cells have higher expression of total VEGF mRNA, it is the thecal cells that have the highest expression of the receptors for VEGF [39], which may relate to vascularity of the theca interna being controlled by the granulosa cells. In support of this, the highest amount of mRNA expression in the thecal and granulosa cells for angiogenic factors, including VEGF, is during the final follicular maturation phase, which corresponds to the high amount of VEGF protein in the follicular fluid [59, 60]. Histological evaluation of bovine preovulatory follicles demonstrated a high expression of VEGF in both theca interna and granulosa layers, while fibroblast growth factor (FGF2) was only in the thecal layer [60].

Using Doppler ultrasonography in dairy cows [58], researchers studied the first follicular wave and discovered that the difference in vasculature is detectable between the largest follicle

and subordinate follicles at follicle deviation [58], when the dominant and subordinate follicles begin to have different growth rates [44]. A group of reproductive scientists in Turkey [61, 62] have also been using colour Doppler ultrasonography to look at the changes in the blood flow to the follicles in cattle, with similar findings of greater vascularity developing around the dominant follicle [62]. In addition, the dominant follicle of the first wave has been shown to be greater in size, blood supply and steroidogenesis [63-65].

During the luteal phase (high levels of progesterone), the dominant follicle undergoes regression and atresia [44]. Lack of blood flow in the thecal layer has been associated with follicular atresia [29, 66]. This lack of blood flow is also found in anovulatory follicles. This suggests that colour Doppler ultrasonography may be an extremely useful, non-invasive technique to determining which follicles are close to ovulation and others that are anovulatory [25].

In the final ovulatory wave, follicles continue to grow to ovulatory size due to an increase in LH pulse frequency and its relationship with lower plasma progesterone and increasing estradiol concentrations [44]. In cattle, ovulation occurs 24 to 36 hours following the LH surge [25]. The diameter of the ovulatory follicle and its ability to ovulate has been studied extensively in cattle and buffalo [31, 53, 63, 67-69]. However, the evaluation of vascularity surrounding the preovulatory follicle can provide additional information on follicular maturation and ovulatory capacity.

**1.2.2 Vascularity, Follicle Maturation and Ovulatory Capacity**

In spontaneous estrous cycles of cattle, as the dominant follicle approaches ovulation, there is an increase in vascularity in the wall prior to ovulation [25]. In contrast, in cycles that are manipulated with gonadotropin-releasing hormone (GnRH), prior to the LH surge the vascularity of the dominant follicle is restricted to a single region around the follicle, deemed the base. In this case, treatment with GnRH caused an increase in vascularity within 30 minutes, which remains high until ovulation, most likely due to the effect of estradiol on the nitric oxide synthase pathway and dilation of the existing vasculature [25]. By using colour Doppler ultrasonography, researchers determined that preovulatory follicles with greater blood supply correlated with higher pregnancy rates [70].

### 1.2.2.1      Intrafollicular Hormones and Vascularity

Follicle diameter has been used as an easily measurable endpoint that coincides with changes in the fluid within the follicle. In cattle, the dominant follicle averages 8.5 mm at deviation from the largest subordinate follicle [43, 53], while in buffalo the dominant follicle is 7.2 mm [67]. However, research has shown that follicle diameter is not a predictive measure whether a follicle would develop into a CL following follicular aspiration [71]. On the other hand, the estradiol concentration and estradiol to progesterone ratio within the follicular fluid were strongly predictive of the formation of a CL [71], suggesting the necessity for the appropriate follicular environment for production of a functional CL. When intrafollicular fluid was analyzed from cattle ovaries obtained from slaughterhouse and *in vivo* aspirated follicles, the estradiol concentrations increased when comparing follicles that were under 8.5 mm in diameter with those greater than 8.9 mm in diameter [72]. These intrafollicular levels of estradiol have been associated with increased dominant follicle vascularity in both cattle [73] and buffalo [31]. Similarly, in assisted reproduction in humans, there was a decreased resistance to blood flow surrounding the follicles when the plasma estradiol levels were high [74]. Research suggests that estradiol has an effect on the endothelial nitric oxide synthase pathway, thereby causing vasodilation with the increased availability of nitric oxide [75], which is a possible explanation for the increase in vasculature surrounding those dominant follicles that are higher in estradiol [26].

Along the same lines, ovulatory follicles have been shown to have double the concentration of estradiol compared with anovulatory follicles [49]. After deviation, the dominant follicle had higher levels of estradiol and nitric oxide, and a higher estradiol to progesterone ratio in cattle [62], in addition to the increased blood flow mentioned above. Estradiol in dominant follicles of the first follicular wave are higher at three to five days after ovulation than at six to eight days after ovulation, signaling atresia [64, 76]. Follicles undergoing atresia have lower estradiol to progesterone ratio [77]. Subordinate follicles show little estradiol in the intrafollicular fluid [76]. The hormone status within the follicle may be more important than the size of the preovulatory follicle [31] for predicting the health status of the oocyte the follicle contains, although this is difficult to assess as follicles that are aspirated are unable to be followed to an ovulatory event. However, the vascularity of the CL that follows may correlate with the estradiol concentration in the intrafollicular fluid that was aspirated [71, 78]. Similarly, colour Doppler applied to the

preovulatory follicles in water buffalo demonstrated that blood flow was highly correlated to intrafollicular estradiol and insulin-like growth factor, while diameter of the follicle was of less importance [31]. Colour Doppler therefore can provide more information about follicles that are aspirated.

### 1.2.2.2    Hormone Manipulation and Changes in Vascularity

A discussion of the major hormones affecting follicle growth and ovulation is imperative for the understanding of follicular dynamics and the ability to manipulate the estrous cycle for assisted reproductive programs. Manipulation of the estrous cycle in cattle and water buffalo has been used to decrease the inter-estrus interval [6, 79, 80], as well as for superstimulation and superovulation for *in vitro* fertilization and embryo transfer [81-84]. Synchronization using hormone induction of luteolysis, followed by ovulation including OvSynch and Double OvSynch protocols has improved the success of artificial insemination in buffalo [6, 83, 85-87]. The major benefit of hormonal manipulation of the estrous cycle to induce ovulation is that it eliminates or reduces the need for estrus detection [5, 6]. It is important to note that estrus detection in water buffalo is more difficult than in cattle as they rarely exhibit mounting behaviour [88], therefore ultrasonography of the ovaries of this species to detect estrus and preovulatory follicles is invaluable for artificial insemination protocols.

Three hormones will be discussed below as they pertain to the manipulation of estrous cycles in cattle and buffalo in the chapters of this thesis: follicle stimulating hormone (FSH), gonadotropin-releasing hormone (GnRH), and luteinizing hormone (LH).

### 1.2.2.2.1   FSH

Follicle stimulating hormone (FSH) is released from the pituitary in response to gonadotropin-releasing hormone (GnRH) from the hypothalamus and is responsible for the emergence of new follicular waves [43, 44, 89]. FSH is required for the early growth of follicles prior to selection, while LH assists the dominant follicle to reach ovulatory capacity [44], which will be discuss further in a later section. The peak in FSH occurs at the time of wave emergence, or the appearance of the future dominant follicle and largest subordinate follicles, and its lowest at the time of deviation of the dominant follicle [43, 52]. Inhibin is also released from the dominant follicle, and provides a negative feedback for the release of FSH [43, 44]. By

10

increasing the amount of FSH available, cattle [81, 90] and buffalo [82, 83] will respond by continued growth of follicles that would normally regress, although the response to superstimulation is much greater in cattle than buffalo [83]. However, such follicle stimulation (superstimulation or superovulation) disrupts the normal gene expression for steroid producing cells, delaying it compared to single ovulatory cycles [91]. This can be addressed by increasing the duration of superstimulation, thereby allowing adequate time for appropriate follicular gene expression during maturation [92].

Using colour Doppler ultrasonography during superstimulatory treatment may predict the outcome of the response, the production of many large follicles. Early studies in women undergoing follicular stimulation demonstrated that women with a greater ovarian stromal vascularity had a greater number of follicles at the time of oocyte retrieval [21], and those with a lower RI prior to stimulation had a higher number of oocytes retrieved [93]. Additionally, women who required a longer duration of stimulation in order to achieve an appropriate level of estradiol concentration per large follicle (>16 mm or minimum of three follicles >20 mm) had higher resistance to blood flow prior to stimulation [93]. In ewes during superstimulatory treatment, there was an increase in subjective blood flow measurements of the follicles using colour Doppler [94]. However, there was a positive correlation with the number of unfertilized eggs and colour flow to the follicles on the final day of superstimulatory treatment, after treatment with equine chorionic gonadotrophin (eCG) which mimics luteinizing hormone [94]. Whether this is due to operator selection of a single two-dimensional image for analysis or that ewes respond differently is unknown. Conversely, eCG in water buffalo was not stimulatory for vascularization of the CL [95]. Cows may be similar to women, in that the number of small follicles that have blood flow prior to superstimulation may be predictive of superstimulatory response possibly due to having greater nutritional and hormonal transport [4, 58]. However, one study in dairy cattle, using spectral Doppler and PI on the ovarian artery close to the aorta, did not find a relationship between ovarian blood flow parameters and superstimulatory response [96].

Colour flow analysis after superstimulation may also provide valuable information on the expectedquality of the embryo or pregnancy success. Women with lower follicular vascularity after stimulation on the day of intrauterine insemination had fewer large follicles (>16 mm), lower serum estradiol, as well as being significantly older in age than women who demonstrated

11

greater follicular vascularity on the day of insemination [97]. This is similar to a more recent study, showing that as women age, their ovarian stromal blood flow decreases and so does their probability for success during *in vitro* fertilization [98]. Furthermore, no pregnancies were achieved in the women with low follicular vascularity, while women with a high grade of vascularity had a pregnancy rate of 31% [97]. In goats undergoing superstimulation, there was a positive association between viable oocytes and the peak systolic velocity of the ovarian artery [99]. In cows undergoing stimulation with eCG, the blood flow velocity in the ovarian artery increased during stimulation and was highest on the day of corpora lutea assessment (day 7) [96]. Additionally, the velocity of blood flow in the ovarian artery was positively correlated with the number of corpora lutea. However, it appears that little research has been performed using colour Doppler ultrasonography to assess follicles prior to oocyte collection or assessment of corpora lutea that form after aspiration in adult or juvenile cattle undergoing superstimulatory treatment.

### 1.2.2.2.2  GnRH and LH

Gonadotropin-releasing hormone (GnRH) is released from the hypothalamus and signals to the pituitary to release follicle stimulating hormone (FSH) and luteinizing hormone (LH) [100]. GnRH-based protocols were used in lactating dairy cattle without regard to the status of their estrous cycle [5] and was later adopted in water buffalo [101]. GnRH was originally given to induce ovulation, with subsequent formation of a CL, but treatment with GnRH can also induce the emergence of a new wave of follicles [100]. Ovulation occurs between 20 to 32 hours following GnRH treatment in water buffalo [101]. As reported in cattle, GnRH-induced and spontaneous ovulation will give variable results with dependency on the size of the dominant follicle [102].

Luteinizing hormone (LH) is secreted from the pituitary and predominately binds to receptors on the granulosa cells of dominant follicles [55, 56] or the luteal cells of CL. Early in the estrous cycle, progesterone levels are low and LH pulse frequency supports the growth of the dominant follicle until the CL has grown to its full size and progesterone then inhibits LH pulse frequency [76]. This may explain why first wave follicles grow to a larger size [103] than the dominant follicle of second (anovulatory) wav in three-wave cycles. Once the CL is secreting luteal phase levels of progesterone, the dominant follicle of the first wave is no longer supported and regresses [76]. After luteolysis, or during proestrus, LH pulse frequency increases and so

does the diameter of the preovulatory follicle [103]. Given this, lysis of the CL is important for the development of the ovulatory follicle. In cattle, ovulation occurs 26 to 34 hours following the surge in LH [25]. The peak in LH in water buffalo follows approximately 14.8 hours after a peak in estradiol concentration [83]. After treatment with GnRH, LH peaks within 2 hours of administration in water buffalo [101]. In addition to supporting the growth of the dominant follicle, LH also supports the growth of the CL [104].

The LH surge induces an increase in vascularity to the ovulatory follicle [24, 105]. The vascularity of the preovulatory follicle prior to the LH surge is located in a small region near the base of the follicle [25]. During the LH surge, confirmed by its plasma concentrations either endogenously or by control of with a GnRH treatment, the vascularity to the follicle (as measured by time-averaged maximum velocity in spectral Doppler) increases within a half hour of treatment with GnRH [25]. This initial study showed that the velocity of the blood flow remains higher until ovulation. In a later study, heifers that were induced to ovulate with GnRH demonstrated a biphasic pattern of increase in blood flow to the circumference of the follicular wall when measured every hour until ovulation [106]. An initial increase occurred up to three hours after treatment, followed by a decrease to basal levels. Subsequently, a second increase occurred six to eight hours prior to ovulation, with a late decrease one to two hours prior to ovulation [106]. This allows one to hypothesize that vascular flow measures taken 24 hours following treatment with GnRH would provide the greatest increase in vascular flow to a preovulatory follicle in cattle.

### 1.2.2.3    Vascularity and its Relationship with Oocyte Morphology

The use of ultrasound-guided follicular aspiration for oocyte collection *in vivo* has been used in cattle [36, 107], buffalo [108], non-domestic species of Bovidae [109], mares [110], and women [111] that has enabled the repeated collection of oocytes from individuals without removal of their ovaries. However, recovery of the oocyte is dependent on many factors, including season [112], the vascularity surrounding the follicle prior to aspiration [111], needle and tubing diameter, and the vacuum flow rate [113], as well as the skill of the operator. Women undergoing ovarian stimulation and follicular aspiration had greater recovery of oocytes when the resistance to blood flow was decreased [93].

During follicular aspiration, oocytes were more frequently recovered from follicles that showed a greater percent of blood flow in their circumference and a greater increase in blood flow between the time of GnRH treatment and the time of collection [114]. When single preovulatory follicles were aspirated in cattle, there was no difference in the degree of expansion of the cumulus-oocyte-complex (COC) [114]. However, the odds ratio for collecting a good quality COC (greater than four layers of compact cumulus cells and homogenous ooplasm) from a highly vascular follicle was 3.3 times higher than COC collected from avascular follicles when collected at random points in the estrous cycle [73]. Contrary to a study in women [111], a study in mares did not find a relationship between the oocyte recovery and percentage of blood flow to the follicular wall [115], which is possibly due to the position of the ovulatory fossa in this species. When cattle are superstimulated to increase the COC retrieval, animals that undergo a long duration of superstimulation have larger follicles, greater number of expanded COC, greater proportion of good quality oocytes and greater production of embryos [116, 117]. The production of embryos *in vitro* is related to the quality of the oocytes that are retrieved [116]. Taken together, these data suggest that colour Doppler ultrasonography may provide a non-invasive means for predicting subsequent successful retrieval, oocyte maturation, fertilization and culture of the oocytes in cattle and buffalo, which would allow researchers and producers to concentrate resources towards individuals that would be successful donors of good quality oocytes.

### 1.2.2.4    Vascularity and its Relationship with Oocyte Competence

Oocyte competence is the ability for an oocyte to become fertilized and produce a viable embryo [92, 118]. Predictions of developmental competence of the oocyte have been performed using grey-scale ultrasonography prior to slaughter and retrieval of oocytes from follicles of growing, early-static, late-static, or regressing follicles, by assessing the echotexture of the follicular wall, peripheral antrum and the surrounding ovarian stroma [119]. This study found that subordinate follicles that were aspirated on day five of the cycle had lower grey-scale values than those collected at the regressing phase (day seven). Subsequently, these grey-scale parameters measured on the regressing follicle were related to the inability to produce embryos *in vitro*. Oocyte competence is dependent on the developmental stage of the follicles within the ovary, with a large diameter follicle typically containing a more competent oocyte [90, 118].

14

Maternal age also effects oocyte competence, with aging mothers having oocytes with lower developmental competence than their younger relatives [90].

Colour Doppler ultrasonography was used to study the relationship between the vascularity of the wall of the preovulatory follicle prior to oocyte collection and embryo development in cattle [114]. A decrease in the resistance index (an indicator of vascular perfusion) in a vessel within the follicular wall from the time of GnRH and the time of collection was associated with cleavage of the oocytes (two-cell embryo), while oocytes that did not cleave did not demonstrate this change in vascular perfusion [114]. In women, higher peak systolic velocity in the follicular wall was positively related to embryo quality [111]. However, some researchers have found that colour Doppler ultrasonography is predictive in a qualitative manner and not by a quantitative method during the assessment of single ovulatory follicles [120]. Despite some supporting evidence that blood flow in the CL is also related to the blood flow of its ovulatory follicle of origin, and that follicular blood flow correlated with the progesterone production following ovulation [14], subsequent research did not find a relationship between the vascularity of the preovulatory follicle and pregnancy success [121], thus the clinical relevance of the use of colour Doppler as a predictive measurement tool remains controversial.

### 1.2.3 Vascularity and Corpus Luteum Function

The CL develops from the granulosa and theca layers of the follicle after ovulation [44]. It is the main gland that produces progesterone during the estrous cycle of cattle taking an animal from less than 2ng/mL to greater than 6ng/mL [44]. During luteinization, granulosa and theca cells change their production of estradiol and androgens towards a progesterone producing environment [104]. There are two populations of luteal cells, small and large, which differ in their production of progesterone and responsiveness to LH [122]. The small cells are derived from the cells of the theca interna, while large cells arise from granulosa cells of the follicular wall [104]. Both the small and large luteal cells produce progesterone in response to LH *in vitro*, with the small cells responding to low levels and large cells requiring a high level of LH [122]. Angiogenesis is paramount for the normal function of the CL [123-126], including the regulation of two angiogenic factors, vascular endothelial growth factor (VEGF) A and fibroblast growth factor 2 [61]. Accordingly, the highest VEGF mRNA expression levels occur in the early growing CL of cattle [59]. Additionally, FSH stimulation for superovulation in water buffalo

15

increases the capillary bed of the subsequent corpora lutea, and the VEGF expression in luteal cells [95]. It is thought that the capillary network is important for bringing cholesterol components to the growing CL for the conversion to progesterone [104]. Both the size (cross-sectional area) [127] and the blood flow (number of coloured pixels in the luteal area) [128, 129] of the CL are related to peripheral progesterone levels.

### 1.2.3.1    Luteal Growth, Vascularity and Plasma Progesterone

CL structure and echotexture as seen in brightness mode ultrasonography differs throughout the estrous cycle [130]. The echogenicity of the CL in cattle does not differ significantly between metestrus and proestrus, but histological sampling showed that blood vessels were highest during metestrus and lowest in proestrus [130]. The echogenicity of the CL has been evaluated and showed a positive correlation with plasma progesterone in cattle [129, 131]. Physiological changes in the CL coincide with changes in vascular indices including spectral Doppler measurements pulsatility index and  resistance index, and total vascular volume (the vascular ratio by volume of luteal tissue) [132]. A study in humans used power Doppler to detect the blood flow in the CL [132] and demonstrated that the product of the ratio between the blood flow area to the area of the CL and the volume of the CL was correlated with the serum progesterone concentration [132]. Similarly, in cattle, smaller luteal size and lower blood flow are correlated with lower levels of progesterone [128]. This may be explained by the proposed role of the blood flow as a source of cholesterol (low density lipoprotein) to the granulosa cells for the production of progesterone [104, 133]. The CL in buffalo has also been analyzed using colour Doppler imaging and its relationship with concentrations of progesterone measured in whey [134]. It has been found that in cattle, progesterone release is related to the blood flow pattern within the CL, central or peripheral [135]. In a study evaluating the response to human chorionic gonadotropin (hCG) *in vitro*, central regional blood flow increased, whereas peripheral regions did not [135]. A vascular grading system of low, medium, high and very high for the CL was also associated strongly with serum progesterone [18].

### 1.2.3.2    Luteolysis and Vascular Changes

Towards the end of the luteal phase of the estrous cycle, the CL regresses and diminishes in size, blood flow and production of progesterone [44]. This is in response to prostaglandin F2$_{\alpha}$

(PGF) in cattle [44] and buffalo [6, 136] that is released in a pulsatile manner from the endometrium [44, 137]. Prostaglandin analogues have been used to induce luteolysis and subsequent ovulation of the dominant follicle [44]. The production of progesterone from large luteal cells *in vitro* is inhibited by PGF, even under the influence of LH [122]. Additionally, the production of progesterone from small luteal cells *in vitro* is stimulated by PGF [122].

Prostaglandin F2$_\alpha$ is the primary luteolytic component in cattle [44]. However, an initial increase in vascularity following treatment with PGF did not always lead to luteolysis in cattle [138], which could be due to the differential effects of PGF on small versus large luteal cells [122], as well as the luteotrophic effects of endogenous LH [44]. The peripheral region of the bovine CL consists of blood vessels that are smooth muscle actin-positive, and PGF receptors were found in both the large blood vessels and the luteal cells within this region of the mid-cycle CL [139]. PGF treatment causes a transient increase in blood flow in the peripheral region of the CL prior to a decrease in the secretion of progesterone [9, 129]. Additionally, the acute increase in blood flow following PGF treatment also appears to coincide with an acute increase in the expression of endothelial nitric oxide synthase within the peripheral luteal region but not within the central region [139]. Further to this, blocking the binding of nitric oxide to smooth muscles in blood vessels was associated with suppression of the change in blood flow and it delayed luteolysis [139].  Given the segregation of central vs peripheral regional blood flow, there is a requirement to analyze these regions separately.

Colour Doppler ultrasonography has been used to visualize the differential response or lack thereof between the mid-cycle CL and the early CL. The relationship between luteal blood flow and progesterone secretion during PGF induced luteolysis, as well as CL dimensions has been tested, with the mid-cycle CL responding with an initial increase in luteal blood flow then a decrease, while there was no response in the early CL [9]. The central region of the CL appears to respond to LH with an increase in progesterone release when treated with hCG that mimics LH [135].

### 1.2.4 Vascularity and its Relationship with Pregnancy Success

A main function of the CL, that is progesterone secretion, is important in the early establishment of pregnancy and maternal recognition of the presence of an embryo *in utero* [140, 141]. Plasma progesterone increases during early pregnancy and is strongly correlated with

blood flow to the CL [18, 32, 142, 143]. While some researchers have found no difference in the diameter or blood flow of the CL between pregnant cows and non-pregnant cows [69], others have found that the cows are more likely to carry a successful pregnancy if the CL has greater vascularity [27, 121, 144]. Similar contradictions have been demonstrated in water buffaloes. In one study, water buffaloes that were pregnant had a decrease in the resistance index in the wall of the preovulatory follicle five hours after artificial insemination compared with non-pregnant buffaloes; however the CL dimensions and RI taken at day ten after insemination did not differ between pregnant versus non-pregnant buffaloes [145]. In contrast, vascular measurements, RI and time average medium velocity, taken on the CL at ten days following artificial insemination, demonstrated a greater velocity and lower resistance to blood flow for pregnant buffaloes compared to non-pregnant buffaloes [33]. Another study in buffaloes found that RI and PI in the CL were not good indicators of pregnancy status, but that the time-averaged medium velocity between days five and ten tended to be higher in pregnant animals [32]. Whether these conflictions are due to inherent variability in the spectral Doppler measurements on the small vasculature of the CL, or due to variability in study design is unknown.

During embryo transfer, a functional CL is required for successful adherence of an embryo. In cattle, evaluation of the blood flow to the CL can predict better quality recipients that are more likely to maintain a pregnancy after transfer [27, 121]. Additionally, the evaluation of blood flow to the CL on day 20-21 following either ovulation and timed artificial insemination, or embryo transfer at day seven, found a high sensitivity for non-pregnant animals, demonstrating a value of colour Doppler ultrasonography in the management of recipients or detection of non-pregnant animals [146-148]. However, due to high variation between animals, it may not be successful as a tool to diagnose early pregnancy in cattle [17, 143].


**1.3 Three-Dimensional Volumetric Analysis of Vascularity of Ovarian Structures**

The application of colour Doppler ultrasonography in three-dimensions has been performed in human medicine beginning in the early 2000's [38, 149-154], but very little research has been performed in bovine reproduction [20] and to my knowledge no published research has been performed in buffalo reproduction. Additionally, knowledge of CL development in prepubertal calves is limited to morphological or histological evaluation [155-157] with no reports of vasculature or three-dimensional image analysis. The rationale for using three-dimensional

reconstruction of ovarian structures using colour Doppler ultrasonography in human medicine includes the differential changes in blood flow surrounding ovulatory follicles [152, 158]. Three-dimensional Doppler ultrasonography has been used in assisted reproductive medicine for management of individuals undergoing IVF cycles. Its feasibility in human reproductive medicine appears to be similar to two-dimensional sonographic imaging [153].

A recent study in cattle using three-dimensional power Doppler ultrasonography demonstrated that blood flow measured leading up to ovulation increased [159], however there was no description of animals that failed to ovulate. Analysis of multiple images to gather information of the vascularization surrounding the entire follicle is time consuming and is therefore only rarely evaluated during studies using colour Doppler ultrasound data. Keeping in mind that subjective selection of the most vascular region of a follicle or CL may not depict the true vascularity of the structure [20], technological advancement and exploration of a three-dimensional methodology to objectively assess the vascularity of ovarian structures and the relationships with their function in cattle and buffalo are the basis of the studies within this thesis.

# CHAPTER 2: THESIS OBJECTIVES AND HYPOTHESES

The overall thesis objective was to relate changes in follicular and luteal vascularity with functional changes (ovulatory capacity, hormones, oocyte quality, etc.). The hypothesis for this thesis was that vascularity is positively correlated with the function of the ovarian structures. To test this hypothesis, we developed a computer-assisted three-dimensional method of assessing vascular flow from the colour Doppler ultrasound data of ovarian follicles and corpora lutea. Two requirements for this method were that: 1) it should use video segments recorded after free-hand movement of the routine linear-array transducer and 2) does not require a-priori operator selection of images, i.e., is an objective method.

## 2.1 Objectives

Specific objectives that are addressed in the subsequent chapters are:

- To develop an objective method of assessing vascular flow from the colour Doppler ultrasound data of ovarian follicles and corpora lutea (Chapter 3)
- To study the effect of exogenous administration of GnRH or LH on vascular flow to the preovulatory follicle and its correlation with ovulation success or expansion of the cumulus-oocyte-complex (Chapters 3 and 4)
- To study the relationship between the follicular wall vascularity of ovulatory follicles with vascularity of the CL that follows (Chapters 3 and 4)
- To study the relationship between follicular wall vascularity of the ovulatory follicles and corpora lutea with pregnancy outcome (Chapter 3)
- To determine the vascular changes following exogenous LH in superstimulated ovaries of four-month-old calves (Chapter 4)
- To determine the relationship between ovarian and luteal vascularity and relative luteal tissue volume that forms following follicular aspiration with the production of progesterone (Chapter 4)

## 2.2 Hypotheses

Given the above objectives the following hypotheses were formed:

- Vascularity index obtained from three-dimensional volumetric analysis would demonstrate lower variability between animals at the same stage of functional development compared with two-dimensional analysis of single images
- Treatment with GnRH or LH would lead to an increase in vascularity to the follicular wall measured 24 hours following treatment
- An increase in vascularity following treatment with GnRH or LH would increase ovulatory capacity and expansion of the cumulus-oocyte-complex
- The vascularity of the follicular wall would be positively correlated with the vascularity of the CL that follows
- Higher vascularity of preovulatory follicles and corpora lutea would be positively related with pregnancy success
- Superstimulated ovaries in calves under a long duration of FSH would have greater vascularity than those under a short duration of FSH
- Luteal tissue volume and vascularity that develops following follicular aspiration will be positively correlated with the production of progesterone

**CHAPTER 3: A novel volumetric method for assessment of ovarian follicular and luteal vascular flow in water buffalo (*Bubalus bubalis*) using colour Doppler ultrasonography**

**Relationship of this study to the thesis**

The specific objectives that are addressed in this chapter are: to develop an objective method of assessing vascular flow from the colour Doppler ultrasound data of ovarian follicles and corpora lutea, to study the effect of exogenous administration of GnRH on vascular flow to the preovulatory follicle and its correlation with ovulation success, to study the relationship between the follicular wall vascularity of ovulatory follicles with vascularity of the CL that follows, and to study the relationship between follicular wall vascularity of the ovulatory follicles and corpora lutea with pregnancy outcome.

**3.1 Abstract**

The main goal of the study was to develop an objective computer-assisted volumetric method of assessing vascular flow from colour Doppler ultrasound data of ovarian follicles and corpora lutea. We hypothesized that a vascularity index (ratio of region of blood flood to region of ovarian structure) obtained from three-dimensional volumetric analysis would be more predictive (less variable) than conventional two-dimensional analysis of single images in estimating functional status of ovarian structures. The study design also allowed us to 1) compare vascular flow changes in follicles that ovulated or failed to ovulate in response to exogenous GnRH treatment, and 2) assess relationships between vascular flow in the ovulatory follicle, the resultant corpus luteum (CL), and pregnancy outcome. Doppler ultrasound cineloops of dairy water buffaloes (*Bubalus bubalis*; n=22) ovaries were recorded daily from 12 h prior to treatment with GnRH to four days following ovulation. Cineloops were processed using Fiji and Imaris software packages for segmenting and calculating the area (two-dimensional analysis) and the volume (three-dimensional analysis) occupied by colour (blood-flow) or grey regions of the follicle wall (follicular vascularity), luteal tissue, and the region surrounding the CL (vascularity index=volume of blood flow/volume of region of interest). For three-dimensional volumetric measurement, all images in a cineloop were used (i.e., no a-priori selection of images) while for two-dimensional analysis, three images from the region with apparent maximum vascularity were selected for analysis. The volumetric method was verified with theoretical ellipsoidal volumes based on the diameter of the follicles (r=0.96 P<0.01) or corpora lutea (r=0.58 P=0.02). Vascularity index values remained unaffected by assumptions made for the slice thickness in the Z-axis, while absolute volumes of the follicles, corpora lutea, and the blood flow (colour regions) were affected by changes in the Z-axis (P<0.01). Follicular vascularity index demonstrated lower variability among animals using the newly-developed three-dimensional method compared to two-dimensional analysis (0.018 ± 0.002 vs 0.030 ± 0.005, P<0.01), while the variability for CL vascularity was similar between the two methods (P=0.23). An increase in the follicular vascularity index was detected at 12 h after GnRH treatment (n=16) using both methods (two-dimensional: 0.030 ± 0.008, P<0.01; three-dimensional: 0.016 ± 0.006, P<0.02). The pre- to post-GnRH change in vascularity index tended (P=0.06) to be greater for follicles that ovulated (n=13; 0.023 ± 0.005) than those that failed to ovulate (n=3; -0.02 ± 0.01) using the three-dimensional method, whereas no such difference was detected using the two-dimensional

method (0.035 ± 0.009 vs 0.008 ± 0.018, P=0.20). The follicular vascularity index obtained by three-dimensional image analysis at 14 to 16 h after GnRH treatment was positively correlated with the diameter of the follicle (r=0.59; P=0.02). The vascularity index of the preovulatory follicle assessed one day before ovulation and that of the CL four days after ovulation were not correlated (n=16; r=0.38, P=0.20). Further, no relationship was detected between ovarian vascularity indices and pregnancy (P=0.45). In conclusion, a new volumetric method for assessing relative ovarian blood flow changes was developed using Doppler ultrasound cineloops that eliminates the need for a-priori selection of images and making assumptions about the Z-dimension. The volumetric method is more precise than the conventional two-dimensional analysis as a result of decreased technical variability and greater representation of follicular and luteal data.

**Keywords**: colour Doppler ultrasonography, three-dimensional volumetric analysis, ovary, buffalo, reproduction, follicle, blood-flow, vascularity, CL

## 3.2 Introduction

Colour Doppler ultrasonography provides a real-time and non-invasive *in vivo* method to assess blood flow to ovarian structures over time. A positive correlation between blood flow surrounding the preovulatory follicle (follicular vascularity) and successful pregnancy has been reported in cattle [70], mares [160] and women [11, 12, 161, 162]. In heifers treated with gonadotrophin releasing hormone (GnRH), the follicular vascularity increased by the time of artificial insemination (i.e., 26 h after GnRH treatment) in heifers that become pregnant but not in non-pregnant heifers [70]. Follicular vascularity has been proposed as a method to identify the future dominant follicle [12, 70], as a biomarker of intrafollicular hormone concentrations [31, 73, 163], and as an indicator of cumulus-oocyte quality and oocyte maturation [73, 111, 162]. Follicular vascularity has also been used to predict the vascularity of and progesterone production by the subsequent CL [14] as well as embryo quality [114, 162]. In cattle and humans, oocytes from larger follicles and those with greater vascularity or blood velocity had greater *in vitro* fertilization rates and embryo development potential [111, 114]. In water buffalo, follicular vascularity was associated with an increase in follicular fluid estradiol concentrations

[31], but the timing of follicular fluid sampling relative to the luteinizing hormone (LH) surge was not reported.

Ultrasonography has also been used to assess CL function. Computer-assisted echotexture analysis of B-mode ultrasound images of bovine CL revealed differences between diestrus vs metestrus or proestrus, and pixel values were correlated with luteal and plasma progesterone concentrations [130]. Plasma progesterone concentrations in cattle were better correlated with Doppler-assessed blood flow than cross-sectional area of the CL [61, 143], and luteal vascularity paralleled the increase in CL volume during the early luteal phase [25]. Although blood flow to the CL was greater in cows in the 3rd week of pregnancy than in non-pregnant animals [61], and the percentage of the luteal area occupied by blood flow decreased between 14 and 18 days after insemination in non-pregnant but not in pregnant cows, variation was too great to use the technique to diagnose early pregnancy [61, 143, 164]. In buffaloes at ten days after insemination, the vascular velocity in the CL was higher in pregnant than in non-pregnant individuals [34]. Using colour Doppler ultrasonography and plasma progesterone measurements, the effect of season on the function of water buffalo CL was confirmed, whereas the diameter and area of CL did not differ between breeding seasons [34].

While vascular-flow patterns discerned by colour Doppler imaging provides information about the physiological status of ovarian follicles and corpora lutea, assessment of vascularity scoring may be influenced by observer bias. Most of the studies cited above involved assessment of images selected by the operator that represented the most vascular region of the structure of interest, either by "freezing" the image during the examination (single image) or from stored cine-loops (multiple images). The selection of images is, in part, subjective; the operator is in control of the transducer direction and speed, and is making the selection. Furthermore, a given two-dimensional slice of an ovary may not be the most accurate representation of the vascular network surrounding a follicle or CL, particularly in light of recent findings that the vascular supply to ovarian follicles is not evenly distributed [20]. Hence, a volumetric method to evaluate the vascularity of the entire structure, without operator selection, would provide a more objective and representative assessment [20, 165].

The goal of the present study was to develop an objective volumetric method of assessing vascular flow from colour Doppler ultrasound data of ovarian follicles and corpora lutea. We hypothesized that a vascularity index obtained from three-dimensional volumetric analyses will

be more reflective (less variable) of functional status than conventional two-dimensional analysis of single images. The study design allowed us to examine follicle vascular flow changes before and after the pre-ovulatory LH surge, and the relationship between vascular flow to the ovulatory follicle and the resultant CL in relation to pregnancy outcome.

## 3.3 Materials and Methods

The study was conducted at the dairy farm of Guru Angad Dev Veterinary and Animal Science University, Ludhiana, Punjab, India, during June and July ($31.0 \pm 0.04°C$, $67 \pm 2\%$ humidity). The institutional ethics committee of GADVASU approved the protocol for animal experimentation. Computer-assisted data analyses were performed at the One Reproductive Health Research Group imaging facility at the University of Saskatchewan, Saskatoon, Canada.

### 3.3.1 Treatment protocol

Water buffaloes of Murrah and Nili Ravi breed were selected for the study (replicate 1: n=13; replicate 2: n=9). Buffaloes were of $5.5 \pm 0.6$ years (mean $\pm$ SEM) of age (range: 2.2 to 10.1 years), $578 \pm 17$kg (range: 400 to 720kg) with a body condition score of 2.5 to 5 out of 5. Parity (nulliparous n=4; multiparous n=18) ranged from 1 to 7 and they were $195 \pm 44$ days from last parturition date (range: 36-560 days). Buffaloes were managed in an open housing system with access to covered shelters and had free access to water and were fed ad lib.

For the purpose of another study (unpublished data), buffaloes were subjected to either of two modified ovulation synchronization protocols (PGF-GnRH-PGF-GnRH or PGF-GnRH-GnRH-PGF-GnRH). The development of a three-dimensional volumetric analysis of the vascularity in the water buffalo ovary was therefore opportunistic, with the knowledge that evaluation of colour Doppler flow during a natural cycle was being performed on a separate group of animals (unpublished data). At the commencement of the protocols, ultrasound examination of genital tracts and ovaries of buffaloes was performed using transrectal ultrasonography (7.5MHz; Esaote MyLab5) to assess the presence of a CL. Buffaloes with a CL (n=19) were given prostaglandin $F_{2\alpha}$ (PGF, Cloprostenol 500μg im; Vetmate, Provimi Animal Nutrition, India) followed by a GnRH agonist (Buserelin 10 μg im; Receptal, Intervet, India) two days later. Buffaloes that had a large follicle >10 mm but no CL (n=3) were given GnRH only (i.e., PGF treatment was omitted). Buffaloes were artificially inseminated 14 to 16h after the

final GnRH agonist treatment in the respective synchronization groups using frozen semen (two 0.25cc straws) from a single fertile water buffalo bull. For the purposes of the present study, Doppler ultrasound cineloops of both ovaries were recorded daily from the time of the second PGF treatment to four days after insemination. Pregnancy status was assessed via transrectal ultrasonography 45 days after insemination, and confirmed at 60 days after insemination.

### 3.3.2 Ultrasound evaluation of ovarian structures and colour Doppler image acquisition

Ultrasonographic images of ovaries were recorded using a transrectal linear-array 7.5MHz probe (MyLab5, Esaote) in brightness and colour Doppler modes. Ultrasound evaluations were done daily with the same settings for all animals (overall gain 58%, colour gain 65%, depth 5cm, two focal points). Ultrasound recordings of each ovary were made in 20-second cineloops in colour Doppler using free-hand rotation in a medial-to-lateral plane to encompass the entire dimension of the ovaries. Cineloops were captured in AVI format. Colour Doppler ultrasonography cineloops of the ovary containing the preovulatory follicle were recorded 12 h before and 12 h after GnRH treatment and those containing the resultant CL four days after ovulation were selected for further image processing.

### 3.3.3 Image processing for two-dimensional and three-dimensional data generation

In two-dimensional images, the X-axis was taken as the cranial-to-caudal direction of the ovary (viewed in the horizontal plane on the screen), and the Y-axis was taken as the dorsal-to-ventral direction of the ovary (viewed in the vertical plane on the screen). For three-dimensional imaging, the Z-axis was in the medial-to-lateral direction of ovary (i.e., adjacent X- Y-frames in the cineloop). Cineloops in AVI format were cropped in the Z-axis to include one complete scan of an ovary and converted into a series (stack) of TIFF images using VideoMach software (version 5.8.7, www.Gromada.com) running under Microsoft Windows 7 Professional on a desktop imaging workstation. The TIFF stacks of each ovary were imported into Fiji software (ImageJ 1.49a, National Institutes of Health, Bethesda, MD, USA) and the length of the scale bar built into the ultrasound machine was used to set the scale in Fiji from pixels to mm (*straight-line section tool*, *Analyze menu >>Set Scale…*). The imported images were cropped in the X- and Y-axes (*Rectangle selection tool >>Image menu>>Crop*) to remove animal identification and the files were renamed to anonymize data sets for further analyses.

27

**3.3.3.1 Image processing in two-dimensional data analysis**

Images for two-dimensional colour flow analysis were selected based on apparent maximum amount of blood flow to follicle perimeter or luteal region [142]. Three TIFF images were selected for each follicle or CL and processed in Fiji software. Since the theca externa cannot be clearly defined by conventional ultrasonography, the area of the follicular wall was calculated by first selecting the outermost margin of the follicular antrum using the manual selection tool (*Freehand selection tool*), then enlarging the selected area (*Edit menu>>Selection >>Enlarge*) by 1.5 mm (limit of ultrasonographic resolution; [166]) to include adjacent tissue with blood supply. The area between these two selections is defined as the 'follicular wall region' (Fig. 3.1). Similarly, the area of luteal tissue was determined by drawing a border representing the outer margin of the CL in two-dimensions and increasing this border by 1.5 mm to include adjacent tissue with blood supply (defined as "enlarged luteal region"). After removing the region outside (*Edit menu>>Clear Outside*) the area of interest (making the region solid white), the colour threshold feature (*Image menu>>Adjust>>Color Threshold…*) available within Fiji (Saturation: 65; Brightness: 110) was used to select and determine the area (*Analyze menu>>Measure*) of vascular flow in the follicular wall region of preovulatory follicles and in CL. The vascularity index of the follicular wall region was calculated as the ratio of the area of vascular flow (coloured area) to the total area of the region. Similarly, the vascularity index of the enlarged luteal region was calculated as the ratio of the coloured area to the total area of the region. The vascularity index was the average of three selected images for each follicle and CL.

A

B — Follicle Area = 131 mm$^2$

C — Enlarged Follicle Area = 205 mm$^2$

D — Follicular Wall Area = 74 mm$^2$

E — Vascular Area = 1.57 mm$^2$
2D Vascularity Index = 0.021
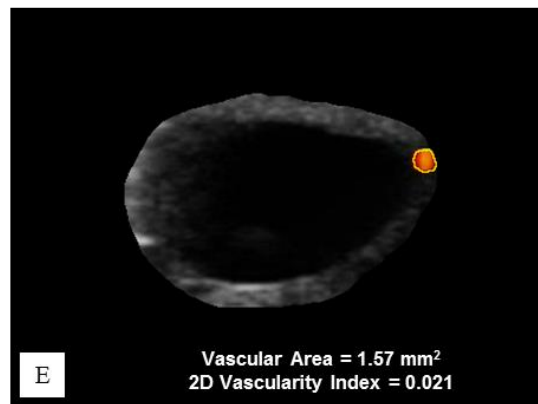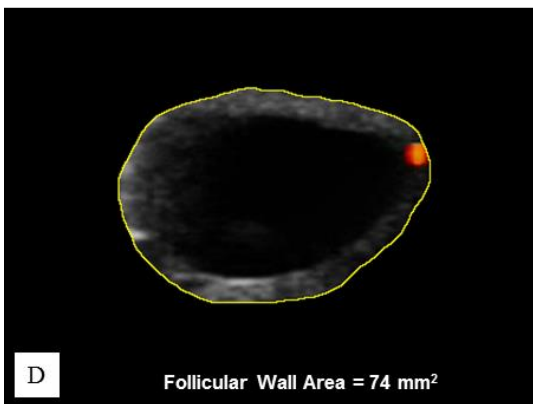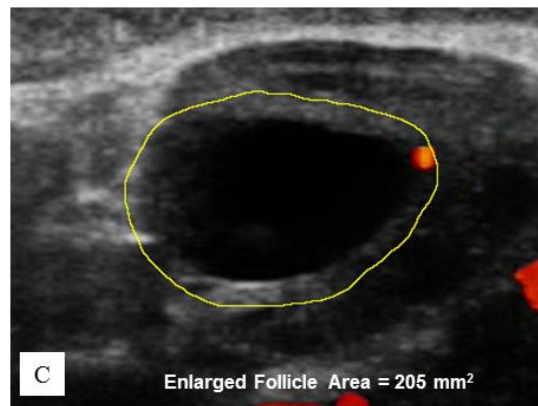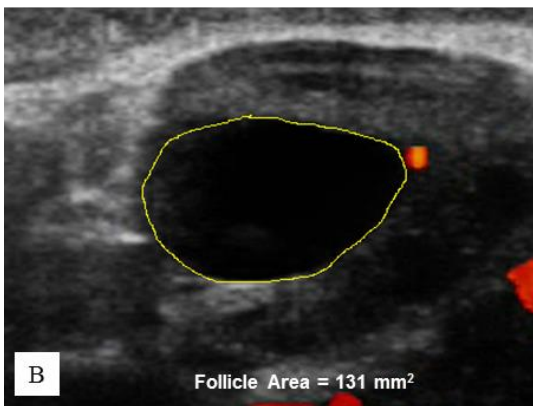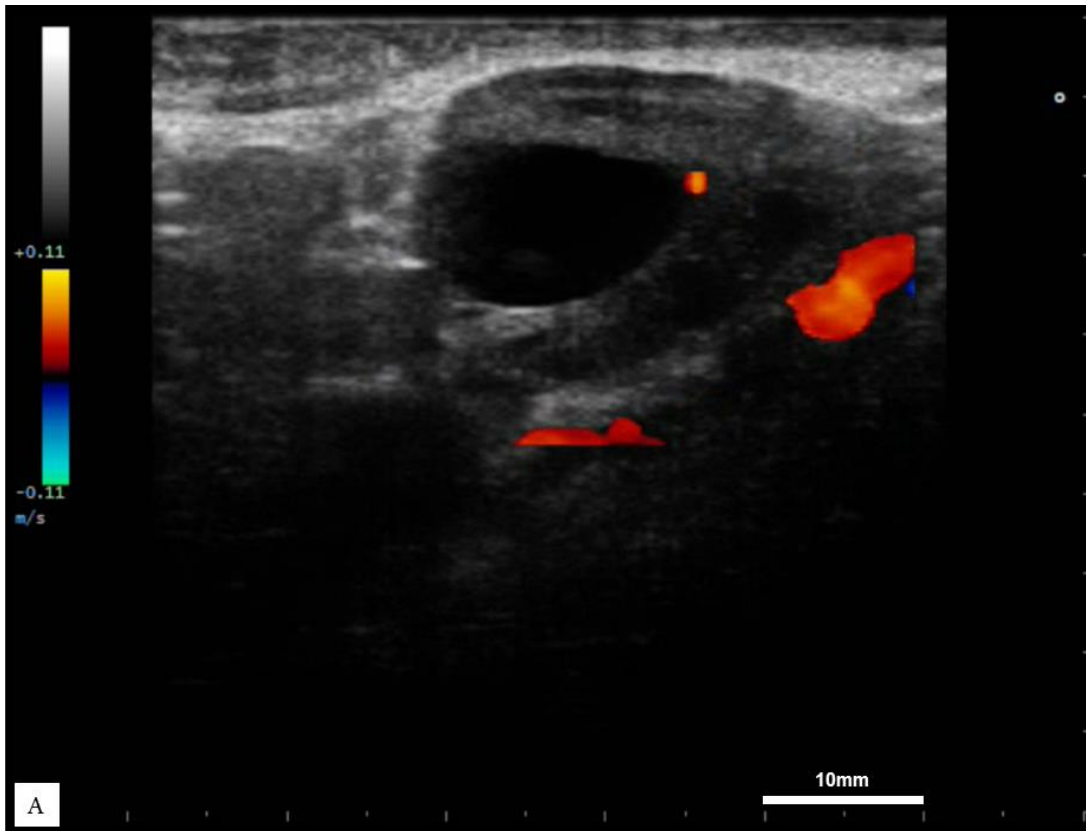
Figure 3.1: Two-dimensional image analysis in Fiji software (ImageJ). A) Original unprocessed image exported from the ultrasound machine. B) Manual selection of follicle area using free-hand selection tool. C) Enlargement of area in B by 1.5 mm. The difference between area in B and A = follicular wall area. D) Clearing region outside the area of interest. E) Selection and area measurement of blood flow by colour thresholding (using Saturation: 65; Brightness: 110) in the follicular wall region. Follicular wall vascular area : follicular wall area ratio was defined as two-dimensional Vascularity Index.

### 3.3.3.2 Image processing for three-dimensional data analysis

The TIFF images for three-dimensional analyses (92 to 494 images for follicles and 161 to 517 images for CL) were imported into Fiji then split into three colour (RGB) channels (*Image menu >> Type >> RGB Stack* followed by *Image menu>>Color>>Split Channels*) and saved as 8-bit TIFF files. The coloured regions were selected in Fiji using the colour thresholds used previously for two-dimensional analysis (saturation: 65, brightness: 110). Each stack of TIFF images was converted to a white on black image (white representing all coloured regions, black representing everything outside coloured regions *Threshold color>>B&W*) using Fiji options in *thresholding* (*Image menu>>Adjust>>Threshold*). The file was then converted to 8-bit (*Image menu>>Type>>8-bit*) and a *binary mask* (*Image menu>> Adjust >> Threshold >> Apply >> Black background (binary mask)*) was used, where white represented all coloured regions in a cineloop and black was the volume outside the coloured regions. The white on black images were saved as a separate TIFF stack and subsequently imported into Imaris software (version 8.1.2, Bitplane, Santa Barbara, California, USA). The frames were adjusted to measure in mm and the *geometry* was changed by accessing the display properties in the Imaris software so that voxel size matched the Fiji measurements (X=0.106 mm, Y=0.106 mm, Z=0.106 mm).

The dominant follicle within the ovary was used to calibrate the Z-axis dimension assuming the average of X- and Y-axes diameter was equal to the Z-axis diameter. The Imaris measurement tool was used to measure the initial Z-axis diameter with the frame rotated by 90° and the depth of points adjusted to be in the plane of the two-dimensional image. Using cross multiplication calculation, the Z-axis was adjusted in the geometry settings. (see Appendix A)

To determine the volume of the follicular wall region, the volume of the follicular antrum was built by using the *surface* feature in Imaris (Fig. 3.2). The volume was then increased by 1.5 mm using the *distance transformation* feature in Imaris. The volume of the follicular wall region

was then obtained by subtracting the volume of the antrum from new enlarged volume. To identify the vascular volume within the follicular wall volume, the enlarged volume was used to exclude (*mask*) all vascular regions outside the enlarged follicle region. Next, a new *surface* was built on the remaining white on black vascular channel. The volumes determined by these *surfaces* were exported into a spreadsheet (Excel, Microsoft Corporation, Redmond, WA, USA) for further analysis. The three-dimensional vascularity index of the follicle was calculated in Excel (Microsoft Corporation, Redmond, WA, USA) as the ratio of the vascular volume to the follicular wall volume. Similarly, to obtain luteal vascularity indices, the border of the CL was outlined by free-hand selection and called luteal volume. The *surface* feature in the luteal volume was used to exclude (*mask*) the volume outside of the CL to exclude these vascular regions and termed luteal vascularity. The luteal volume was enlarged by 1.5 mm to include vessels entering the CL by using the *distance transformation* feature and was termed enlarged luteal volume and similarly, the *mask* feature was used to exclude the vascular regions outside the enlarged luteal region and termed enlarged luteal vascularity. The difference between enlarged and luteal was subsequently termed peripheral luteal region and peripheral vascularity. After calibration of the Z-axis, as described above, to validate our new three-dimensional method of determining vascular volume, the measurements of follicular and luteal volumes were compared with theoretical volumes of an ellipsoid: $Volume = \pi \frac{4}{3} \times \left( r_x \times r_y \times \left( \frac{r_x + r_y}{2} \right) \right)$ where $r_x$=1/2 of diameter (mm) in the X-axis and $r_y$=1/2 of diameter (mm) in the Y-axis.

A

**B**     Follicle Volume = 1045 mm³

**C**     Enlarged Follicle Volume = 2049 mm³
       Follicular Wall Volume = 1004 mm³

**D**     Follicular Wall Vascular Volume = 55.5 mm³

**E**     3D Vascularity Index = 0.055

32
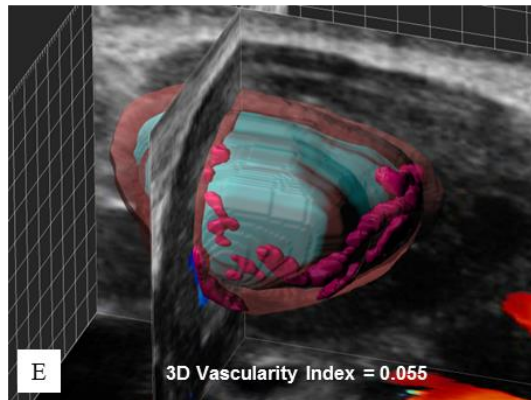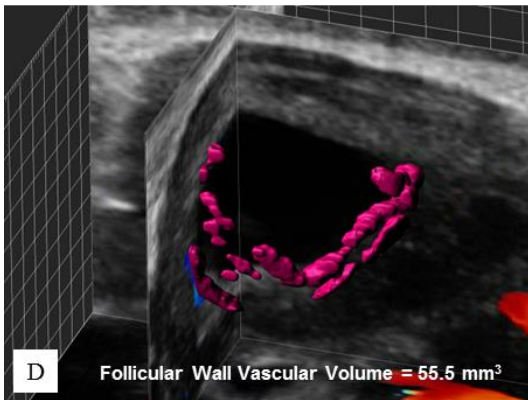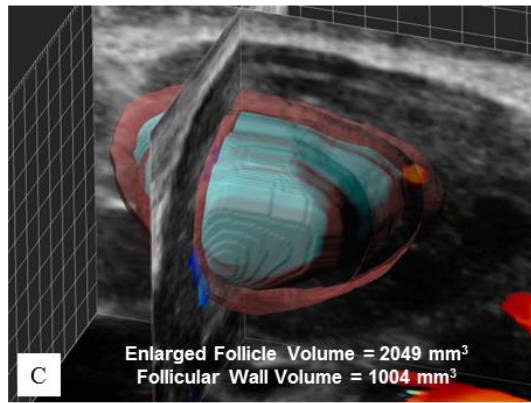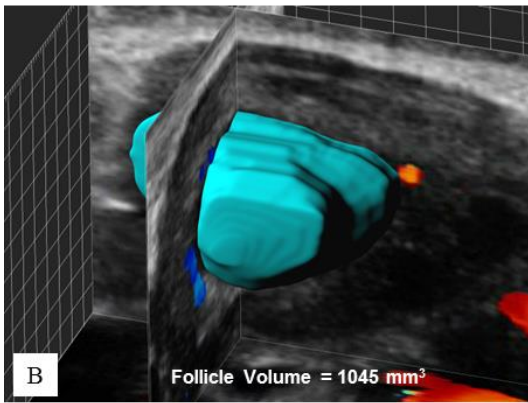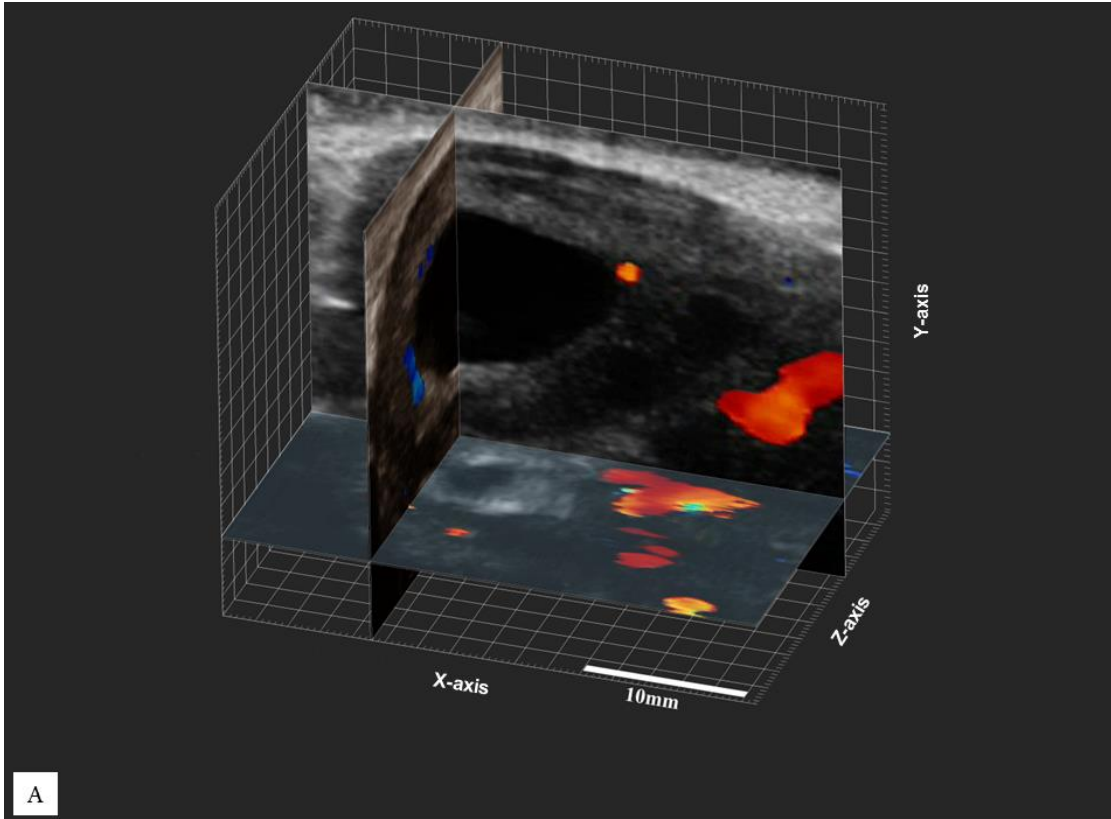
Figure 3.2: Three-dimensional image analysis using Imaris software. A) Importation of TIFF image series into X, Y, Z-axes. B) Surface built for follicle volume. C) Enlargement of surface by 1.5 mm. D) Surface built for blood flow regions by selection of colour. E) Three surfaces used to calculate volumetric vascularity index. Follicular wall vascular volume : follicular wall volume ratio was defined as three-dimensional Vascularity Index.

### 3.3.4 Statistics

Statistical analyses were performed using SPSS (version 24, IBM, Armonk, New York, USA). Numerical data are reported as mean ± SEM. Probability values <0.05 were considered significant. Data were tested for normality using a Shapiro-Wilk test. Measured volumes were compared with theoretical volumes using Pearson's correlation, linear regression, and Kruskal Wallis with Mann-Whitney U and Bonferroni adjustment post hoc. Levene's test was used to test for equal variance, unless the normality assumption was violated, then the variability between groups was assessed by Wilcoxon signed-rank test on the absolute value of the residuals (variability index) for follicular vascularity index. Follicle data were combined over time points (pre-GnRH and post-GnRH when present) for variability index only. The luteal vascularity index measured in three-dimensions at four days after ovulation was compared with the peripheral luteal vascularity in three-dimensions by paired t-test. Vascularity index for preovulatory follicles were compared pre-GnRH and post-GnRH using paired t-test. CL at four days following ovulation were compared using paired t-test on enlarged vascularity index (two-dimensional versus three-dimensional). For comparison between synchronized versus non-synchronized buffaloes, analysis was done using Mann-Whitney U test, where normality assumption was violated. Logistic regression was used to assess the odds of pregnancy given vascularity index of the follicles and/or CL.

### 3.4 Results

All postpartum buffalo cows that were less than 100 days postpartum had a CL at the start of the study and were therefore considered to have returned to reproductive cyclicity. One buffalo ovulated before the final GnRH treatment, but did not appear to form a CL and was therefore excluded from the analyses (n=21). Five animals ovulated before insemination, thus

they were not included in analyses of pre- vs post-GnRH. Buffalo that had a follicle at pre-GnRH (n=20) and post-GnRH (n=16) were used to test variability of vascularity indices.

### 3.4.1 Verification of volumetric analysis

The measurements for follicular volumes using Imaris were positively and strongly correlated with the theoretical volumes of an ellipse (r=0.96, P<0.01, Fig. 3.3A). Additionally, the ratio of the theoretical volume over the measured volume averaged 1.03 ± 0.03 (range 0.68-1.42) and the difference in the mean volumes did not differ (P=0.13, data not shown). Similarly, the calculated follicular wall volume measured in Imaris was positively and strongly correlated with the theoretical wall volume (r=0.95, P<0.01, Fig. 3.3B). As such, the ratio of the theoretical wall volume over the measured follicular wall volume averaged 1.06 ± 0.02 (range 0.81-1.33). A measure of follicle diameter was strongly predictive of follicle volume (adjusted $R^2$=0.86, P<0.01, Fig. 3.3C). When the volume of the CL measured in Imaris was compared with a theoretical calculated volume of an ellipsoid, the positive correlation was moderate (r=0.58, P=0.02, Fig. 3.3D), and the ratio of theoretical to measured CL volume averaged 1.03 ± 0.13 (range 0.38-2.46). The ratio of theoretical to measured peripheral CL volumes averaged 0.96 ± 0.08 (range 0.53-1.75) and were moderately correlated (r=0.58, P=0.02, Fig. 3.3E). The CL diameter measured using the calipers on the ultrasound machine was a weak predictor of the measured volume (adjusted $R^2$=0.26, P=0.02, Fig. 3.3F).
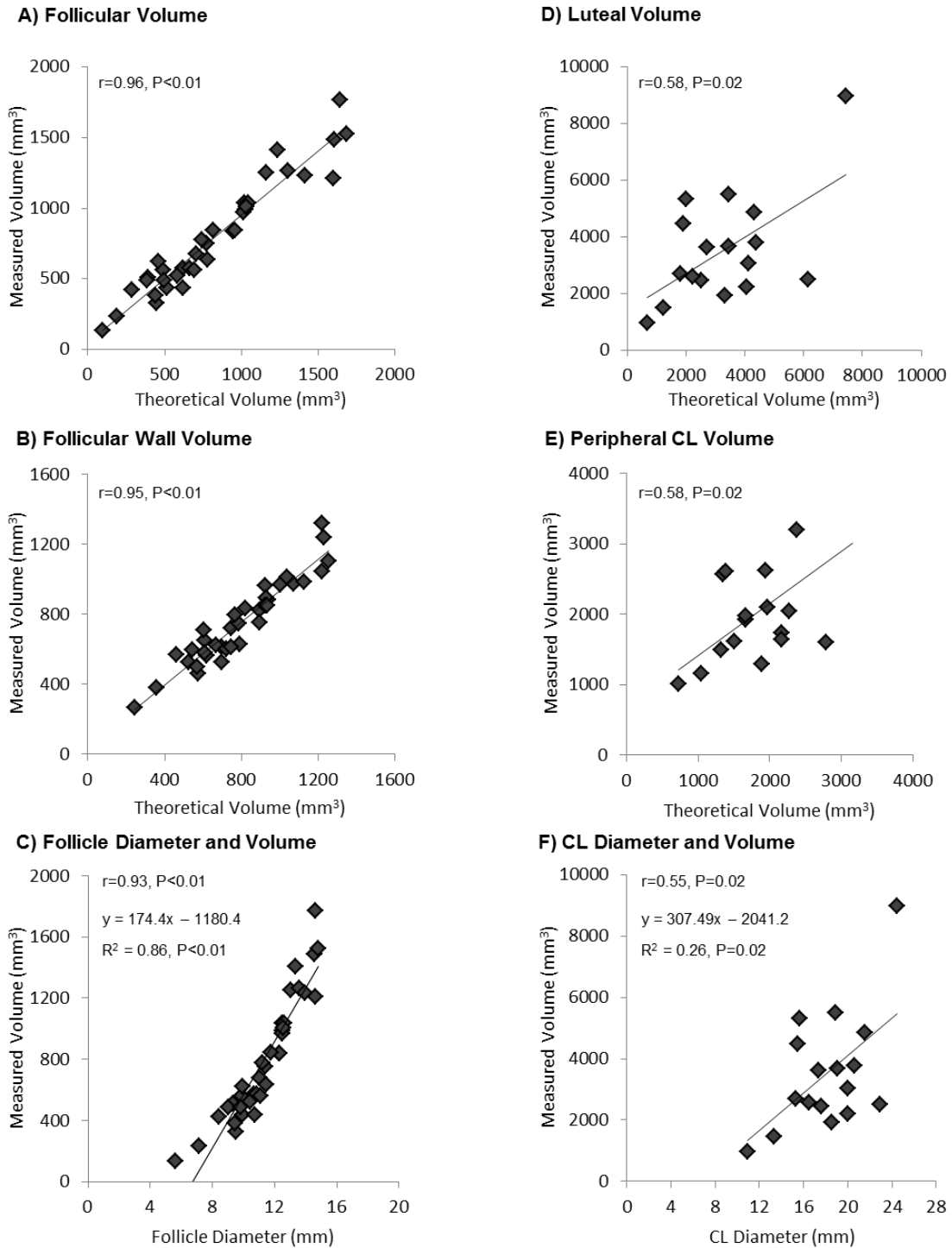
Figure 3.3: Relationships between theoretical volume (calculated ellipsoid volume based on measured vertical and horizontal diameters), measured volume by three-dimensional analysis in Imaris software, and diameter for ovarian structures. Follicle data is combined over time (n=20 pre-GnRH and n=16 post-GnRH); CL data (n=17) were recorded four days after ovulation. A) Follicular volume. B) Follicular wall volume. C) Follicle diameter and volume. D) Luteal volume.

E) Peripheral CL volume. F) CL diameter and volume. P = P-value of the test, r = Pearson's correlation coefficient, $R^2$ = adjusted linear regression coefficient.

## 3.4.2 Effect of slice thickness assumption on three-dimensional measurements

Doppler ultrasound cineloops were recorded using free-hand movement necessitating standardization of slice thickness (Z-axis) based on follicle diameter in X and Y dimensions. To select an endpoint for further analysis that remains unaffected by slice thickness, the voxel size along the Z-axis was assigned three arbitrary values in Imaris software (standardized based on follicle diameter, equal to X and Y dimension, i.e. isotropic voxel size, and 1 mm) to mimic the variation in the operator's speed of scanning. The effects of these changes on CL volume, CL vascular volume and CL vascularity index (CL vascular volume : CL volume ratio) were evaluated. There was no difference between vascularity indices for the CL when the Z-dimension was manipulated, either by using standardization to a follicle, isotropic or 1 mm value (Fig. 3.4). However, increasing the size of the voxel along the Z-axis increased the absolute volume of the structure and the vascular volume (P<0.01). Given that there was no difference in the vascularity index despite changes in the Z-dimension, all other analyses were performed using the vascularity indices for follicles and corpora lutea.
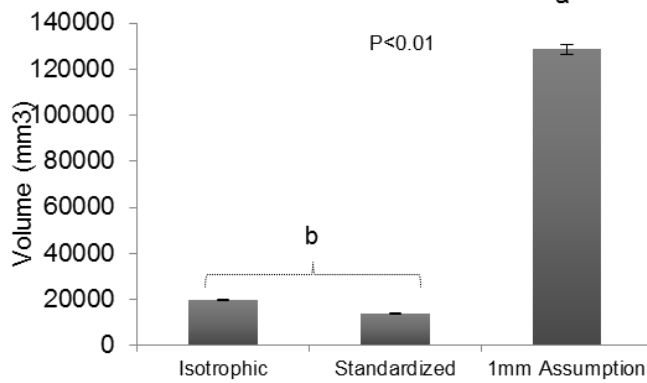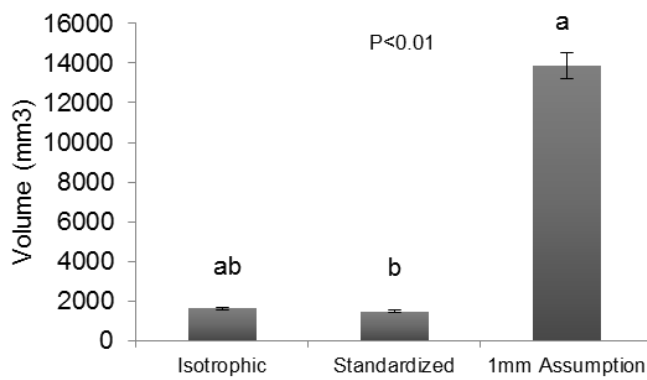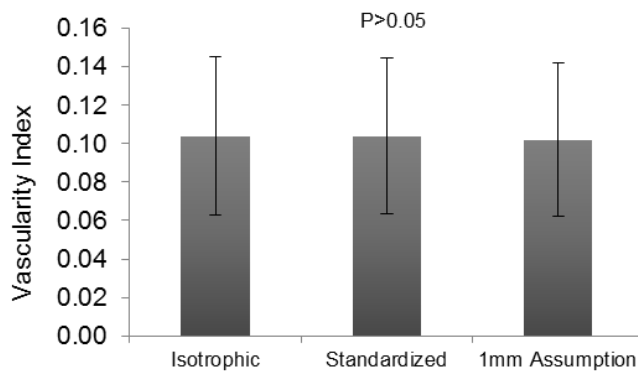
Figure 3.4: Effect of voxel size assumption in Z-direction on (A) measured volume of CL, (B) measured blood flow volume of CL, and on (C) vascularity index of CL (blood flow volume : CL volume ratio). Voxel size was based on scale bar measurement from ultrasound images in X and Y dimensions while Z-dimension was assumed to be the mean of X and Y (Isotrophic: left bars), standardized in Imaris software based on diameter of follicles (middle bars), or arbitrary assumed

37

to be 1 mm (right bars). Measured values for CL volume and blood flow volume were assumption dependent (i.e. differed between groups) while vascularity index was independent of voxel size in Z-direction. Kruskal Wallis test with Mann-Whitney and Bonferroni adjustment Post Hoc. Values with different letters (a,b) differed P<0.01

Three-dimensional analysis of CL four days after ovulation showed that luteal vascularity index did not differ from peripheral vascularity index (P=0.27, Fig. 3.5), therefore all luteal vascularity index analyses were subsequently performed on the enlarged vascularity for the CL.
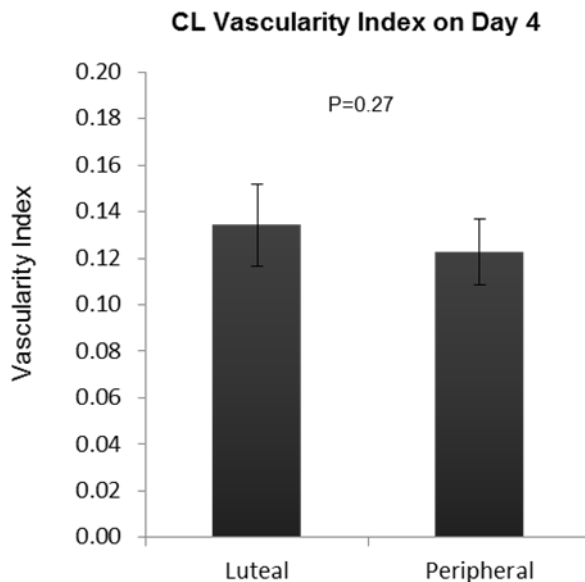


Figure 3.5: Vascularity index for corpus luteum four days after ovulation comparing luteal versus peripheral vascularity using three-dimensional method. Paired t-test, P=0.27

## 3.4.3 Comparison of vascularity indices by two-dimensional versus three-dimensional analysis method

Vascularity index was greater for two-dimensional method compared with three-dimensional method for pre-GnRH and post-GnRH follicles, as well as corpora lutea four days after ovulation (P<0.01, Fig. 3.6A). Method variability was assessed by using residuals (Fig. 3.6B) and the absolute value of the residuals (variability index; Fig. 3.6C). The residuals (value for a given follicle minus the group mean) for follicular vascularity index were not normally distributed (Shapiro-Wilk P<0.01, Fig. 3.6B), therefore, comparison of homogeneity of variance

38

by Levene's test may not be robust. The follicular variability index (pre- and post-GnRH follicles combined) was larger for the two-dimensional method (0.030 ± 0.005) than the three-dimensional method (0.018 ± 0.002; P=0.01 by Wilcoxon rank test and P=0.05 by paired t-test). The residuals for vascularity index of CL four days after ovulation were normally distributed (P>0.10, Fig. 3.6B) and the Levene's test of homogeneity of variance (Fig. 3.6B; P=0.21) and variability index (Fig. 3.6C; Paired t-test P=0.23) did not differ between two-dimensional and three-dimensional image analyses.

For the buffaloes (n=16) that had a follicle present both on the day of GnRH (pre-GnRH) and the day of insemination (post-GnRH), the two-dimensional analysis demonstrated a larger change in vascularity index than the three-dimensional analysis (P<0.05, data not shown).
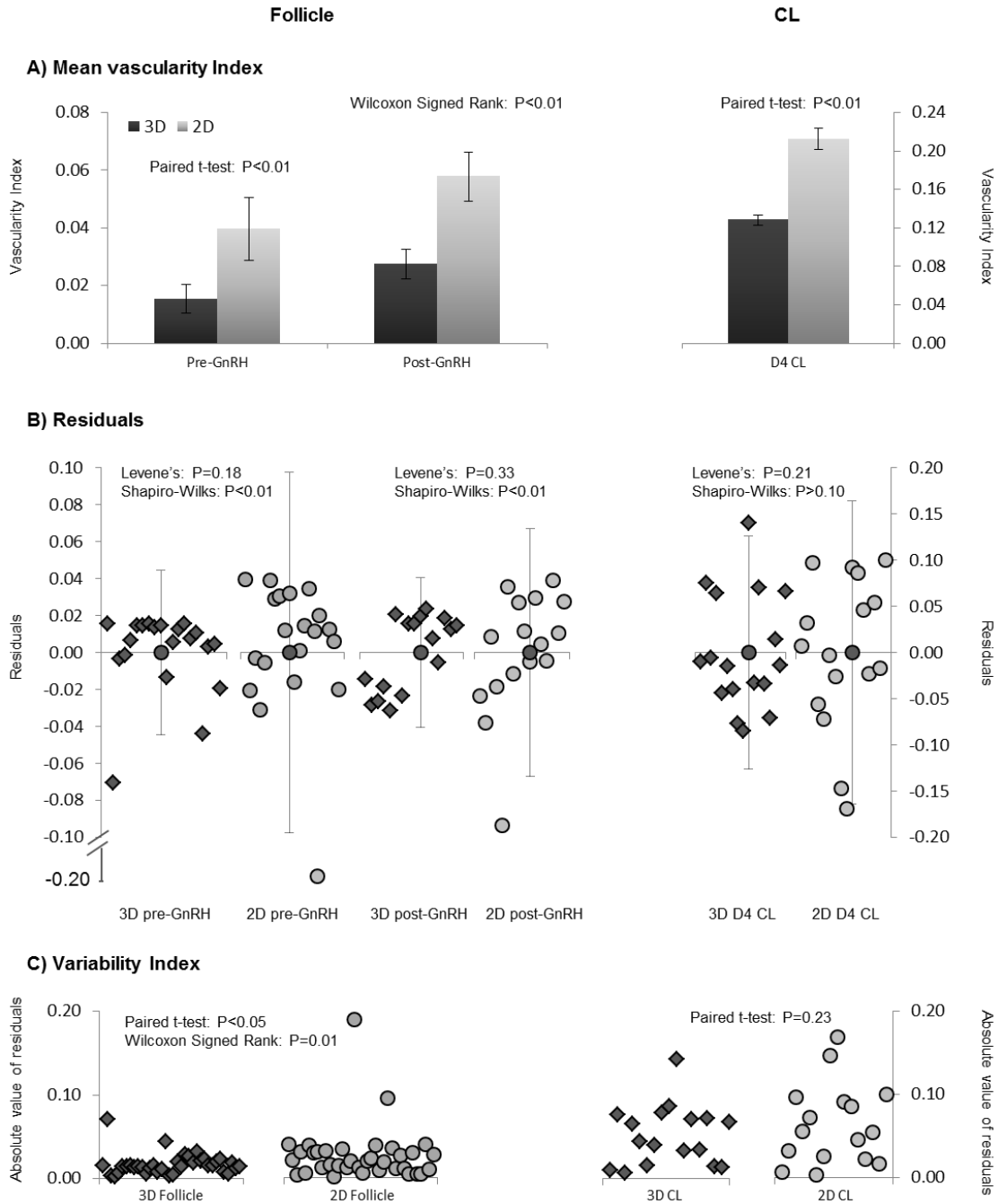
Figure 3.6: Comparison of three-dimensional and two-dimensional method variability in vascularity index values of preovulatory follicles 12 h before (pre-GnRH; n=20) or after (post-GnRH; n=16) GnRH treatgnrhment, and the corpus luteum four days after ovulation (n=17). A) Vascularity index values (mean ± SEM) for pre-GnRH and post-GnRH follicles, and the CL are smaller for three-dimensional versus two-dimensional (2D) method. B) Distribution of residuals (follicle value minus group mean) for vascularity index (three-dimensional (3D) = diamonds, two-dimensional (2D) = circles) around the group mean ± 95% confidence interval (vertical lines) to

40

illustrate smaller technique variance for three-dimensional (3D) method. C) Compared to two-dimensional method, three-dimensional method had lower variability index (absolute values of residuals) for follicles (pre- and post-GnRH values combined; n=36) but not for CL.

### 3.4.4 Relationship between follicle diameter, follicular vascularity and ovulatory capacity

Data from 16 buffaloes were available for analysis of follicular blood flow. Two-dimensional analysis showed an increase of $0.030 \pm 0.008$ (P<0.01) in follicular vascularity index, while three-dimensional analysis showed an increase of $0.016 \pm 0.006$ (P<0.02).

Thirteen buffaloes ovulated within 40 h of GnRH treatment (synchronous ovulation group) and three did not ovulate by 84 h after GnRH treatment (non-responding group). Two-dimensional image analysis was unsuccessful at detecting a difference between ovulating and non-responding animals ($0.035 \pm 0.009$ vs $0.008 \pm 0.018$; Mann-Whitney U, P=0.20, Fig. 3.7A). Conversely, when data were compared using three-dimensional image analysis, synchronous ovulating animals showed an increase in vascularity index ($0.023 \pm 0.005$) that tended to differ (P=0.06) from those of non-responding animals ($-0.02 \pm 0.01$) (Fig. 3.7B).

**Change in vascularity index of dominant follicle between pre-GnRH and post-GnRH**
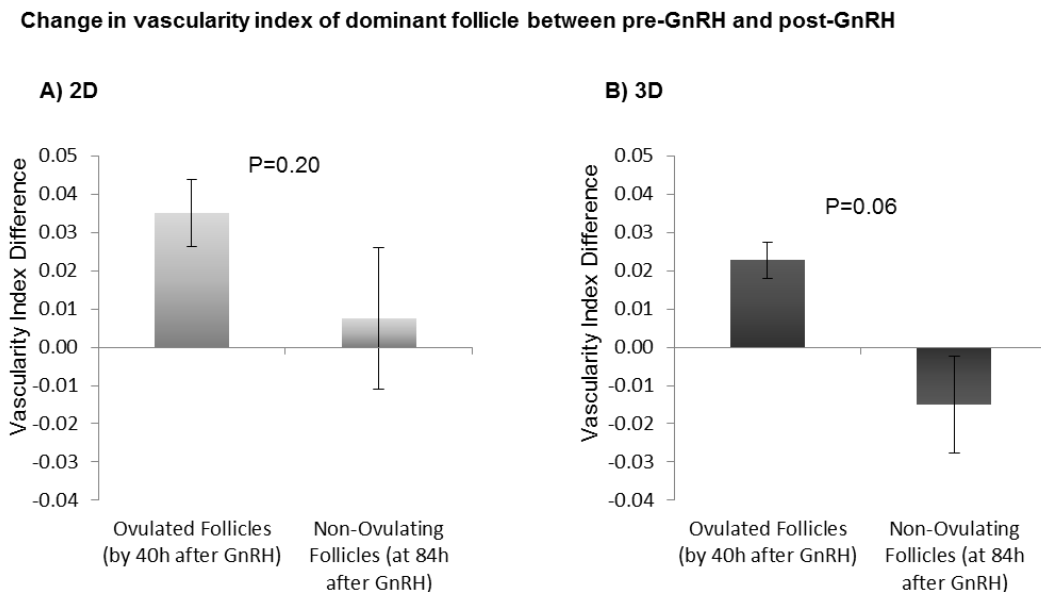


Figure 3.7: The change in vascularity index (24 h post-GnRH value minus pre-GnRH value for each follicle; mean ± SEM) of dominant follicles due to GnRH treatment of buffaloes that ovulated after GnRH treatment (n=13) by 40 h after GnRH treatment of failed to respond (n=3) by 84h after GnRH. A) Two-dimensional (2D) method showing no difference between groups

41

(Mann-Whitney U test, P=0.20). C) Three-dimensional (3D) method detected a trend towards a greater change in ovulated follicles versus those that failed to ovulate (Mann-Whitney U test, P=0.06).

The diameter of the preovulatory follicle 12 h after GnRH in synchronous ovulating animals did not differ from that of non-responding animals (12.3 ± 0.5 mm vs 10.2 ± 1.7 mm, P=0.14). The diameter of the preovulatory follicle at pre-GnRH (12 h prior) treatment was not related to vascularity (r=-0.06, P=0.80), while diameter was moderately and positively correlated with vascularity post-GnRH (r=0.59, P=0.02, Fig. 3.8).



**Vascularity Index and Diameter of Dominant Follicle**
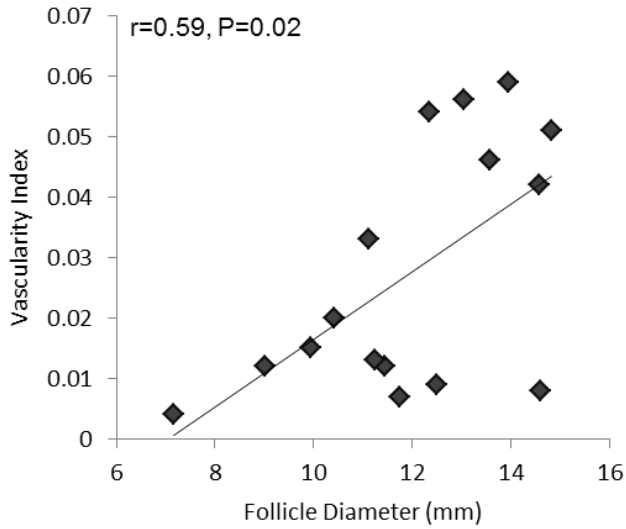
Figure 3.8: The relationship between post-GnRH follicle diameter and three-dimensional vascularity index demonstrating a moderate positive correlation. r = Pearson's correlation coefficient.

### 3.4.5 Follicular vascularity and vascularity of the corpus luteum

There was no correlation detected between the three-dimensional vascularity index of the preovulatory follicle and the vascularity index for the CL four days after ovulation (n=16, r=0.38, P=0.20).

### 3.4.6 Relationship between follicular and corpus luteum vascularity and pregnancy success

The pregnancy rate was 52% (n=11/21), and was not influenced by parity (P=0.90), body weight (P=0.93), days in milk (P=0.96), or the diameter of the ovulatory follicle (pregnant $12.3 \pm 0.7$ mm versus non-pregnant $11.7 \pm 0.8$ mm; P=0.53). Neither the change in follicular vascularity index from pre- to post-GnRH treatment nor the CL vascularity index four days after ovulation were predictive of pregnancy (P=0.45) using either the two-dimensional or three-dimensional method.

### 3.5 Discussion

This study reports a novel method for volumetric assessment of ovarian structures and their vascularity from Doppler ultrasound video segments recorded by free-hand movement of the transducer without a priori selection of images and was validated by comparing the measured volume of structures with theoretical volumes. One of the significant findings in the current study was that the new method developed for three-dimensional image analysis had lower technique variability than the conventional method and therefore was able to discriminate between ovulating follicles (increase in the vascularity index as the dominant follicle approached ovulation) and those that failed to respond (a decrease in vascularity index after GnRH treatment). This difference in blood flow was not detected by the commonly used two-dimensional method based on selection of the Doppler images with the most vascular cross-sectional area. To our knowledge this is the first study using a three-dimensional reconstruction of water buffalo ovarian structures to compare vasculature at critical stages of ovulatory follicle and CL development.

Colour Doppler ultrasound data was acquired with free-hand scanning of buffalo ovaries in-situ. As the scanning speed varied among animals, we calibrated the voxel size in the Z-axis (i.e. slice thickness of volumetric datasets) based on the assumption that follicles are ellipsoid structures (i.e., assumed the follicle diameter along the z coordinate = average of measured diameter in X and Y directions). The measured volume of follicles was accurate when compared to the calculated theoretical volume thereby validating our method. We discovered that the measured diameter of the dominant follicle was strongly related to the computed volume of the follicle and volume of follicular wall region. However, the relationship between the diameter of

43

the early CL and its volume was not as strong. Given the assumption that ovarian structures would follow an ellipsoid shape, follicles fit this very well, while corpora lutea only moderately related to their diameters.

The variability estimates for the vascularity indices for follicles were markedly lower for the three-dimensional image analysis when compared to two-dimensional analysis. A likely explanation for this higher variation in the two-dimensional analysis is the subjective selection of the most vascular follicular wall region. It has been shown that more variation exists in the blood flow area of bovine follicles when a cross-section is taken of the same follicle at different angles [20] and similar results have been demonstrated in studies of human ovarian follicles when measured at greater than 20 hours after the LH surge [158]. Contrary to our observation on the vascular supply to follicles, the variations in the vascularity indices for the corpora lutea were similar between two- and three-dimensions. Whether this is due to our current small sample of 17 animals that produced a CL four days after ovulation, or that corpora lutea have less variable vascular networks than were demonstrated for follicles has yet to be explored.

The current study demonstrates the importance of both vascularity index and the diameter of the follicles for the assessment of the follicular environment and future ovulatory status. Comparison of the vascularity indices conducted in two- and three-dimensions showed that follicles demonstrated a greater vascularity index in two-dimensional image analysis than was found in three dimensions. A functional relationship between the vascularity of the preovulatory follicle and plasma estradiol and LH has been proposed [26, 29]. Using the three-dimensional vascularity assessment methodology we developed, we confirmed that vascular flow in the follicle wall region increased by 12 h following GnRH treatment. In buffaloes, an increased blood flow to the follicle as seen with colour Doppler ultrasonography was more related to higher amounts of estradiol and insulin like growth factor in the follicular fluid than the diameter of the follicle [31]. In cattle, serum estradiol was only weakly correlated with the size of the ovulatory follicle [167], however vascularity was positively associated with the estradiol to progesterone ratio [168]. A stronger positive association between follicle size and its vascularity at 12 h post-GnRH was observed in the current study than previously reported (r=0.59 compared with r=0.21 [31]).

In the present study, the follicles that ovulated within 40 h post-GnRH treatment were similar in size to follicles that did not respond immediately to treatment (but ovulated later than

84h; presumably due to endogenous LH surge). However, ovulated follicles had a greater difference in the blood flow measured in three-dimensions. The over-estimation of the vascularity index measured in two-dimensions masked the decrease in vascular flow that was found in follicles that did not ovulate within 40 h post-GnRH. Two-dimensional analysis has limitations when assessing the blood flow to a follicle over time as the observer would not be able to obtain the exact cross-sectional area of the follicle at serial time points in order to assess a decrease or increase in blood flow in that region thereby leading to greater technical variability. The reported three-dimensional analysis method obviates this problem as all images are used for the analysis resulting in lower variability in measurements. Based on these observations, the change in vascularity of the dominant follicle as measured in three-dimensions prior to GnRH compared with 12 h after treatment may assist in early detection of non-ovulatory follicles.

In the current study, vascularity index of the CL four days following ovulation could not be used to predict pregnancy status. There was an appreciable increase in the dominant follicle vascularity by 12 h post-GnRH treatment compared to pre-GnRH follicular vascularity values. However, it did not differ for pregnant versus non-pregnant animals. This is similar to a previous study, when the luteal vascularity was assessed in buffaloes, the resistance index at day ten and day 20 after AI was similar in pregnant and non-pregnant buffaloes [145]. Conversely, in a study in embryo transfer in cattle there was greater vascular area in the CL at the time of transfer (day seven) for animals that became pregnant compared to those that were not pregnant on day 30 [27]. Additionally, pregnant buffaloes tend to have greater velocity of blood flow to their CL alongside serum progesterone when assessed between days five and ten [32]. However, other blood flow indices and size of the CL were not related to pregnancy in buffalo measured from days five to ten [32], which corroborates with our study. Finally, we cannot exclude individual buffalo variation given the variability in our animal collection (age and days from last parturition).

### 3.6 Conclusions

In conclusion, the reported three-dimensional image analysis of colour Doppler ultrasound data is a novel objective method that does not require a-priori selection of images by an expert and had less technical variability than the conventional two-dimensional image analysis of ovarian data. Further, the described Vascularity Index parameter is independent of the voxel size

along the Z-coordinate and therefore free-hand scanning of the tissue of interest can be used without making any assumptions about the shape. By comparing a cineloop acquired on the day of GnRH treatment (pre-GnRH) and 12 h post-GnRH, three-dimensional analysis of colour flow of preovulatory follicles was able to detect differences in blood-flow characteristics of follicles that ovulated or failed to respond to GnRH treatment; in contrast, conventional two-dimensional analysis based on three operator-selected images of each preovulatory follicle was not sufficient to detect these subtle changes. The current study showed that while three-dimensional image analysis of colour Doppler ultrasound data was more labor-intensive than two-dimensional analysis, it was able to detect biologically significant ovarian events, including the failure to ovulate, that would have been missed using two-dimensional image analysis alone.

## 3.7 Acknowledgements

**CHAPTER 4: The relationship between ovarian vascularity, cumulus-oocyte morphology and luteal development in four-month-old calves after FSH stimulation**

**Relationship of this study to the thesis**

The specific objectives that are addressed in the following chapter are: to study the effect of exogenous administration of LH on vascular flow to the preovulatory follicle and its correlation with expansion of the cumulus-oocyte-complex, to study the relationship between the follicular wall vascularity of ovulatory follicles with vascularity of the CL that follows, to determine the vascular changes following exogenous LH in superstimulated ovaries of four-month-old calves, and to determine the relationship between ovarian and luteal vascularity and relative luteal tissue volume that forms following follicular aspiration with the production of progesterone.

## 4.1 Abstract

The ovaries of prepubertal calves may be superstimulated to produce oocytes for *in vitro* embryo production to decrease the generation interval. The objectives of this study were to determine the effect of LH on the vascularity of ovaries of 4-month-old calves after FSH stimulation, and the relationship between ovarian vascularity and the morphology of the cumulus-oocyte-complexes (COC). Additionally, to determine the relationships between luteal tissue volume that forms following follicular aspiration, the ovarian and luteal vascularity, and production of progesterone. We expected that ovarian vascularity, as detected by Doppler ultrasonography, would increase in response to LH, and a greater increase in vascularity would produce greater expansion of COC. Additionally, greater ovarian volume and vascularity measured from Doppler ultrasonographic cineloops using 3D image analysis were expected to predict the development of luteal tissue volume and vascularity, as well higher levels of plasma progesterone. Ovarian superstimulation was induced in 4-month-old beef calves (n=16) and 16-month-old postpubertal beef heifers (n=6) and two primiparous cows (2.5 year old) using either a traditional 4-day or an extended 7-day FSH protocol (n=8 calves and n=4 control animals per group). Power Doppler ultrasonography was performed on the day of LH treatment 12 h after the last FSH treatment, on the day of ultrasound-guided follicular aspiration for oocyte collection 24 h after LH, and 3 and 7 days after follicular aspiration to assess luteal tissue volume and vascularity. Recorded video segments were exported for analysis in Fiji and Imaris software to assess the ovarian vascularity index (ratio of blood flow volume to tissue volume) at each time point; luteal vascularity and volume indices were determined on days 3 and 7 after follicular aspiration. The ovarian vascularity index tended to increase in response to exogenous pLH in both prepubertal calves (pre-LH 1.5 ± 0.4% vs post-LH 2.6 ± 0.7%; P=0.08) and postpubertal heifers and cows (pre-LH 2.2 ± 0.6% vs post-LH 4.7 ± 0.9%; P=0.07). Calves with a greater proportion of expanded COC (>75% partially to fully expanded) had a higher ovarian vascularity index (10.7 ± 2.6% vs 4.8 ± 1.6%; P=0.06) and luteal vascularity index (15.7 ± 4.5% vs 5.7 ± 2.1%; P<0.05) 7 days after aspiration. Calves of the 7-day FSH protocol had greater progesterone production on Day 3 (12.69 ± 7.33ng/ml vs 1.17 ± 0.35ng/ml; P<0.05) and Day 5 (50.59 ± 28.02ng/ml vs 4.45 ± 1.04ng/ml; P<0.05), and luteal vascularity index at 7 days after follicle aspiration (13.7 ± 4.6% vs 7.7 ± 2.8%; P<0.05) than calves of the 4-day FSH protocol, while no difference (P>0.05) was found in control heifers. In conclusion, there was an increase in

ovarian vascularity between the time of pLH treatment and 24h after treatment for prepubertal calves and postpubertal heifers and cows, as assessed by 3D image analysis of power Doppler ultrasound data. The duration of the FSH protocol significantly affected the production of greater expansion of COCs, and the development of functional luteal tissue and luteal vascularity in calves, but not in adult heifers.

**Keywords**: colour Doppler ultrasonography, prepubertal cattle, calf reproduction, ovarian vascularity, FSH stimulation, follicle development, luteal development, cumulus-oocyte-complex, ovum pick-up

## 4.2 Introduction

Similar to adult cows, prepubertal calves demonstrate a wave-like pattern of follicular development and regression as demonstrated by daily observation using transrectal ultrasonography [107, 169]. Oocytes from these follicles can be obtained using a transvaginal ultrasound guided technique in calves as young as ten weeks of age [107], however the quality of the oocytes is variable [170] and requires further understanding of follicle function during the prepubertal period. During recruitment and selection of the dominant follicle, small follicles with perifollicular vascularity grow to a larger diameter than follicles without blood flow [58]. These changes in blood flow can be assessed by colour and power Doppler ultrasonography [1, 7]. A three-dimensional (3D) follicular wall vascularity index can be calculated by analyzing cineloops of ultrasound images to quantify the changes in blood flow in the wall of the follicles [149][Caunce et al., 2017 – Chapter 3]. In adult heifers, the vascularity of the ovulatory follicle increases by 26h after gonadotrophin releasing hormone (GnRH) treatment in pregnant but not in non-pregnant animals [70]. Likewise, histological sectioning of bovine follicles demonstrated an increase in vascularity of the theca interna in dominant follicles compared with anovulatory follicles [65]. Additionally, the expression of vascular endothelial growth factor is associated with a higher estradiol to progesterone ratio in the intrafollicular fluid, as well as having an association with thecal and granulosa cell proliferation and vascularity [168]. This increase in perifollicular vascularity is associated with the luteinizing hormone surge [25, 106]. It is

plausible to postulate that similar changes in perifollicular vascularity will also occur during the prepubertal period and may provide diagnostic predictive value for clinical applications.

Stimulation of the ovaries using treatments of follicle stimulating hormone (FSH) rescues follicles during recruitment of a wave, preventing subordinate follicle atresia and increasing the number of mature follicles for cumulus-oocyte-complex (COC) retrieval [84]. Superstimulation has been performed with success in calves [36, 156, 171, 172]. It is interesting that FSH treatment for seven days produced an increase in the number of >9mm follicles than four days of FSH in six-month-old calves [Krause et al., unpublished data], as it does in adult animals [116]. Our research group has documented that genes required for angiogenesis were not fully activated after traditional (4 day) FSH treatment in adult cows when compared with a single ovulatory follicle [91]. An additional three days of stimulation allowed follicles to reach appropriate maturation status through transcription factors associated with oocyte competence and responsiveness to luteinizing hormone (LH) [91, 92]. Further, the seven-day protocol increased the proportion of expanded COC [84, 116], proportion of mature oocytes, i.e. those at the MII stage [116, 173], and the oocytes contained greater amount of ATP [174]. Increasing the duration of superstimulation to seven days may allow time increased transcription of the appropriate genes required for ovulation [84] and development luteal tissue.

A surge in luteinizing hormone (LH) is required for development of luteal tissue, whether it is preceded by a natural ovulation or follicular aspiration by an operator [78]. The breakdown of the basement membrane between the granulosa and theca layers of the follicular wall in response to LH is important for the development of vascularization to the CL [175]. In adult cattle, luteal blood flow is a better reflection of the luteal function (i.e. plasma progesterone) than was the size of the CL [17, 142]. Additionally, changes in luteal blood flow tend to occur prior to changes in luteal size [128]. Assessment of the ovary by ultrasonography following follicular aspiration can be used as a retrospective analysis of the quality of the follicle prior to retrieval of the cumulus-oocyte-complex (COC), as measured by the estradiol concentration and the ratio of estradiol to progesterone within the follicular fluid [71]. However the CL that develops after follicle aspiration is smaller and has less progesterone secretion than that of natural ovulation [176], most likely due to removal of granulosa cells during ovum pick-up. Following superovulatory treatment by hormonal induction of ovulation, calves form corpora lutea as in adults [155, 156]. Further, progesterone production is related to the number of corpora lutea formed and begins to

rise 40 to 68 hours following the LH surge in calves [156]. Given the relationships between blood flow to the follicular wall, increased follicular diameter, and the follicular environment (estradiol to progesterone ratio in the follicular fluid), studying these relationships using the minimally invasive technique of Doppler ultrasonography may provide insight to LH responsiveness and subsequent functional luteal tissue production.

It is not known if the blood vessels in the wall of ovulatory follicles induced by prolonged (7-day) FSH treatment during the early prepubertal period will develop blood flow in the ensuing luteal tissue that is greater than those calves treated with a traditional 4-day FSH protocol. A recent study on dairy buffaloes in our laboratory found a significant difference in the three-dimensional follicular wall vascularity index by 12 h after the time of GnRH treatment in animals that ovulated compared to those that did not [Caunce et al, 2017 – Chapter 3] while the commonly used analysis method of operator-selected of two-dimensional Doppler images failed to detect those subtle changes. Additionally, single image clips are not appropriate for ovaries under superstimulation; therefore three-dimensional reconstruction of power Doppler ultrasonographic data may be more appropriate to gain additional information on the function of ovarian structures in calves under superstimulation.

The objectives of this study were: to determine the effect of exogenous LH on blood flow changes in superstimulated ovaries of four-month-old beef calves, to determine the relationship between ovarian vascularity with the morphology of the cumulus-oocyte-complexes aspirated from ovarian follicles, and to determine the relationship between the ovarian and luteal vascularity and relative luteal tissue volume that forms following aspiration and production of progesterone. Our hypotheses were that ovarian vascularity will increase between the day of LH treatment and the time of COC collection (i.e. 24 hours following LH). Calves with greater increase in vascularity index would produce greater number of expanded COCs compared with calves with minimal increase in vascularity index. Following aspiration, ovaries with greater volume of luteal structures and with greater vascularity would demonstrate higher levels of plasma progesterone compared with ovaries with lesser luteal volume and low vascularity. Given the superstimulatory protocols used during this study, it was also predicted that superstimulation of ovaries for a seven day protocol would produce more vascular ovaries at the time of collection than those under a traditional four day protocol. Additionally, a protocol with seven days of FSH would produce greater amount of luteal tissue than a four day protocol.

## 4.3 Materials and Methods

The study was conducted from July to August 2016 and the study site was located near Saskatoon, Saskatchewan, Canada at the Goodale Research Farm. Procedures were conducted in accordance with the guidelines of the Canadian Council in Animal Care and were approved by the University Animal Care Committee Animal Research Ethics Board of the University of Saskatchewan. Computer-assisted data analyses were performed at the One Reproductive Health Research Group imaging facility at the University of Saskatchewan, Saskatoon, Canada.

### 4.3.1 Treatment protocol

Prepubertal cross-bred Hereford cross-bred female calves (*Bos taurus*) were selected (n=16) based on the weight at birth, and calf replicates born within one week of each other to multiparous females. The prepubertal calves were 16 to 17 weeks of age with a mean body weight of 181 ± 5kg (ranging between 150 and 221kg) at the start of the experiment and were kept in outdoor paddocks with their mothers for the duration of the experiment. The prepubertal calves were randomly assigned to two groups: short FSH (four days; n=8) and long FSH (seven days; n=8). Two primiparous cows (2.5 year old) and six nulliparous 16-month-old postpubertal heifers were used as control animals and randomly assigned to one of two groups (adults n=4 each treatment group). The date for the start of the treatment was staggered to allow oocyte retrieval from three animals (two calves and one control) per collection day. The collection of oocytes from control animals were alternated between the collection days. The development of a three-dimensional volumetric analysis of the vascularity in prepubertal calf ovaries was opportunistic, with the knowledge that evaluation of colour Doppler flow during a natural wave in calves has not been previously evaluated. Additionally, data regarding antral follicular count at the time of wave emergence, anti-Müllerian hormone analysis, as well as *in vitro* embryo development is reported elsewhere (Krause et al., unpublished data).

On day -1 (Day 0 = day of wave emergence) (Fig. 4.1), all animals underwent transvaginal ultrasound-guided ablation of follicles >5 mm in diameter from both ovaries (as in [36, 107]). For follicular aspiration, two mL 2% lidocaine HCl with epinephrine USP (Bimeda-MTC Animal Health Inc, Cambridge, Ontario, Canada) was injected in the caudal epidural space for

relaxation of the rectum and local anesthesia. The perineal region was washed with betadine solution and the operator's hand was passed within the rectum to position the ovary towards the vaginal fornix while a transvaginal 5MHz convex-array transducer with custom-designed handle (similar to [107]) with needle guide was placed cranially within the vagina. An 18G one and a half inch vacutainer needle attached to a needle guide with silicone tubing and a six mL syringe was used for follicular aspiration. In prepubertal calves, a progestagen norgestomet ear implant (3mg; Crestar®; Intervet, Cotia, São Paulo, Brazil) was inserted subcutaneously along the ear following a local anesthetic treatment with subcutaneous lidocaine 2% with epinephrine (1mL); the entry point was sealed with tissue adhesive. In control heifers and cows, a progesterone releasing device (1.38g progesterone; CIDR®; Zoetis, Kirkland, Quebec, Canada) was placed in the vagina. Starting on Day 0.5 (i.e., 36 hours following follicular ablation), animals were given 25mg of FSH (Folltropin®-V, Vetoquinol, Lavaltrie, Quebec, Canada) by intramuscular treatment every 12 hours for 4 days (short protocol; 8 treatments) or 7 days (long protocol; 14 treatments). Control animals were given two treatments of prostaglandin analogue (500 μg cloprostenol sodium USP, Estrumate®, Merck Animal Health, Kirkland, Quebec, Canada) along with the last two FSH treatments. Progesterone releasing devices (Crestar® in calves or CIDR® in control animals) were removed at the time of the last FSH treatment. Luteinizing hormone (12.5mg pLH, Lutropin®-V, Vetoquinol, Lavaltrie, Quebec, Canada) was given intramuscularly 12 hours following the last treatment with FSH and a blood sample was obtained via jugular venipuncture for hormone analysis. Twenty-four to 26 hours following LH treatment, COC were collected by ultrasound-guided follicle aspiration.

For COC collection, similar to ablation, a caudal epidural of two to three mL (calves) or four to five mL (heifers) was used to ease collection. A short beveled 18G two inch needle was used in the needle guide attached to a vacuum system at a flow rate of approximately 25mL per minute (similar to [36]). Blood samples were collected via jugular venipuncture on the day of collection, and days three, five and seven following aspiration for progesterone analysis.
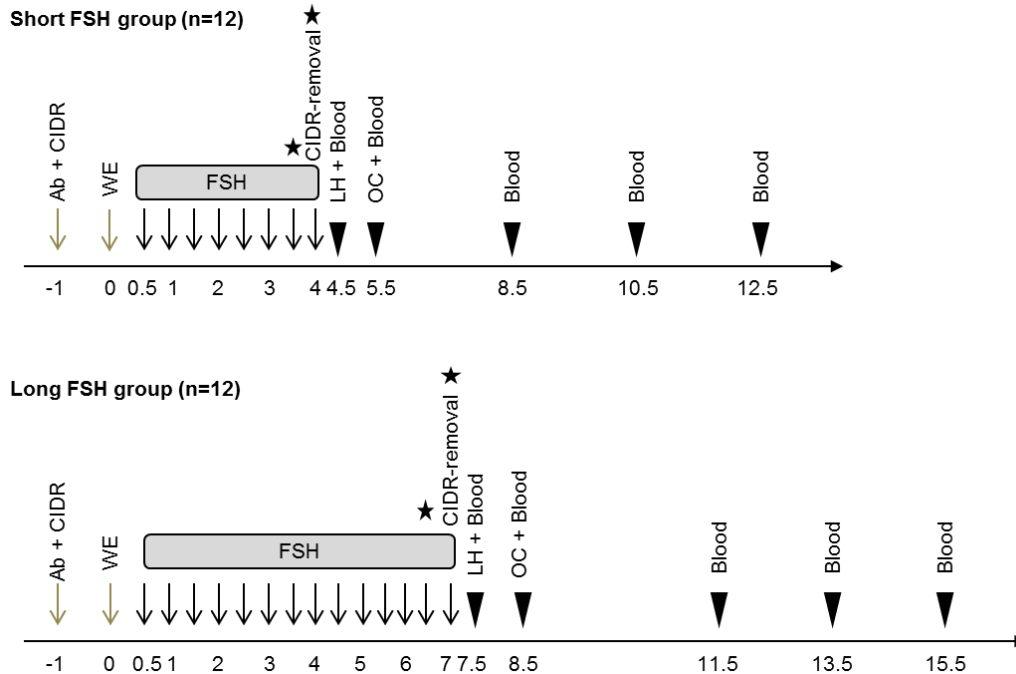
Figure 4.1: Treatment protocol: Four day (Short; calves n=8, adults n=4) follicle stimulating hormone (FSH) intramuscular treatments and seven day (Long; calves n=8, adults n=4) FSH treatment. Ab = follicular ablation; CIDR = progesterone releasing device (adults: CIDR®; calves: Crestar®); WE = wave emergence; LH = luteinizing hormone treatment; OC = oocyte collection; Blood = blood sample for progesterone; arrow heads = power Doppler ultrasonography; stars = PGF analogue in adults only

### 4.3.2 Ultrasonography of ovaries and power Doppler image acquisition

Transrectal ultrasonography of both ovaries was performed in B-mode, colour and power Doppler (MyLab Alpha, 7.5MHz linear-array transducer, Esaote, Canadian Veterinary Imaging, Georgetown, Ontario, Canada). A video clip of 15 to 30 seconds in duration (cineloop; AVI format) were recorded for each mode for the day of LH (Day 4.5 = short; Day 7.5 = long) and the day of COC collection (Day 5.5 = short; Day 8.5 = long). Colour gain 58% remained constant for all recordings. Animals were also examined and cineloops recorded on days three, five and seven following follicle aspiration to assess luteal tissue development (Fig. 4.2).
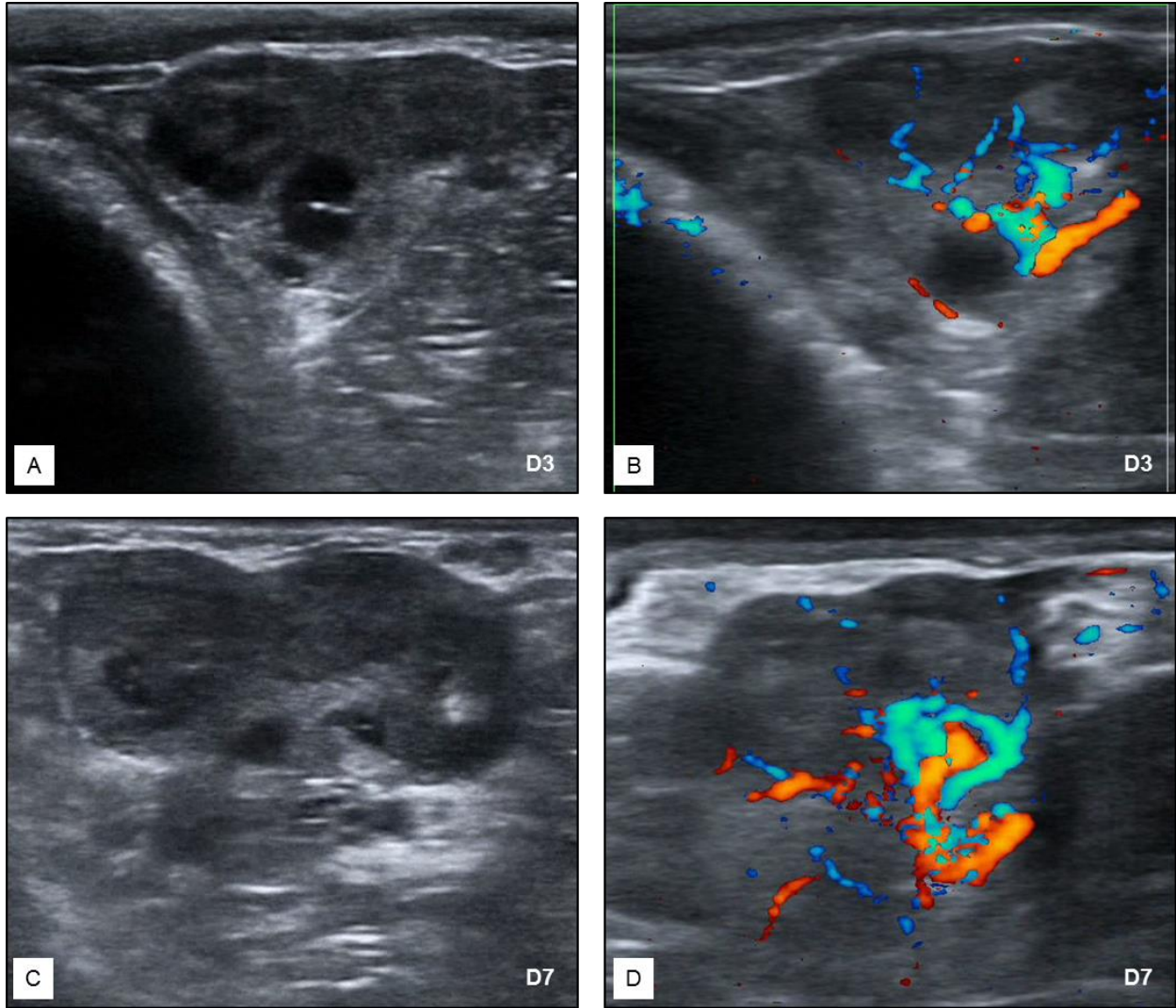
Figure 4.2: Ultrasonographic examination of a four-month-old heifer on day three following follicular aspiration in brightness mode (A) and power Doppler mode (B) and on day seven after aspiration in brightness mode (C) and power Doppler (D). Esaote MyLab Alpha, 7.5 MHz, linear-array

In the current study all image analyses were performed on the power Doppler cineloops, given the assumption that power Doppler is advantageous to colour Doppler in detection of low flow regions, as well as reducing the artefact of aliasing [7, 15, 28]. Similar to Caunce et al, 2017 (Chapter 3), cineloops were exported from the MyLab Alpha machine for analysis using proprietary software. Briefly, AVI cineloops were converted to TIFF stacks using Videomach software and randomized to avoid observer bias. TIFF stacks were then imported into Fiji (ImageJ, 1.49a, National Institutes of Health, Bethesda, MD, USA) for scale calibration and

colour thresholding. TIFF stacks for red, green, blue (RGB) and for colour selection were converted to 8-bit for use in Imaris (8.1.2, Bitplane, Santa Barbara, CA). Imaris 'surface' build function was used to segment the ovarian volume and exclude all regions outside its border by freehand drawing a border along the edge of the ovary for every tenth frame. After excluding all regions outside the ovarian 'surface', the volume was used to select ovarian vascular regions. A vascularity index was determined by the ratio of vascular volume over ovarian volume. In Caunce et al, 2017 (Chapter 3), it was determined that relative vascularity index is not affected by the voxel size along Z-axis coordinate (i.e., scanning direction). Therefore, all measures of volume in the current study were in relative percentages to allow increased efficiency of image analysis on superstimulated ovaries. Ovaries that were larger than the ultrasound transducer length (4.5 cm) were considered in a partial manner, with the assumption that follicles outside the region were of similar size to those within the view of the transducer. Additionally, vascularity indices were also assumed to be similar in the regions outside the probe's length of visualization.

Luteal tissue following aspiration was determined by operator identification and selection of areas of typical luteal echogenicity. Hyperechoic regions (suspected fibrous tissue) and anechoic regions (follicular fluid/luteal cavitations) were excluded by adjusting the intensity during 'surface' build of luteal tissue (intensity range of 10 to 60). The volume for luteal tissue was recorded. An additional 'surface' was built on the blood flow only channel after exclusion of vascular regions detected outside the luteal 'surface' build. In this regard, two vascularity indices were calculated for days following aspiration. Ovarian vascularity index was calculated as the percentage of vascular volume within the total ovarian volume. Luteal vascularity index was calculated as a percentage of vascular volume within luteal volume. Additionally, a luteal volume index was determined as the percentage of luteal volume within ovarian volume.


### 4.3.3 Oocyte collection and morphological grading

Following collection, oocytes were washed with rinsing medium (dPBS + heparin) and filtered using EmCon$^{TM}$ filter (Partnar Animal Health, Ilderton, Ontario, Canada) similar to [116]. The retentate was then rinsed into 10cm Petri dishes and COCs were located and classified using stereomicroscopy. COCs were transferred to clean holding medium (dPBS and 5% calf serum) until searching was deemed complete by two technicians. COCs were transferred from

the farm to the IVF laboratory in cryo-vials at 37 degrees Celsius within two hours of collection. COCs were graded based on the level of expansion of cumulus cells (i.e. compact, partially expanded, expanded and denuded). COC were processed further for the purposes of another study (Krause et al., unpublished data).

### 4.3.4 Progesterone assay

Jugular venipuncture was performed on the day of LH treatment, day of oocyte collection, and three, five and seven days following collection in 10mL Li-Heparin Vacutainer® collection tubes (Becton Dickinson and Co., Franklin Lakes, NJ, USA). Centrifugation (1500x g for 15 min) of the samples was performed, plasma separated into storage tubes then frozen at -20°C until analysis. Progesterone concentration (ng/mL) was assessed using radioimmunoassay (ImmuChem[TM] Progesterone ^{125}I RIA kit, ICN Pharmaceuticals, Inc. Costa Mesa, California, USA) in a single assay. The range of the standard curve was 0.15 to 80 ng/mL. The intraassay coefficients of variation were 9.45%, 7.27%, and 6.04% for low ($0.83 \pm 0.05$ ng/mL), medium ($4.30 \pm 0.09$ ng/mL) and high ($8.76 \pm 0.33$ ng/mL) standards respectively.

### 4.3.5 Statistics

Right and left ovaries were compared using a paired t-test. Animals that lost their progesterone devices during the superstimulatory treatment were compared with animals that maintained their devices using an independent t-test or Mann-Whitney U test when the normality assumption was violated. Assumption of normal distribution of data was tested using a Shapiro-Wilk test. Statistical significance of a test was set at $P<0.05$. Values are reported as the mean ± SEM values.

For the comparison across repeated measures of time modeling with the effects of treatment and age, the Proc Mixed procedure was applied (SAS Enterprise Guide version 6.1, SAS Institute Inc., Cary, NC, USA). The random effects of replicate and a lost progesterone device were incorporated in mixed modelling. Best fit models were selected based on the lowest AICC (simple for luteal vascularity, Huynh-Feldt for high and low proportions of expanded COCs, and heterogeneous compound symmetry for all other analyses). If the interaction terms differed ($P\leq0.05$), post-hoc comparisons were done using Tukey's test.

57

For the relationships between progesterone concentrations and ovarian vascularity, luteal vascularity or luteal volume indices, multiple linear regressions were applied after Pearson's correlation (SPSS version 24, IBM, Armonk, New York, USA). For all multiple linear regression models, coding was based on Age: Adult Control=0, Calf=1; Trt: Short=4, Long=7; P4Device: Lost=0, Kept=1.

## 4.4 Results

We opted to report ovarian vascularity index, luteal volume index and luteal vascularity index as these index endpoints represent the ratio of one volume to another and thereby are independent of the assumption of voxel size along the free-hand scanning direction (Caunce et al., 2017; Chapter 3). The ovarian vascularity index at the end of FSH stimulation (12 h after last FSH and immediately before pLH treatment) and 24 h after LH treatment (i.e., the day of oocyte collection) did not differ between right and left ovaries (paired t-test, P=0.41). Additionally, the ovarian vascularity (P=0.93), luteal vascularity (P=0.90) and luteal volume (P=0.21) indices on Days 3 (D3) and 7 (D7) following follicular aspiration did not differ between right and left ovaries (paired t-test). Given that there was no difference between the right and left ovaries, the average values between the two ovaries were used for all other analyses.

In one adult animal in the long protocol, the CIDR was accidently removed on Day 6, 12 h before the last treatment of FSH, therefore she ovulated prior to oocyte collection. A second adult lost her device prior to removal, but did not ovulate, therefore was included in all analyses. Additionally, prepubertal four calves from the long FSH protocol lost their norgestomet implant during the treatment. When calves of the long protocol where compared between lost device (n=4) or kept the device (n=4), the ovarian vascularity did not differ on the day of oocyte collection (P=0.31) or D3 (P=0.38) and D7 (P=0.08) following follicular aspiration (independent t-test). Given this information, the lost progesterone device for adults (n=2) and calves (n=4) was added as a random effect in the mixed modelling procedures below.

### 4.4.1 The effect of LH on changes in ovarian vascularity in calves

Overall, the ovarian vascularity increased between the day of LH treatment (recorded before LH treatment) and 24 h after LH treatment (all calf and adult groups combined; Proc Mixed P<0.01, Fig. 4.3). When data were analyzed separately, both calves and adult animals demonstrated similar tendency towards an increase in vascularity between pre-LH treatment and

24 h post-LH treatment (i.e. on the day of oocyte collection)(P=0.08, P=0.07, respectively, data not shown). There was a tendency for an effect of treatment (4-day vs 7-day FSH; P=0.09).
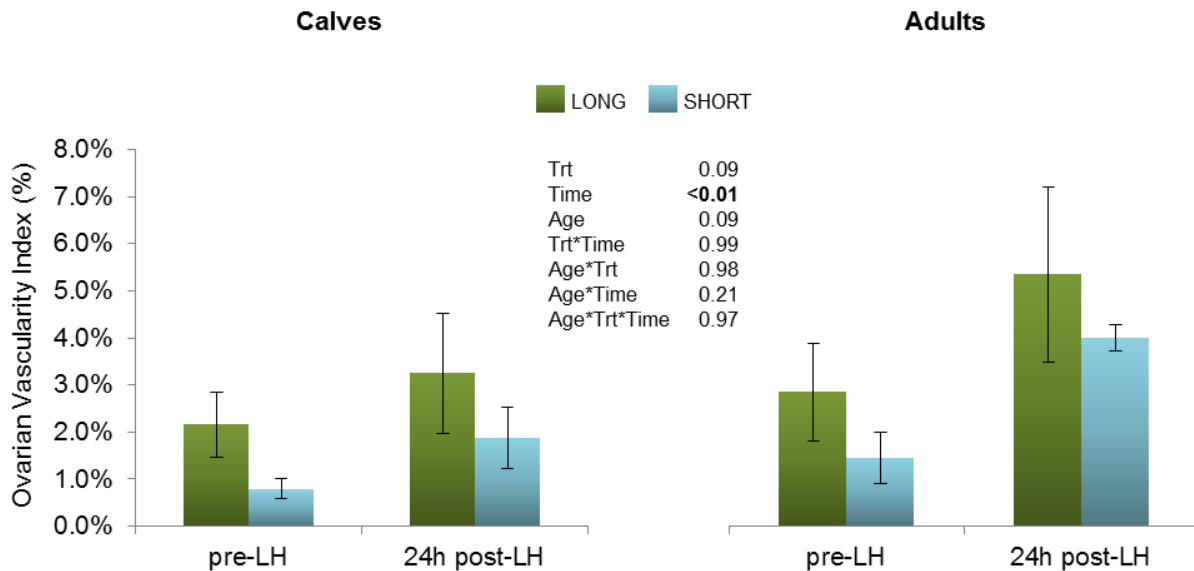


Figure 4.3: Ovarian vascularity indices (mean ± SEM) on the day of luteinizing hormone (pre-LH) treatment and 24 h after LH treatment (i.e., the day of oocyte collection) for superstimulated calves and adult animals. There was a main effect of time (pre- vs post-LH) demonstrating greater vascularity on the day of oocyte collection following LH treatment (P<0.01). Trt = Long or Short; Time = pre-LH or 24 h post-LH; Age = Calf or Adult

## 4.4.2 The development of luteal tissue in ovaries following superstimulation and follicular aspiration

The luteal volume index (luteal volume : ovarian volume ratio) was assessed on D3 and D7 following follicular aspiration. Calves in the long FSH group showed greater luteal volume index than calves of the short FSH group but adult animals did not differ between FSH protocols (Fig. 4.4A, Proc Mixed, age*treatment interaction P=0.04). Overall, luteal volume index did not differ between Day 3 and Day 7 (P=0.46; data combined between age and treatment groups); similar results were found when calves (P=0.15) and adults (P=0.71) were analyzed separately (data not shown).

**Calves**         **Adults**

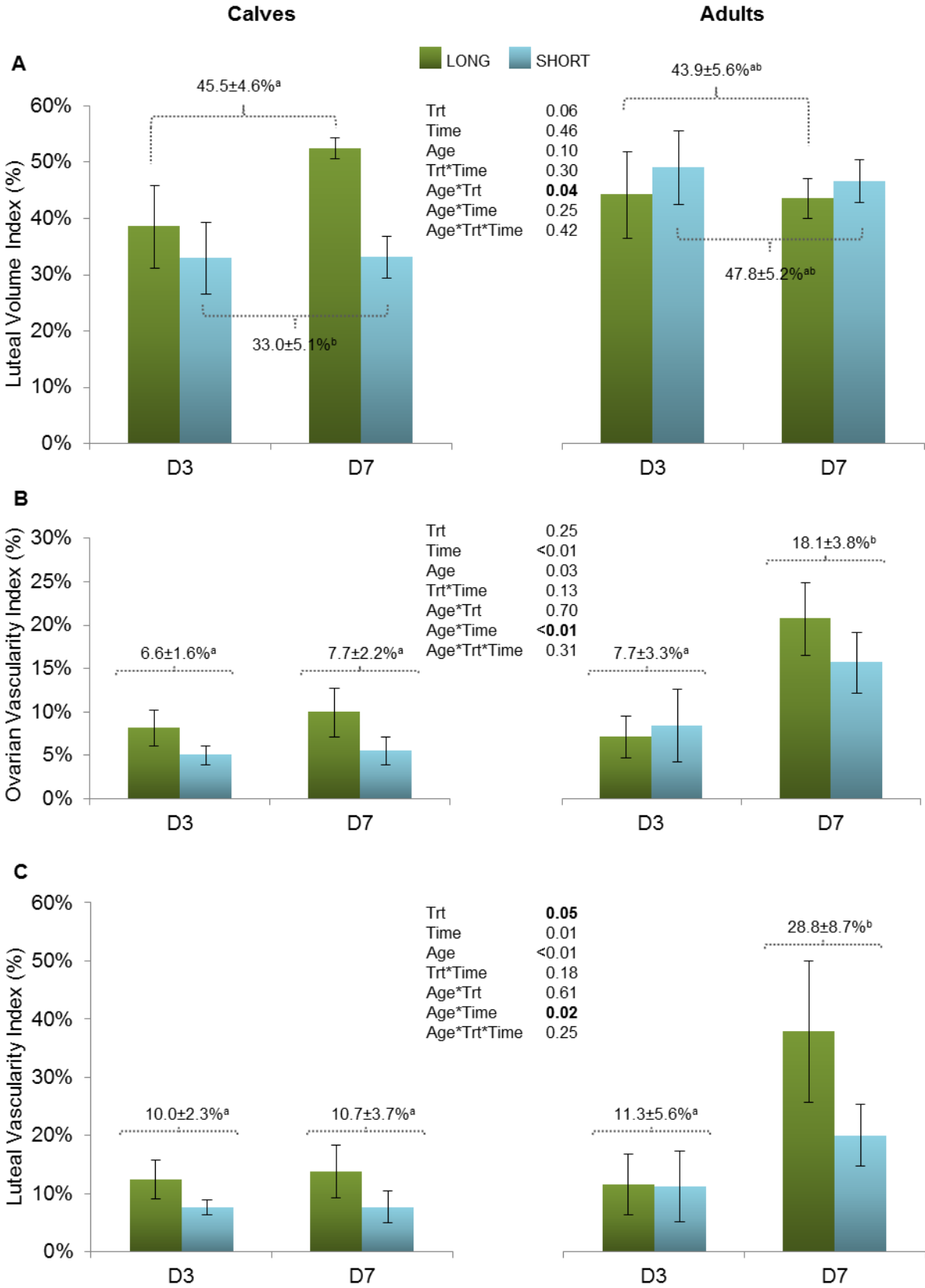Figure 4.4: Ovarian indices (mean ± SEM) on Days three (D3) and seven (D7) after follicular aspiration for superstimulated calves and adult animals. A) Luteal volume as a percentage of ovarian volume (luteal volume index): Age*Trt interaction where calves under the short protocol showed lower luteal volume index compared with calves in the long protocol. B) Ovarian vascularity as a percentage of ovarian volume (ovarian vascularity index): Age*Time interaction where adults showed greater ovarian vascularity index on Day 7 than Day 3. C) Luteal vascularity as a percentage of luteal volume (luteal vascularity index): Age*Time interaction where adults had greater luteal vascularity on day seven. Trt = Long or Short; Time = D3 or D7; Age = Calf or Adult. Values without a common letter (a-f) differed, P<0.05. Dotted line indicates the mean of the two indicated groups were compared with the mean of the other two groups.

Adult animals had a greater ovarian vascularity index (ovarian vascular volume : ovarian volume ratio) on D7 compared with D3 while calves did not differ (Fig. 4.4B, Proc Mixed age*time interaction P<0.01). There was no effect of treatment (long versus short FSH groups) on the ovarian vascularity on these days (P=0.25; data from age and treatment groups combined). When data from calves and adult animals were analyzed separately (data not shown), calves in the long FSH group demonstrated greater ovarian vascularity index compared with short FSH group (P<0.01), while adult animals did not differ (P=0.46).

The luteal vascularity index (luteal vascular volume : luteal volume ratio) showed an interaction between age and time (Fig. 4.4C, Proc Mixed, P<0.01) where adult animals showed higher luteal vascularity on D7 compared to all other groups. Overall, the long FSH groups had higher luteal vascularity than the short FSH groups (combined over age and time; P=0.05). When calves and adult animal datasets were analyzed separately, calves in the long protocol had greater luteal vascularity index than the short FSH group (P=0.01) but this effect was not seen in the adult animals (P=0.15; data not shown).

### 4.4.3 The relationship between ovarian vascularity index on 24 h post-LH with Day 3 and Day 7 after follicle aspiration

Changes in the ovarian vascularity index over time (follicles in the ovaries at pre-LH and 24 h post-LH; luteal tissue at Day 3 and Day 7 after follicle aspiration) were compared between long and short FSH groups by repeated measures (Proc Mixed) analysis (Fig. 4.5). There was a time*age interaction (P=0.01) and ovarian vascularity index of calves on Day 7 in the short FSH group was lower than those of the short and long FSH groups in adults; long FSH calf group was

61

intermediate. The ovarian vascularity index on Day 3 was similar to Day 7 for calves of both FSH protocols while ovarian vascularity index on Day 7 in adults was greater than Day 3 in the both short and long FSH protocols.
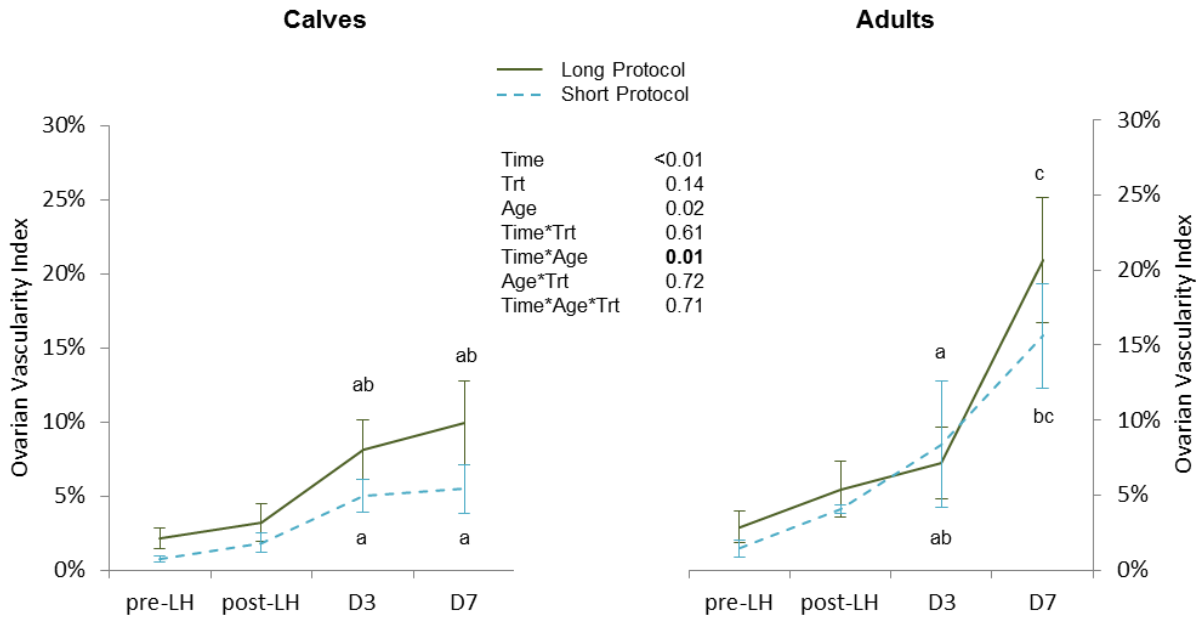


Figure 4.5: Ovarian vascularity changes over time by superstimulation protocol and age (calves and adults). Time: the day of luteinizing hormone treatment (pre-LH), 24 h after treatment (post-LH; i.e., the day of oocyte collection), and days three (D3) and seven (D7) following follicular aspiration. Trt: long FSH protocol, short FSH protocol, Age: calf or adult. Proc Mixed. Values without a common letter (a,b,c) differed (P<0.05) by post-hoc comparison.

The correlation between the ovarian vascularity index at 24 h post-LH versus Day 3 after follicle aspiration tended to differ (Pearson's correlation coefficient r=0.36, P=0.09; Fig. 4.6A; combined data from calves and adults); the calves in the long protocol had a strong and positive association in ovarian vascularity index at 24 h post-LH versus Day 3 after follicle aspiration (r=0.78, P=0.02; Fig. 4.6B). Likewise, the ovarian vascularity index at 24 h post-LH was moderately and positively related to the ovarian vascularity index on Day 7 following aspiration (r=0.60, P<0.01, Fig. 4.6C; combined data from calves and adult animals)  however the correlation did not reach statistical significance when data from long FSH group calves or short FSH were analyzed separately (Fig. 4.6D).

**Calves and Adults**   **Calves**

**A**

**Day 3**

D3 Ovarian Vascularity (%)

r=0.36
p=0.09

**B**

● Calf-Long, **r=0.78, p=0.02**
◇ Calf-Short, r=-0.30, p=0.47

D3 Ovarian Vascularity (%)

**C**

**Day 7**

D7 Ovarian Vascularity (%)

r=0.60
<p=0.01

**D**

● Calf-Long, r=0.58, p=0.13
◇ Calf-Short, r=-0.09, p=0.83

D7 Ovarian Vascularity (%)

Ovarian Vascularity 24h post-LH     Ovarian Vascularity 24h post-LH

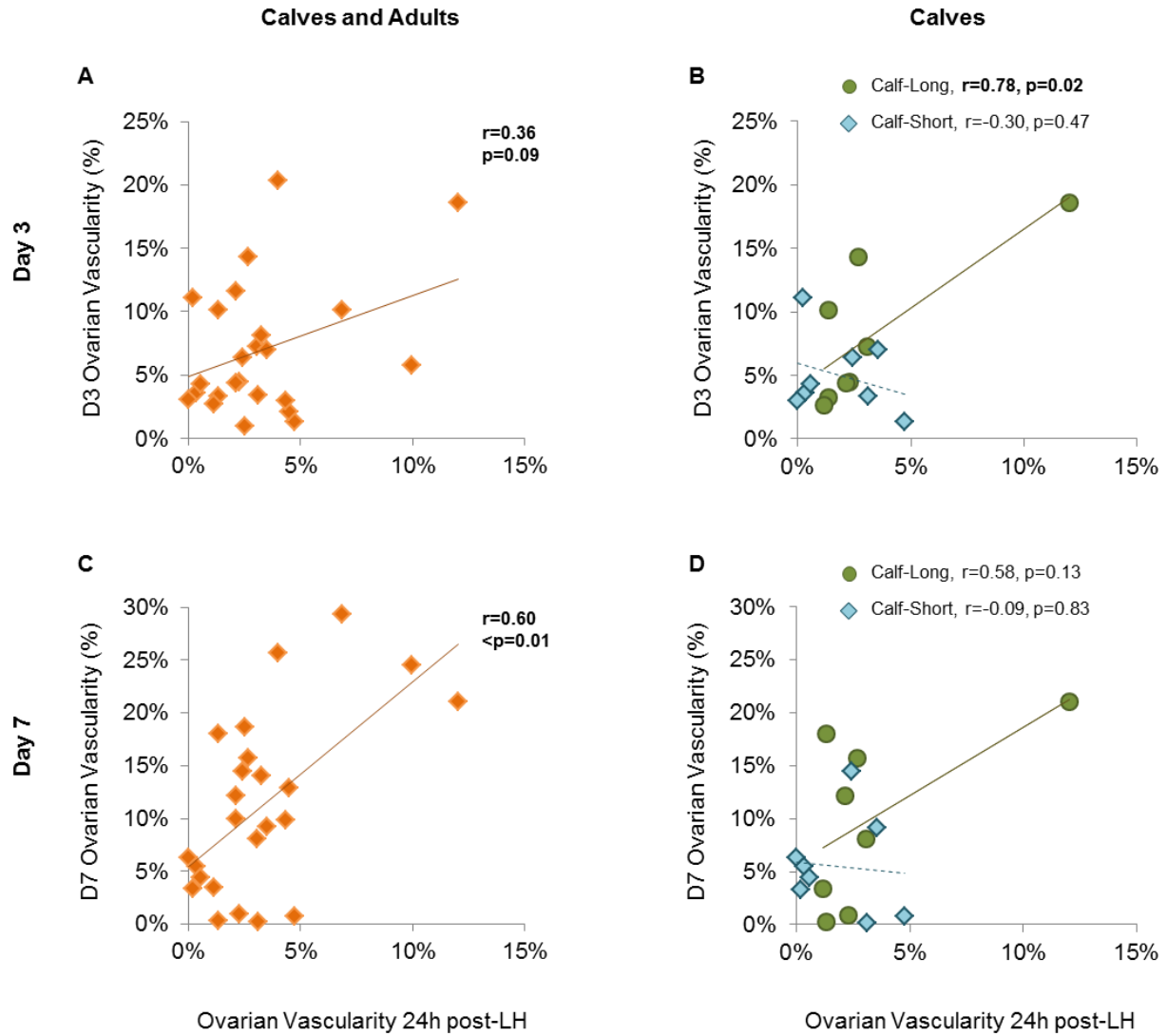Figure 4.6: The relationships between ovarian vascularity indices: (A, B) on the day of oocyte collection (OC; 24 h post-LH) and day three (D3) following follicular aspiration, and (C, D) at 24 h post-LH (i.e. the day of oocyte collection) and day seven (D7) following follicular aspiration for combined data (A, C) and for calves only (B, D); long protocol solid lines, short dotted lines. Pearson's correlation r is reported.

**4.4.4 The relationship between vascularity indices and the rise of plasma progesterone over time after follicle aspiration**

Plasma progesterone was measured at 24 h post-LH, and Days three, five, and seven after follicle aspiration. Progesterone levels differed between long and short FSH calf groups on Days three and five following follicular aspiration (Table 4.1, Mann-Whitney U, $P<0.05$), but not on Day seven (Mann-Whitney U, $P=0.20$). Additionally, calves did not differ from adults in levels of plasma progesterone on Day 7 following follicle aspiration (Calves: $31.63 \pm 15.55$, Adults: $19.40 \pm 5.00$; Mann-Whitney U, $P=0.45$; data combined between long and short FSH groups).

Table 4.1: Plasma progesterone (ng/ml) for four-month-old calves superstimulated using a short (four day) and long (seven day) follicle stimulating hormone (FSH) protocol for: 24 h post-LH treatment (i.e., on the day of oocyte collection), and three, five, and seven days following follicular aspiration.

|  | | DAY | | |
| --- | --- | --- | --- | --- |
| Protocol | Post-LH[a] | D3[b] | D5[b] | D7[b] |
| Short | 0.10±0.03 | *1.17±0.35 | **4.45±1.04 | 8.83±3.17 |
| Long | 0.80±0.28 | *12.69±7.33 | **50.59±28.02 | 54.43±29.62 |

a. Independent t-test, P=0.06
b. Mann-Whitney U, *P=0.03, **P=0.02

For each animal, the rate of change of plasma progesterone (progesterone slope) was calculated by fitting a linear regression model using 24 h post-LH, and Days 3, 5 and 7 after follicle aspiration values. Progesterone slope was moderately and positively correlated to the ovarian vascularity index at pre-LH time ($r=0.65$, $P<0.01$), 24 h post-LH ($r=0.65$, $P<0.01$, Fig. 4.7A) and at the Day 3 after follicular aspiration ($r=0.54$, $P<0.01$), but not the ovarian vascularity index on Day 7 ($r=0.32$, $P=0.13$) or the difference between ovarian vascularity indices on Day 24 h post-LH and pre-LH days ($r=0.32$, $P=0.12$; data combined among all groups). Calves in the long FSH group showed a stronger association between the progesterone slope and the difference between ovarian vascularity indices on Day 24 h post-LH and pre-LH days ($r=0.95$, $P<0.001$, Fig. 4.7B) but not for the short FSH group ($r=-0.21$, $P=0.62$, Fig. 4.7C).

**A**  **All animals**

r=0.65, P<0.01

Progesterone slope OC to Day 7 (ng/ml/day)

Ovarian Vascularity 24h post-LH

**B**  **Calves, Long FSH group**

r=0.95, P<0.001

Progesterone slope OC to Day 7 (ng/ml/day)

**C**  **Calves, Short FSH group**

r=-0.21, P=0.62

Progesterone slope OC to Day 7 (ng/ml/day)
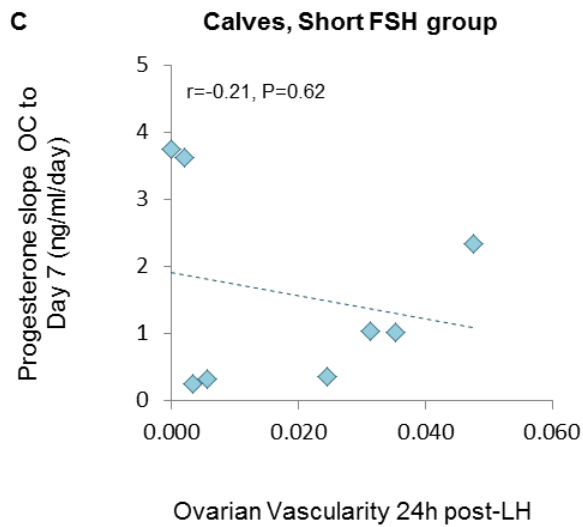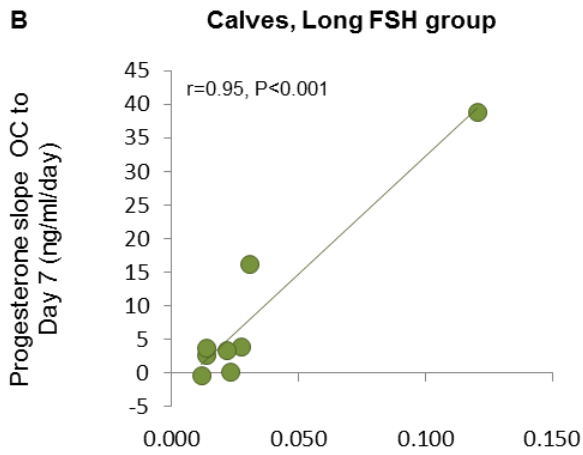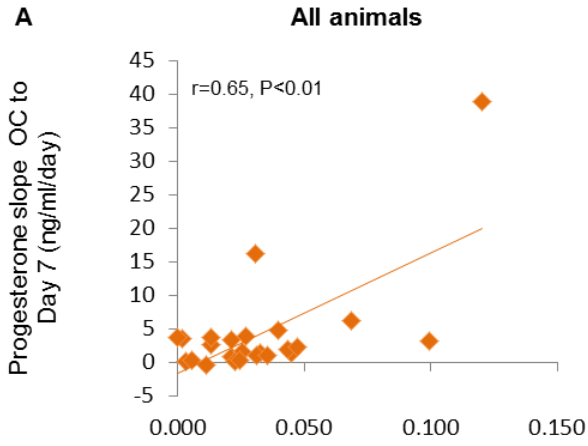
Ovarian Vascularity 24h post-LH

Figure 4.7: The relationship between ovarian vascularity 24 h post-LH treatment (i.e. on the day of oocyte collection) and the rate of change (slope: ng/ml/day) of plasma progesterone from the day

of oocyte collection (OC) to seven days following follicular aspiration for: A) all animals, B) calves in long protocol, and C) calves in short protocol. Pearson's correlation r is reported.

To explain the progesterone slope, a multiple linear regression model using four predictors was developed ($F_{(4,19)}$ = 14.464, P<0.001, $R^2$ = 0.75, $R^2_{Adjusted}$ = 0.70): Progesterone slope = 1.29*(age*trt interaction) + 166.80*Ovarian vascularity index at 24 h post-LH + 36.27*luteal volume index at Day 3 + 4.99 * P4Device -13. (β for all covariates P<0.05, Table 4.2). A reduced model with one predictor (ovarian vascularity index at 24 h post-LH) was not as strong a predictor of the progesterone slope ($R^2_{Adjusted}$=0.59). The four predictor model was checked for outliers (Std. Residual min = -1.45, max=1.72), collinearity (Ovarian vascularity index at 24 h post-LH: Tolerance = 0.80 VIF=1.26, luteal volume index on Day 3: Tolerance=0.79 VIF=1.26; Age*Trt interaction: Tolerance=0.91 VIF=1.10; P4Device: Tolerance=0.87 VIF=1.14), residuals were normally distributed (Shapiro-Wilk, P=0.43), and the model met the assumption of independent errors (Durbin-Watson=1.94) and non-zero variance (Ovarian vascularity index at 24 h post-LH =0.001, luteal volume index on Day 3=0.007, Progesterone Slope=65.26, age*trt interaction=8.58, P4Device=0.20).

Table 4.2: Linear regression coefficients (β) for best fit models for the rate of change of plasma progesterone (ng/ml/day) (Slope(P4)), plasma progesterone concentrations (ng/ml) for day three (D3) and day seven (D7) following follicular aspiration. Age: 0=adult, 1=calf; Trt: 4=short, 7=long; $OvV_{OC}$=ovarian vascularity on day of oocyte collection; $LutV_{D3}$=luteal vascularity on day three following aspiration; P4Device: 0=lost, 1=kept.

| | Age*Trt | $OvV_{OC}$ | $LutV_{D3}$ | P4Device | Intercept | $R^2$ | $R^2_{Adjusted}$ | $F_{(4,19)}$ | P-value |
|---|---|---|---|---|---|---|---|---|---|
| Slope(P4) | *1.29 | *166.80 | *36.27 | **4.99 | *-13.39 | 0.75 | 0.70 | 14.464 | <0.001 |
| $P4_{D3}$ | *2.09 | *291.89 | **42.40 | ***6.24 | *-20.65 | 0.73 | 0.68 | 13.069 | <0.001 |
| $P4_{D7}$ | *8.63 | *1134.42 | **203.66 | **32.37 | *-88.17 | 0.76 | 0.71 | 14.852 | <0.001 |

β: *P<0.001, **P<0.05, ***P=0.12

**4.4.5 The relationship between ovarian vascularity index and cumulus-oocyte morphology**

The proportion of partially to fully expanded COCs did not differ (t-test, P=0.80) between calves in the short FSH (0.69 ± 0.34) compared with the long FSH (0.73 ± 0.06) groups. Therefore, all animals (calves and adults combined) were ranked according to the proportion of partially and fully expanded COCs, then re-grouped based on the top half (n=11) and the bottom half (n=12). The group with higher number of partially to fully expanded COCs tended to have greater ovarian vascularity on Day 7 after follicle aspiration (independent t-test, P=0.08), however the two groups were not different for the pre-LH day, 24 h post-LH and for Day 3 after aspiration.

A mixed modelling procedure was applied with the ovarian vascularity as the dependent variable repeated over the day of oocyte collection and days three and seven afterwards, to assess for any differences in animals that produce a higher number of partially to fully expanded COCs (Fig. 4.8A). There was no three way interaction between the group (high versus low proportion of expansion of COCs), age (calf versus adult), or time (day of OC, D3 or D7) (Proc mixed, P=0.19). However there was an interaction between time and age (Proc mixed, P<0.01), where calves and adults did not differ on the day of collection (P=0.16) or the third day after aspiration (P=0.84), but differed on the seventh day following collection (P<0.01). There was also a group by time interaction (Proc mixed, P=0.04). On post hoc assessment, the animals in the high group tended to have greater ovarian vascularity on D7 (P=0.06) which was appreciable in the calves (P=0.06) more than adult animals (P=0.33) Additionally, there was a difference in luteal vascularity seen between the higher proportion group of calves compared to low proportion group on day seven but not on day 3 (Proc mixed, P<0.05, Fig. 4.8B).
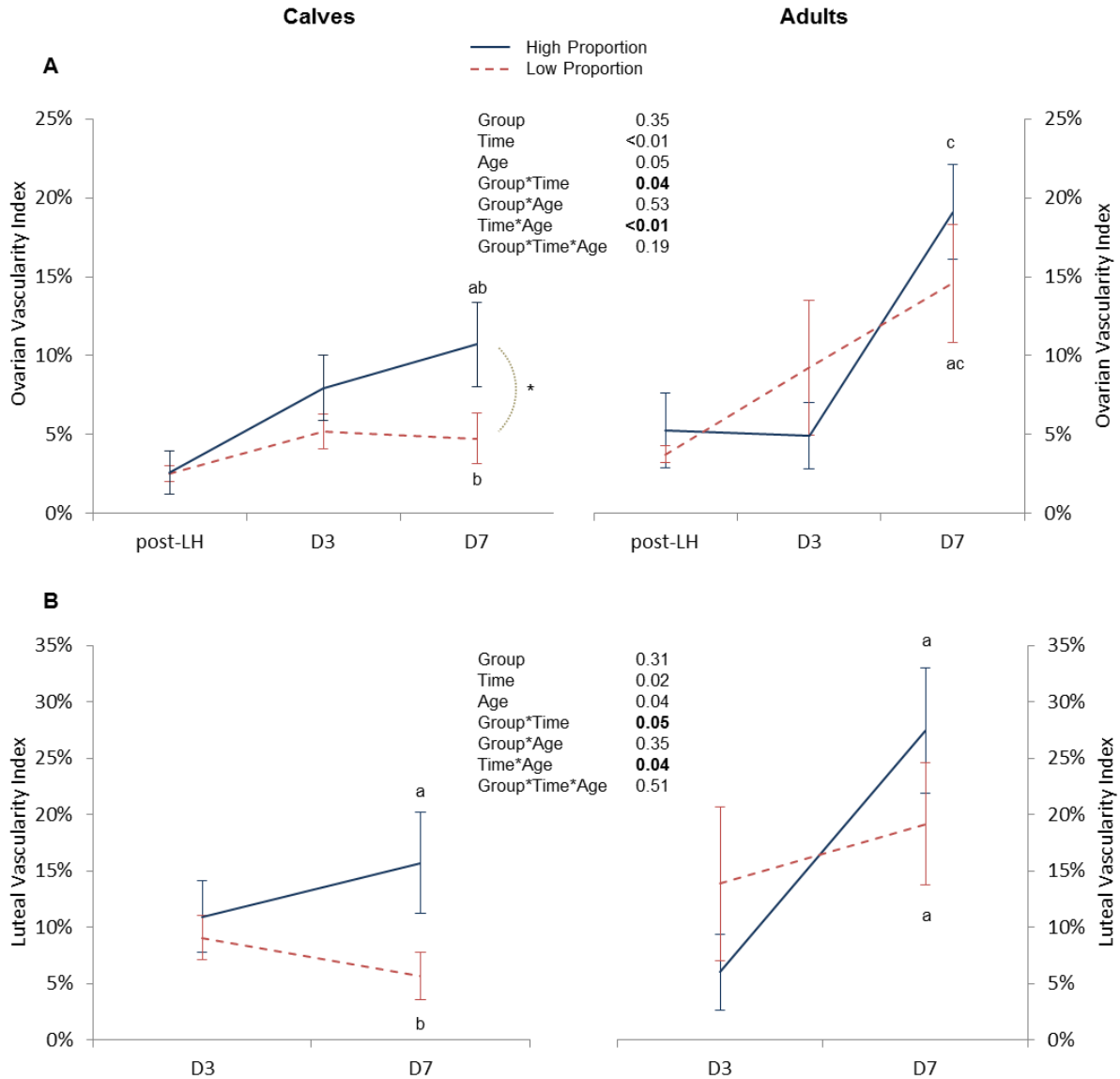
Figure 4.8: Changes in vascularity over time, grouped by proportion of partially to fully expanded cumulus-oocyte-complexes. Group: High proportion partially to fully expanded (calves n=8; adults n=3); Low proportion partially to fully expanded (calves n=8; adults n=4), Time: 24 h post-LH treatment (i.e., oocyte collection), days three (D3) and seven (D7) after collection. Age: calf or adult. A) Ovarian vascularity. B) Luteal vascularity. Proc mixed. Values without a common letter (a,b,c) differed on D7 by post-hoc Tukey's test, P<0.05. *P=0.06

**4.5 Discussion**

The study aimed to characterize the vascularity of the ovary during superstimulation in four-month-old prepubertal beef heifers and its relationships with the status of the cumulus-oocyte-complex following follicular aspiration and luteal tissue development and function. Power Doppler ultrasonographic images were evaluated on an external computer for the day of luteinizing hormone treatment, the day of oocyte collection, and the third and seventh days following follicular aspiration for prepubertal calves and adult animals that underwent superstimulation under a traditional four-day protocol or a lengthened duration of seven days of FSH stimulation. Ovarian vascularity index was calculated for all four time points, while luteal vascularity and the relative luteal volume index were calculated on days three and seven. Notably, we were able to document that calves exhibit an increase in vascularity in response to an exogenous treatment of pLH, and possibly due to the endogenous surge in LH with the suppression of the LH surge using a progestagen. Longer 7-day FSH stimulation protocol was more important in calves than in adults in relation to the production of progesterone and the neovascularization of the luteal structures that developed following follicular aspiration. Furthermore, calves that had greater expansion of the cumulus-oocyte-complexes after 24 hours following treatment with pLH demonstrated greater ovarian and luteal vascularity on day seven after aspiration.

Power Doppler ultrasonographic images that were collected on the day of oocyte collection demonstrated an increase in vascularity from the day of the luteinizing hormone treatment. This is consistent with research in single ovulations in adult animals [25]. Additionally, when calves and adults were analyzed separately, it was shown that calves follow a similar pattern to adults in their vascularity. This increase in vascularity is likely due to the responsiveness of the existing vasculature through the nitric oxide synthase pathway to relax the endothelial smooth muscle [26, 105]. Additionally, the levels of estradiol modulates nitric oxide levels [26] and thus intrafollicular fluid analysis from calves may find a relationship between high estradiol to progesterone ratio in the follicles with greater vascularity [73].

When the duration of FSH stimulation was increased from the traditional four day protocol to a seven day protocol, there was a tendency for greater ovarian vascularity changes between the day of LH and the day of oocyte collection. The effect of treatment was much stronger in calves than in adult animals, which demonstrates that increasing the duration of FSH stimulation

69

improves ovarian perfusion in calves that is not seen in adult animals. Development of luteal tissue following follicular aspiration in adult cattle is also related to the protocol used during superstimulation prior to collection of oocytes, with cattle under a long duration of superstimulation having greater luteal tissue development than those in a four-day protocol followed by FSH 'starvation' or a coasting period (i.e. 84h) prior to follicular aspiration [Dias et al 2013 study, unpublished data].

The tendency for greater vascularity in ovaries prior to aspiration for the long protocol was consistent with a significantly greater percentage of luteal tissue development in prepubertal calves of the long protocol compared to the short protocol. Adult animals showed no difference between protocols when assessing the percentage of luteal tissue volume. It appears that increasing the FSH duration improves luteal development in calves, which is not seen in adult animals. It has been found previously that longer duration of superstimulation produces greater number of larger follicles in both calves [Krause et al., unpublished data] and adult animals [116], yet the differential luteal tissue development between the two FSH protocols in calves was not seen in adults in the current study. The ultrasonographic evaluation of volume of luteal tissue was consistent with the plasma progesterone values, where calves of the short protocol had significantly lower concentrations overall compared with calves of the long protocol. This study confirmed that Doppler ultrasonography may be utilized to gain valuable information on the vascularity of the luteal tissue in calves when undergoing superstimulation or superovulation. In previous studies, the use of a long FSH protocol of seven days was compared with a four day FSH protocol followed by a 'coasting' period of FSH starvation (84 hours) and it was found that the protocols differed in the quality of oocytes and cleavage rate [116], and luteal tissue development following aspiration, where starvation of the follicle from gonadotrophins for this length of time prevented the granulosa and thecal cells from developing into functional luteal cells, which was determined by both ultrasonographic evaluation following aspiration and by progesterone concentration in plasma [unpublished data, Dias et al, 2013]. It has been shown that gene expression of the granulosa cells differs between a long FSH protocol and starvation of FSH, including genes that are related to LH responsiveness [92]. Given the importance of the LH binding for development of luteal tissue, even following aspiration [78], it can be hypothesized that those animals who develop luteal tissue following aspiration likely have the presence of LH receptors. Follicular maturation is characterized by the acquisition of LH receptors and activation

of genes responsible for angiogenesis which are important prior to the luteinizing hormone surge [92]. Follicles are required to reach ovulatory capacity, both in size and acquisition of LH receptors, prior to exogenous treatment of LH for the induction of ovulation [177]. By allowing the follicles to grow for a longer duration by increasing the length of time of FSH exposure, it is possible that more follicles acquire LH receptors and therefore, additional luteal tissue is produced. The current study compared calves of a short FSH protocol (four days) and a long FSH protocol (seven days). The luteal tissue development was dependent on the age group and protocol interaction, where calves of the longer duration protocol produced greater percentage of luteal volume than calves of the short protocol, while adult animals demonstrate similar percentage of their ovaries occupied by luteal tissue regardless of protocol. Therefore, it appears the duration of FSH stimulation has a stronger effect on the amount of luteal tissue produced for prepubertal calves than for adult heifers. In an early study on the corpora lutea formed in prepubertal heifers after superovulation, the volume of luteal tissue extracted from calves was similar to mature heifers, yet the progesterone production *in vitro* was lower than adult animals [178]. However, after incubation with LH, calves produced the same level of progesterone *in vitro* as mature heifers. This leads to the hypothesis that calves require continued support of endogenous secretion of LH for progesterone production following ovulation or follicular aspiration. Indeed, calves demonstrate continued elevation in LH plasma concentrations until returning to basal levels at ten days following an ovulatory dose of pregnant mare serum gonadotropin [179]. Additionally, plasma levels of progesterone from prepubertal calves following superovulation were reported to be higher than that of adult animals, rising to levels of approximately 100ng/mL by day eight to ten [179], which is similar levels in this study. Regardless of the FSH stimulation protocol in the current study, the plasma progesterone concentrations taken on day three after follicular aspiration were positively associated with the luteal vascularity index, while no relationship was found between the progesterone values and luteal volume index. The luteal vascularity index was greater for the long duration protocol than the short protocol, irrespective of age group.

Vascularization of the CL is imperative to its function [123]. The current study demonstrated that ovarian vascularity on day seven following follicular aspiration is improved in calves to the level of adult animals under traditional four days of superstimulation by increasing the duration of superstimulation from four to seven days. Overall, calves have an increase in

71

vascularity from the day of LH treatment through collection and seven days after. This increase in vascularity paralleled the rate of change of plasma progesterone concentration. The analysis of power Doppler ultrasound images correlated well with the rate of change of progesterone, and both the measurement of vascularity within the ovary at the time of oocyte collection and the luteal vascularity at three days after collection were strong predictors of the increase in progesterone in the circulation. Similarly, point measurements of plasma progesterone on days three and seven could be predicted by similar parameters, ovarian vascularity on the day of collection and luteal vascularity at day three. While the current study did not show luteal volume index as a strong predictor of progesterone production, it should be mentioned that the measure is of relative volume and not absolute volume, therefore animals with a small volume of luteal tissue can have a high relative percentage of their ovaries occupied by luteal tissue following superstimulation. More importantly, the current study is consistent with research in adult animals in which luteal tissue perfusion visualized with colour Doppler ultrasonography is a predictive measure of the functional secretion of the CL [61, 142]. While it was not performed in the current study, biopsies of luteal tissue *in vivo* is a possible direction to confirm that four-month-old heifers can be stimulated to have ovulatory capacity, followed by luteal tissue development that is achieved at a minimum of seven days following removal of the oocyte.

Expansion of the cumulus cells surrounding the oocyte is one of the markers of oocyte maturation [180]. In the current study, calves that had a larger proportion of partially to fully expanded cumulus-oocyte-complexes also demonstrated the greatest ovarian and luteal vascularity on the seventh day following follicular aspiration. However, this increase in vascularity was not evident on the day of oocyte collection or on the third day following collection. Whether the production of greater amount of luteal vascularity is also associated with oocyte competency and embryonic development has yet to be explored. Binding of luteinizing hormone is associated with an increase in vascularity of the existing blood vessels within the theca interna surrounding a follicle [106], possibly through activation of vasoactive peptides (endothelin-1) [26]. Estradiol may have a local effect on the production of nitric oxide through nitric oxide synthase for vasodilation of blood vessels in the ovary [26]. Nitric oxide is also present in follicular fluid and may play a role in oocyte maturation [73, 181]. Yet, endothelial nitric oxide synthase in the thecal cells may differ in function to the intrafollicular fluid nitric oxide synthase (iNOS) [181]. The proliferation of endothelial cells within the developing CL

occurs long after the LH surge and elevated estradiol therefore may have different regulation than exiting vasculature in the thecal interna (i.e. VEGF and FGF).

Proliferation of endothelial cells during development of the CL following ovulation is under the control of vascular endothelial growth factor as well as fibroblast growth factor [123]. Luteal angiogenesis is blocked by treatment with a VEGF antibody in primates [125]. In this study, granulosa and thecal cell proliferation into luteal cells occurred without substantial morphological changes to the luteal cells. Blocking GnRH in the early development of the primate CL causes disorganization of the luteal cells, smaller cells with an increase in lipid accumulation and  is associated with a decrease in plasma progesterone [124]. These studies confirmed that both LH and VEGF are required for appropriate development of functional luteal tissue [124, 125]. An *in vitro* study on the maturation of bovine oocytes found that adding VEGF to media at the beginning of *in vitro* maturation produced more embryos that reached the cleavage stage and more blastomeres were formed [182]. It is unknown at this time whether calves undergoing superstimulation with a short versus long FSH protocol have differential gene expression of VEGF in granulosa cells, as it is in adult cattle [92]. As thus, it could be hypothesized that increasing the VEGF expression from granulosa cells prior to collection of the oocytes from calves may increase the oocyte competency. It is possible that the production of larger follicles with increased duration of FSH would cause larger volume of luteal cells, however in this study the relative vascularity of the luteal tissue is greater for the longer protocol than shorter, and vascularity index is independent of size of the ovary and luteal tissue volume. Therefore, confirming that in calves, progesterone production is reliant on appropriate vascularization of the luteal tissue as it is in adults. Further work on superovulation in calves with biopsy of the luteal tissue or gene expression of granulosa cells during superstimulation with a long duration of FSH may help to confirm this hypothesis.

**4.6 Conclusions**

In conclusion, there was an increase in ovarian vascularity between the time of pLH treatment and 24 h after treatment for prepubertal calves and postpubertal heifers and adult cows, as assessed by three-dimensional image analysis of power Doppler ultrasound data. Additionally, ovarian vascularity prior to follicular aspiration was associated with ovarian and luteal vascularity up to seven days after follicular aspiration. The duration of the FSH protocol

significantly affected the production of greater expansion of COCs, and the development of functional luteal tissue and luteal vascularity in prepubertal calves, but not in adult heifers.

## 4.7 Acknowledgements

# CHAPTER 5: GENERAL DISCUSSION

The overall thesis objective was to relate changes in follicular and luteal vascularity with functional changes (ovulatory capacity, hormones, oocyte quality, etc.). In order to address this objective, first a computer-assisted three-dimensional method was developed to assess ovarian structures, follicles and corpora lutea, and their vascularity. Then, the three-dimensional method was verified with single image measurements of the follicles and corpora lutea in two-dimensions. This novel method uses video segments recorded after free-hand movement of the routine linear-array transducer, obtained 3D vascularity index values are independent of speed of transducer movement, and the method does not require a-priori operator selection of images, i.e., is an objective method. The development of this new three-dimensional method was addressed in Chapter 3, and Appendix A that follows this discussion is a short version of the integral steps to reproduce ovarian structures in three-dimensions using Imaris software. Finally, the method was used to assess the vascularity to follicles and corpora lutea in a study in water buffalo, and a study in four-month old beef calves.

In Study 1 (Chapter 3), colour Doppler ultrasonography was used to assess the ovaries of water buffalo (*Bubalus bubalis*) who were induced to ovulate using a gonadotropin-releasing hormone analogue. Ultrasonographic examinations were performed daily to assess ovulation and subsequent CL development. This study was designed to develop and validate the three-dimensional method therefore a comparison of the new method was made with a more subjective two-dimensional method in which the observer selects the most vascular region of the structure of interest, which is similar to studies performed previously in cattle [70] and buffalo [31]. The study found that three-dimensional image analysis of water buffalo ovaries was less variable for follicular data compared with two-dimensional analysis, even when the average of three still-images was used for the latter method. This is likely due to a high variability in the vascular network surrounding a follicle that has been previously described in cattle [20]. However, three-dimensional image analysis had similar variation between animals compared with two-dimensional analysis when analyzing the CL. This is probably due to a more uniform vascularity within the CL compared with follicles, despite there being a difference in hormonal control of the peripheral and central regions of a CL [135, 139]. In comparison to the current image analysis methods, a noteworthy feature of the new three-dimensional method is that it is an

objective method without need for a-priori selection of the images by an expert operator thereby eliminating subjectivity and human bias. Accuracy of volume measurement of structures of interest was verified by comparison with theoretical calculations and requires one assumption (i.e., follicle diameter in Z-axis = average of diameter along X-axis and Y-axis); however, the '3D vascularity index' endpoint (vascular volume : volume of the structure of interest) is independent of the slice thickness, i.e., the speed of hand movement along the Z-direction.

In Study 2 (Chapter 4), power Doppler ultrasonography was used to assess the ovaries of four-month-old beef calves (*Bos taurus*) who were superstimulated using two FSH protocols. Ultrasonographic examinations were performed on the day of LH treatment (pre-LH, 12 h after last FSH treatment), the day of oocyte collection (24 h post-LH treatment), and the third and seventh day following ultrasound-guided follicular aspiration for oocyte collection. The three-dimensional method developed in Study 1 was used to calculate vascularity indices for all time points. Ovarian vascularity was then related to the expansion of the cumulus-oocyte-complexes that were retrieved, as well as the luteal tissue that developed following aspiration. Luteal tissue and vascularity indices were also related to plasma progesterone concentrations.

Following the development and verification of the three-dimensional method, it was subsequently applied to demonstrate changes in vascularity between the day of GnRH treatment (12 h before treatment) and the time of AI (14-16 h following treatment) in water buffalo (Chapter 3). It was previously found in cattle that there is a biphasic pattern of increase and decrease of vascular flow to the preovulatory follicle following treatment with GnRH [106]. In study 1, water buffalo were not scanned on an hourly basis therefore we cannot assume that buffalo exhibit this biphasic pattern. However, in this study it was found that buffalo that ovulated within 24 hours of AI (within 40 h following GnRH treatment) exhibited an increased blood flow at the time of AI, compared to the day of GnRH treatment (i.e. by 12 h of LH treatment). More importantly, we detected that buffalo that did not ovulate within 40 hours following GnRH (animals n=3 ovulated at greater than 84 h), had decreased blood flow on the day of AI, compared to the day of GnRH. This decrease in blood flow was not detected using the subjective selection of the most vascular cross-section of the follicle when calculated in two-dimensional image analysis. Therefore, it is reasonable to assume that three-dimensional image analysis was superior in detecting animals that did not ovulate following treatment with GnRH. It is possible that the non-ovulatory follicles were in late-static phase or undergoing atresia, as it

is consistent with a study in cattle where anovulatory follicles had less blood flow [25]. The use of a three-dimensional assessment of the vascularity may be important for future management of AI programs, as producers and AI technicians could modify their protocol for individuals that are highly likely ovulate versus not ovulate given the colour Doppler ultrasound data, perhaps saving the semen from a valuable bull for an animal that has a higher chance of ovulating to the GnRH treatment. Lastly, it should be mentioned that, these conclusions are independent of follicle diameter, i.e. the size of the preovulatory follicle in buffaloes that did not ovulate was similar to those that ovulated. The difference in follicular vascularity is possibly due to a seasonal effect, given the high temperatures that water buffalo experience in the summers of India, and the seasonal effect on vascular flow [34], or individual variation given the smaller sample size of this study.

The study on water buffalo was not able to find an association between colour Doppler measurements of vascularity to the early (day four) or mid-cycle (day 9-10) CL and pregnancy rate. Analysis of the blood flow to the CL has been used on day seven, the day of embryo transfer in cattle, showing that recipients with a greater vascularity to their CL had a higher chance of holding the pregnancy after transfer [27]. Water buffalo that demonstrated a decrease in resistance to blood flow to their CL when assessed on day ten, were more likely to be pregnant than those with lower velocity of blood flow [33]. The reason why our study did not show this relationship is unknown. However increasing the number of buffalo that are assessed during this period may improve the efficiency of the use of colour Doppler ultrasonography for the selection of appropriate recipients for embryo transfer or early diagnosis of non-pregnant water buffalo.

In contrast, the luteal structures that were evaluated in prepubertal calves on day seven following follicular aspiration demonstrated a relationship between a higher proportion of expanded COC and the vascularity of the luteal tissue on day seven (Chapter 4). The quality of the COC, as measured by the number of cumulus layers and homogeneity of the ooplasm, is associated with an increase in follicular blood flow in cattle, where higher grade of COC had greater vascular flow [73]. Oocytes obtained from calves, however, have different developmental capacity compared with adult animals [170]. The oocytes from calves were smaller in diameter, had lower pyruvate and glutamine metabolism, as well as a decrease in protein synthesis during *in vitro* maturation compared with adults [170]. In prepubertal calves, oocytes obtained from larger follicles (>8 mm in diameter) tend to produce greater number of blastocysts [68], which is

77

similar to adult animals [116]. There has been an association between follicle size and the increase in perifollicular blood flow in adults [24, 28], that has not been explored in calves. If oocytes from calves were collected at random, the quality of the COC may be greater from follicles with higher vascularity, compared with those with less vascularity, as seen in adult cattle [73]. The number of large follicles available for oocyte collection can be improved by using follicle stimulating hormone treatments (superstimulation) during wave emergence to prevent follicular atresia and allow co-dominance of the follicles [84]. In contrast to the water buffalo study (Chapter 3), analyses in superstimulated prepubertal calves were performed over the entire ovary and single preovulatory follicles were not evaluated in calves during our study. While previous studies in cattle demonstrated the increase in perifollicular vascularity from the time of induction of ovulation on single follicles [25, 106], the assessment of individual perifollicular vascularity indices is difficult in superstimulated animals, especially given that some calves had greater than 40 follicles per ovary. Likewise, ovarian stromal blood flow has been used as an evaluation method in women [21, 23, 98]. Women who demonstrated low ovarian stromal vascularity were considered less fertile, and stromal blood flow prior to collection can be used to assess the oocyte recovery rate [111]. Women with greater ovarian stromal blood flow had a higher response to stimulation (increased numbers of large follicles) [21]. However, ovarian stromal vascularity was not assessed prior to stimulation in calves to compare those with little stromal blood flow and their response to superstimulation. Recently, there has been an interest in predictive measures of superstimulation response in calves for the purpose of selecting the best responders as donor animals [183]. Antral follicular count, or the number of follicles recruited into a wave [184], has been found to be related to anti-Müllerian hormone (AMH); both measures have significant correlations with the response to superstimulation as an adult [183, 185-188]. AMH has been studied in women with polycystic ovarian syndrome, where AMH was higher in women with polycystic ovaries [189]. Additionally, ovarian stromal blood flow was also higher in women with polycystic ovarian syndrome [189, 190]. Ovarian stromal blood flow may also be related to maternal age [150], for which the bovine model may be a suitable candidate for testing this hypothesis. The relationship between stromal vascularity and antral follicular count or anti-Müllerian hormone in prepubertal calves has not been determined.

Analyses of follicular fluid in buffalo and cattle have found the estradiol to progesterone ratio, estradiol concentration, and concentration of angiogenic factors within the fluid were

related to vascularity surrounding the follicle [31, 39, 59, 60, 71, 73]. During follicular aspiration in our study, all follicles were collected into a single collection tube, therefore individual follicular fluid analyses would not be possible based on our design. However, sacrifice of a few follicles per ovary for fluid analysis is possible in superstimulated animals. It can be hypothesized that calves with greater vascularity to their follicles would also have higher estradiol to progesterone ratio and the expression of angiogenic factors as in adult animals. The analysis of luteal tissue that develops following follicular aspiration is also related to the estradiol content of the follicular fluid [71]. Thereby, the CL can be used to retrospectively assess the maturation status of the follicle. In our study on calves, the long FSH protocol compared with the short protocol demonstrated greater luteal tissue development and greater luteal vascularity that was also related to the concentration of progesterone within the plasma. Given that the longer duration of FSH stimulation produced larger diameter follicles and larger number of follicles in calves [Krause et al., unpublished data] and in adult animals [116], this may also be associated with the amount of luteal tissue development. Interestingly, there was no relationship between the increasing vascularity from the time of LH treatment (12 h after last FSH treatment) to the time of oocyte collection (24 h following LH) and COC expansion. This is similar to single aspirations from preovulatory follicles in mature heifers [114].

In the buffalo study (Chapter 3), some animals did not ovulate, regardless of the size of the preovulatory follicle at the time of GnRH treatment. Additionally, the diameter of the follicle was not a predictive measure of whether a CL would form after follicular aspiration in adult cows [71]. A study in adult cattle used the longer duration of FSH compared with an FSH starvation protocol (four days of FSH followed by 84h of 'coasting') and assessed the development of corpora lutea using B-mode ultrasonography and plasma progesterone [Dias et al., 2013, unpublished data]. This study demonstrated that FSH starvation of >96 h impeded the development of the corpora lutea, with no corpora lutea forming even after treatment with LH for *in vivo* maturation. Analysis of gene expression of granulosa cells comparing these protocols showed a disruption in angiogenic factors during superstimulation that was returned if the duration of stimulation was prolonged by three days [90, 92, 116]. It is well known that vascularity is important for appropriate luteal development [123-126, 129], which the current study has demonstrated in calves.

Luteal tissue development is important for the production of progesterone. Additionally, some research has shown that the luteal vascularity is a stronger predictor of plasma progesterone than the cross-sectional area of the CL [128, 129]. In the calf study (Chapter 4), relative luteal volume was increased in calves under the long duration of FSH stimulation, but ovarian and luteal vascularity were related to plasma progesterone, where the best predictive model for plasma progesterone values included the ovarian vascularity on the day of collection and the luteal vascularity on day three following follicular aspiration (in addition to whether the animal kept its norgestomet implant until experimental removal). It appeared that the relationship between ovarian vascularity prior to aspiration and the development of luteal tissue in the current study was consistent with single ovulations in cows [14]. While progesterone concentration was not evaluated in the buffalo study (Chapter 3), the follicular wall vascularity was positively though weakly associated with the vascularity of the CL. It can be postulated from other studies in buffalo that these animals would exhibit a similar relationship with plasma progesterone and the luteal vascularity [33]. The use of colour Doppler ultrasonographic evaluation of the CL provides additional information on the functionality, which is progesterone secretion, of the structure that would be missed with B-mode ultrasound alone.

## 5.1  Conclusions

In conclusion, the newly-developed three-dimensional image analysis of colour Doppler ultrasound images is an objective and unbiased method that had lower technical variability and was superior to two-dimensional in detecting water buffaloes with large follicles that did not ovulate. The three-dimensional method was also applied to calves undergoing superstimulation and was able to detect that luteal vascular flow from power Doppler ultrasound data was positively correlated to progesterone production following follicular aspiration. The increase in vascularity of the preovulatory follicles following treatment with GnRH or LH in water buffalo and beef calves was consistent with prior studies in adult cattle. Additionally, there was a significant effect of superstimulatory protocol on the production of a functional luteal tissue following follicular aspiration. Finally, the expansion of the COC was not related to the ovarian vascularity at the time of collection in 4-month old calves; however animals with a higher proportion of expanded COC demonstrated greater luteal vascularity on the seventh day following collection.

## 5.2 Future Directions

Three-dimensional image analysis of colour and power Doppler ultrasound data appears to be useful in the analysis of preovulatory follicles prior to artificial insemination. Additionally, it may have a use in evaluation of the CL prior to embryo transfer, though controversial for pregnancy diagnosis in cattle and buffalo. Our studies confirmed that luteal vascularity is dependent on the follicular vascularity, however oocyte competency in prepubertal calves and its relationship with ovarian stromal blood flow or individual follicular wall vascular flow is still open for evaluation. Additionally, pixel evaluation of the wall of the follicle may assist in identifying the level of the theca interna [64], the region which contains the greatest vasculature prior to the breakdown of the basement membrane of the follicle, to further evaluate the vascularity within the wall of the ovarian follicle. Furthermore, assessment of ovarian stromal blood flow prior to superstimulation to predict stimulatory response (the production of a greater number of larger follicles) could be applied to calves, in conjunction with antral follicular count or assessment of anti-Müllerian hormone. The importance of luteal development on day seven and its relationship with the prior expansion of the COC requires further assessment. It is possible to biopsy the CL, without removal of the ovary, in adult cattle [191]. Therefore it may provide an avenue of exploration in young animals for assessment of hormonal or genetic relationships found in the CL and use this information to gain a greater understanding of the developmental competence of oocytes *in vitro* from prepubertal animals. Our study in prepubertal calves confirmed that luteal vascularity was a stronger predictor of plasma progesterone than the relative luteal tissue volume. An assessment of the duration of the luteal phase in calves can be assessed with the minimally invasive tool of colour and power Doppler ultrasonography. Finally, our studies confirmed that three-dimensional analysis of colour Doppler ultrasound data had less technical variation compared to traditional two-dimensional method when assessing follicular vascularity. Therefore, researchers should consider modifying their two-dimensional methods when selecting of single images of preovulatory follicles. Furthermore, this new method does not require an operator to select images for analysis and thereby avoids subjective selection and human bias. This will likely provide an increase in accuracy of the changes in vascularity that surrounds follicles.

# CHAPTER 6: REFERENCES

[1] Ginther OJ. How ultrasound technologies have expanded and revolutionized research in reproduction in large animals. Theriogenology. 2014;81:112-25.

[2] Singh J, Adams GP, Pierson RA. Promise of new imaging technologies for assessing ovarian function. Animal Reproduction Science. 2003;78:371-99.

[3] Fricke PM. Scanning the Future - Ultrasonography as a Reproductive Management Tool for Dairy Cattle. J Dairy Sci. 2002;85:1918-26.

[4] Matsui M, Miyamoto A. Evaluation of ovarian blood flow by colour Doppler ultrasound: practical use for reproductive management in the cow. Veterinary Journal. 2009;181:232-40.

[5] Pursley JR, Mee MO, Wiltbank MC. Synchronization of ovulation in dairy cows using PGF2alpha and GnRH. Theriogenology. 1995;44:915-23.

[6] De Rensis F, Lopez-Gatius F. Protocols for synchronizing estrus and ovulation in buffalo (Bubalus bubalis): a review. Theriogenology. 2007;67:209-16.

[7] Ginther OJ. Ultrasonic Imaging and Animal Reproduction: Color-Doppler Ultrasonography, Book 4. Cross Plains, WI, USA.: Equiservices Publishing; 2007.

[8] Dickey RP. Doppler ultrasound investigation of uterine and ovarian blood flow in infertility and early pregnancy. Human Reproduction Update. 1997;3:467-503.

[9] Acosta TJ, Yoshizawa N, Ohtani M, Miyamoto A. Local Changes in Blood Flow Within the Early and Midcycle Corpus Luteum after Prostaglandin F2 Injection in the Cow. Biology of Reproduction. 2002;66:651-8.

[10] Herzog K, Bollwein H. Application of Doppler ultrasonography in cattle reproduction. Reprod Dom Anim. 2007;42:51-8.

[11] Bhal PS, Pugh ND, Chui DK, Gregory L, Walker SM, Shaw RW. The use of transvaginal power Doppler ultrasonography to evaluate the relationship between perifollicular vascularity and outcome in in-vitro fertilization treatment cycles. Human Reproduction. 1999;14:939-45.

[12] Chui DK, Pugh ND, Walker SM, Gregory L, Shaw RW. Follicular vascularity - the predictive value of transvaginal power Doppler ultrasonography in an in-vitro fertilization programme: a preliminary study. Human Reproduction. 1997;12:191-6.

[13] Ginther OJ, Utt MD. Doppler ultrasound in equine reproduction: principles, techniques, and potential. Journal of Equine Veterinary Science. 2004;24:516-26.

[14] de Tarso SG, Gastal GD, Bashir ST, Gastal MO, Apgar GA, Gastal EL. Follicle vascularity coordinates corpus luteum blood flow and progesterone production. Reprod Fertil Dev. 2015.

[15] Rubin JM. Power Doppler. Eur Radiol. 1999;9:S318-S22.

[16] Chen C-K, Wu H-M, Soong Y-K. Clinical Application of Ultrasound in Infertility: From Two-dimensional to Three-dimensional. Journal of Medical Ultrasound. 2007;15:126-33.

[17] Luttgenau J, Bollwein H. Evaluation of bovine luteal blood flow by using color Doppler ultrasonography. Reprod Biol. 2014;14:103-9.

[18] Kaya S, Kacar C, Polat B, Colak A, Kaya D, Gurcan IS, Bollwein H, Aslan S. Association of luteal blood flow with follicular size, serum estrogen and progesterone concentrations, and the inducibility of luteolysis by PGF2alpha in dairy cows. Theriogenology. 2016.

[19] de Tarso SGS, Ishak GM, Gastal GDA, Bashir ST, Gastal MO, Gastal EL. Novel prospects for evaluation of follicle wall blood flow using color-Doppler ultrasonography. Animal Reproduction. 2016;13:762-71.

[20] Arashiro EKN, Palhao MP, Santos JRL, Fontes RC, Siqueira LG, Henry M, Viana JH. Three-dimensional modeling of color Doppler images: a new approach to study follicular vascularization in cattle. Anim Reprod. 2013;10:662-9.

[21] Zaidi J, Barber J, Kyei-Mensah A, Bekir J, Campbell S, Lin Tan S. Relationship of ovarian stromal blood flow at the baseline ultrasound scan to subsequent follicular response in an in vitro fertilization program. Obstet Gynecol. 1996;88:779-84.

[22] Razik MA, Farag MAH, Sheta M. Uterine and ovarian arteries blood flow during the mid luteal phase in women with unexplained infertility. Middle East Fertility Society Journal. 2014.

[23] Younis JS, Haddad S, Matilsky M, Radin O, Ben-Ami M. Undetectable basal ovarian stromal blood flow in infertile women is related to low ovarian reserve. Gynecol Endocrinol. 2007;23:284-9.

[24] Miyamoto A, Shirasuna K, Hayashi K, Kamada D, Kawashima C, Kaneko E, Acosta TJ, Matsui M. A Potential Use of Color Ultrasound as a Tool for Reproductive Management: New Observations Using Color Ultrasound Scanning that were not Possible with Imaging Only in Black and White. Journal of Reproduction and Development. 2006;52:153-60.

[25] Acosta TJ, Hayashi KG, Ohtani M, Miyamoto A. Local changes in blood flow within the preovulatory follicle wall and early corpus luteum in cows. Reproduction. 2003;125:759-67.

[26] Acosta TJ, Miyamoto A. Vascular control of ovarian function: ovulation, corpus luteum formation and regression. Anim Reprod Sci. 2004;82-83:127-40.

[27] Kanazawa T, Seki M, Ishiyama K, Kubo T, Kaneda Y, Sakaguchi M, Izaike Y, Takahashi T. Pregnancy prediction on the day of embryo transfer (Day 7) and Day 14 by measuring luteal blood flow in dairy cows. Theriogenology. 2016;86:1436-44.

[28] Bollwein H, Heppelmann M, Luttgenau J. Ultrasonographic Doppler Use for Female Reproduction Management. Vet Clin North Am Food Anim Pract. 2016;32:149-64.

[29] Acosta TJ. Studies of follicular vascularity associated with follicle selection and ovulation in cattle. J Reprod Dev. 2007;53:39-44.

[30] Viana JH, Arashiro EKN, Siqueira LG, Ghetti AM, Areas VS, Guimaraes CRB, Palhao MP, Camargo LSA, Fernandes CA. Doppler ultrasonography as a tool for ovarian management. Anim Reprod. 2013;10:215-22.

[31] Varughese EE, Brar PS, Honparkhe M, Ghuman SP. Correlation of blood flow of the preovulatory follicle to its diameter and endocrine profile in dairy buffalo. Reprod Domest Anim. 2014;49:140-4.

[32] Neglia G, Restucci B, Russo M, Vecchio D, Gasparrini B, Prandi A, Di Palo R, D'Occhio MJ, Campanile G. Early development and function of the corpus luteum and relationship to pregnancy in the buffalo. Theriogenology. 2015;83:959-67.

[33] Vecchio D, Neglia G, Gasparrini B, Russo M, Pacelli C, Prandi A, D'Occhio MJ, Campanile G. Corpus luteum development and function and relationship to pregnancy during the breeding season in the Mediterranean buffalo. Theriogenology. 2012;77:1811-5.

[34] Di Francesco S, Neglia G, Vecchio D, Rossi P, Russo M, Zicarelli L, D'Occhio MJ, Campanile G. Influence of season on corpus luteum structure and function and AI outcome in the Italian Mediterranean buffalo (Bubalus bubalis). Theriogenology. 2012;78:1839-45.

[35] Campanile G, Baruselli PS, Neglia G, Vecchio D, Gasparrini B, Gimenes LU, Zicarelli L, D'Occhio MJ. Ovarian function in the buffalo and implications for embryo development and assisted reproduction. Anim Reprod Sci. 2010;121:1-11.

[36] Brogliatti GM, Salamone DF, Adams GP. Ovarian follicular wave synchronization and superstimulation in prepubertal calves. Theriogenology. 1997;47:1253-64.

[37] Ghetti AM, Brandao FZ, Siqueira LG, Areas VS, Arashiro EKN, Fernandes CA, Palhao MP, Viana JH. Comparison of objective and subjective methods for evaluating the vascular pattern of the preovulatory follicle using color Doppler. Anim Reprod. 2012;9:657.

[38] Jokubkiene L, Sladkevicius P, Rovas L, Valentin L. Assessment of changes in volume and vascularity of the ovaries during the normal menstrual cycle using three-dimensional power Doppler ultrasound. Hum Reprod. 2006;21:2661-8.

[39] Ortega Serrano PV, Guzman A, Hernandez-Coronado CG, Castillo-Juarez H, Rosales-Torres AM. Reduction in the mRNA expression of sVEGFR1 and sVEGFR2 is associated with the selection of dominant follicle in cows. Reprod Domest Anim. 2016;51:985-91.

[40] Yamada O, Abe M, Takehana K, Hiraga T, Iwasa K, Hiratsuka T. Microvascular Changes During the Development of Follicles in Bovine Ovaries: A Study of Corrosion Casts by Scanning Electron Microscopy. Archives of Histology and Cytology. 1995;58:567-74.

[41] Pierson RA, Ginther OJ. Ultrasonography of the Bovine Ovary. Theriogenology. 1984;21:495-504.

[42] Sirois J, Fortune JE. Ovarian Follicular Dynamics during the Estrous Cycle in Heifers Monitored by Real-Time Ultrasonography. Biology of Reproduction. 1988;39:308-17.

[43] Ginther OJ, Wiltbank MC, Fricke PM, Gibbons JR, Kot K. Selection of the Dominant Follicle in Cattle. Biology of Reproduction. 1996;55:1187-94.

[44] Adams GP, Singh J. Ovarian follicular and luteal dynamics in cattle. In: Hopper RM, editor. Bovine Reproduction. Ames, Iowa: John Wiley & Sons, Inc.; 2015. p. 219-44.

[45] Manik RS, Madan ML, Singla SK. Ovarian follicular dynamics in water buffaloes (*Bubalus bubalis*): ultrasonically monitoring individual follicles for wave hypothesis. Theriogenology. 1994;41:246.

[46] Baruselli PS, Mucciolo RG, Visintin JA, Viana WG, Arruda RP, Madureira EH, Oliveira CA, Molero-Filho JR. Ovarian follicular dynamics during the estrous cycle in buffalo (*Bubalus bubalis*). Theriogenology. 1997;47:1531-47.

[47] Bergfelt DR, Lightfoot KC, Adams GP. Ovarian synchronization following ultrasound-guided transvaginal follicle ablation in heifers. Theriogenology. 1994;42:895-907.

[48] Bo GA, Adams GP, Pierson RA, Mapletoft RJ. Exogenous control of follicular wave emergence in cattle. Theriogenology. 1995;43:31-40.

[49] Adams GP, Jaiswal R, Singh J, Malhi P. Progress in understanding ovarian follicular dynamics in cattle. Theriogenology. 2008;69:72-80.

[50] Pfeifer LF, Adams GP, Pierson RA, Singh J. Ultrasound biomicroscopy: a non-invasive approach for in vivo evaluation of oocytes and small antral follicles in mammals. Reprod Fertil Dev. 2013;26:48-54.

[51] Pfeifer LF, Siqueira LG, Adams GP, Pierson RA, Singh J. In vivo imaging of cumulus-oocyte-complexes and small ovarian follicles in cattle using ultrasonic biomicroscopy. Anim Reprod Sci. 2012;131:88-94.

[52] Jaiswal RS, Singh J, Adams GP. Developmental pattern of small antral follicles in the bovine ovary. Biol Reprod. 2004;71:1244-51.

[53] Sartori R, Fricke PM, Ferreira JCP, Ginther OJ, Wiltbank MC. Follicular Deviation and Acquisition of Ovulatory Capacity in Bovine Follicles. Biology of Reproduction. 2001;65:1403-9.

[54] Beg MA, Ginther OJ. Follicle selection in cattle and horses: role of intrafollicular factors. Reproduction. 2006;132:365-77.

[55] Nogueira MF, Buratini J, Jr., Price CA, Castilho AC, Pinto MG, Barros CM. Expression of LH receptor mRNA splice variants in bovine granulosa cells: changes with follicle size and regulation by FSH in vitro. Mol Reprod Dev. 2007;74:680-6.

[56] Luo W, Gumen A, Haughian JM, Wiltbank MC. The role of luteinizing hormone in regulating gene expression during selection of a dominant follicle in cattle. Biol Reprod. 2011;84:369-78.

[57] Acosta TJ, Gastal EL, Gastal MO, Beg MA, Ginther OJ. Differential blood flow changes between the future dominant and subordinate follicles precede diameter changes during follicle selection in mares. Biol Reprod. 2004;71:502-7.

[58] Acosta TJ, Hayashi K, Matsui M, Miyamoto A. Changes in Follicular Vascularity during the First Follicular Wave in Lactating Cows. Journal of Reproduction and Development. 2005;51:273-80.

[59] Berisha B, Schams D, Rodler D, Pfaffl MW. Angiogenesis in The Ovary - The Most Important Regulatory Event for Follicle and Corpus Luteum Development and Function in Cow - An Overview. Anat Histol Embryol. 2016;45:124-30.

[60] Berisha B, Schams D, Kosmann M, Amselgruber W, Einspanier R. Expression and localisation of vascular endothelial growth factor and basic fibroblast growth factor during the final growth of bovine ovarian follicles. Journal of Endocrinology. 2000;167:371-82.

[61] Bollwein H, Luttgenau J, Herzog K. Bovine luteal blood flow: basic mechanism and clinical relevance. Reprod Fertil Dev. 2013;25:71-9.

[62] Pancarci SM, Gungor O, Atakisi O, Cigremis Y, Ari UC, Bollwein H. Changes in follicular blood flow and nitric oxide levels in follicular fluid during follicular deviation in cows. Anim Reprod Sci. 2011;123:149-56.

[63] Miura R, Haneda S, Lee HH, Miyamoto A, Shimizu T, Miyahara K, Miyake Y, Matsui M. Evidence that the dominant follicle of the first wave is more active than that of the second wave in terms of its growth rate, blood flow supply and steroidogenic capacity in cows. Anim Reprod Sci. 2014;145:114-22.

[64] Singh J, Pierson RA, Adams GP. Ultrasound image attributes of bovine ovarian follicles and endocrine and functional correlates. Journal of Reproduction and Fertility. 1998;112:19-29.

[65] Singh J, Adams GP. Histomorphometry of dominant and subordinate bovine ovarian follicles. The Anatomic Record. 2000;258:58-70.

[66] Fraser HM. Regulation of the ovarian follicular vasculature. Reprod Biol Endocrinol. 2006;4:18.

[67] Gimenes LU, Carvalho NA, Sa Filho MF, Vannucci FS, Torres-Junior JR, Ayres H, Ferreira RM, Trinca LA, Sartorelli ES, Barros CM, Beltran MP, Nogueira GP, Mapletoft RJ, Baruselli PS. Ultrasonographic and endocrine aspects of follicle deviation, and acquisition of ovulatory capacity in buffalo (Bubalus bubalis) heifers. Anim Reprod Sci. 2011;123:175-9.

[68] Kauffold J, Amer HAH, Bergfeld U, Weber W, Sobiraj A. The In Vitro Developmental Competence of Oocytes from Juvenile Calves is Related to Follicular Diameter. Journal of Reproduction and Development. 2005;51:325-32.

[69] de Tarso SGS, Apgar GA, Gastal MO, Gastal EL. Relationships between follicle and corpus luteum diameter, blood flow, and progesterone production in beef cows and heifers: preliminary results. Animal Reproduction. 2016;13:81-92.

[70] Siddiqui MA, Almamun M, Ginther OJ. Blood flow in the wall of the preovulatory follicle and its relationship to pregnancy establishment in heifers. Anim Reprod Sci. 2009;113:287-92.

[71] Vernunft A, Weitzel JM, Viergutz T. Corpus luteum development and its morphology after aspiration of a preovulatory follicle is related to size and steroid content of the follicle in dairy cows. Veterinarni Medicina. 2013;58:221-9.

[72] Beg MA, Bergfelt DR, Kot K, Wiltbank MC, Ginther OJ. Follicular-Fluid Factors and Granulosa-Cell Gene Expression Associated with Follicle Deviation in Cattle. Biology of Reproduction. 2001;64:432-41.

[73] Pancarci SM, Ari UC, Atakisi O, Gungor O, Cigremis Y, Bollwein H. Nitric oxide concentrations, estradiol-17beta progesterone ratio in follicular fluid, and COC quality with respect to perifollicular blood flow in cows. Anim Reprod Sci. 2012;130:9-15.

[74] Battaglia C, Regnani G, Marsella T, Facchinetti F, Volpe A, Venturoli S, Flamigni C. Adjuvant L-arginine treatment in controlled ovarian hyperstimulation: a double-blind, randomized study. Human Reproduction. 2002;17:659-65.

[75] Chen Z, Yuhanna IS, Galcheva-Gargova Z, Karas RH, Mendelsohn ME, Shaul PW. Estrogen receptor a mediates the nongenomic activation of endothelial nitric oxide synthase by estrogen. J Clin Invest. 1999;103:401-6.

[76] Lucy MC, Savio JD, Badinga L, De La Sota RL, Thatcher WW. Factors That Affect Ovarian Follicular Dynamics in Cattle. J Anim Sci. 1992;70:3615-26.

[77] Sunderland SJ, Crowe MA, Boland MP, Roche JF, Ireland JJ. Selection, dominance and atresia of follicles during the oestrous cycle of heifers. J Reprod and Fert. 1994;101:547-55.

[78] Hayashi K, Matsui M, Acosta TJ, Kida K, Miyamoto A. Effect of the dominant follicle aspiration before or after luteinizing hormone surge on the corpus luteum formation in the cow. J Reprod Dev. 2006;52:129-35.

[79] Honparkhe M, Singh J, Dadarwal D, Dhaliwal GS, Kumar A. Estrus induction and fertility rates in response to exogenous hormonal administration in postpartum anestrous and subestrus bovines and buffaloes. J Vet Med Sci. 2008;70:1327-31.

[80] Martinez MF, Adams GP, Bergfelt DR, Kastelic JP, Mapletoft RJ. Effect of LH or GnRH on the dominant follicle of the first follicular wave in beef heifers. Animal Reproduction Science. 1999;57:23-33.

[81] Bo GA, Mapletoft RJ. Historical perspectives and recent research on superovulation in cattle. Theriogenology. 2014;81:38-48.

[82] Drost M, Wright Jr JM, Cripe WS, Richter AR. Embryo transfer in water buffalo (*Bubalus bubalis*). Theriogenology. 1983;20:579-84.

[83] Singh J, Nanda AS, Adams GP. The reproductive pattern and efficiency of female buffaloes. Animal Reproduction Science. 2000;60-61:593-604.

[84] Mapletoft RJ, Garcia Guerra A, Dias FCF, Singh J, Adams GP. *In vitro* and *in vivo* embryo production in cattle superstimulated with FSH for 7 days. Anim Reprod. 2015;12:383-8.

[85] De Rensis F, Ronci G, Guarneri P, Nguyen BX, Presicce GA, Huszenicza G, Scaramuzzi RJ. Conception rate after fixed time insemination following ovsynch protocol with and without progesterone supplementation in cyclic and non-cyclic Mediterranean Italian buffaloes (Bubalus bubalis). Theriogenology. 2005;63:1824-31.

[86] Mirmahmoudi R, Souri M, Prakash BS. Endocrine changes, timing of ovulation, ovarian follicular growth and efficacy of a novel protocol (Estradoublesynch) for synchronization of ovulation and timed artificial insemination in Murrah buffaloes (Bubalus bubalis). Theriogenology. 2014;81:237-42.

[87] Mirmahmoudi R, Prakash BS. The endocrine changes, the timing of ovulation and the efficacy of the Doublesynch protocol in the Murrah buffalo (Bubalus bubalis). Gen Comp Endocrinol. 2012;177:153-9.

[88] Perera BM. Reproductive cycles of buffalo. Anim Reprod Sci. 2011;124:194-9.

[89] Adams GP, Kot K, Smith CA, Ginther OJ. Selection of a dominant follicle and supression of follicular growth in heifers. Animal Reproduction Science. 1993;30:259-71.

[90] Dias FC, Khan MI, Adams GP, Sirard MA, Singh J. Granulosa cell function and oocyte competence: Super-follicles, super-moms and super-stimulation in cattle. Anim Reprod Sci. 2014;149:80-9.

[91] Dias FC, Khan MI, Sirard MA, Adams GP, Singh J. Differential gene expression of granulosa cells after ovarian superstimulation in beef cattle. Reproduction. 2013;146:181-91.

[92] Dias FCF. Effects of follicular aging and duration of superstimulation on oocyte competence and granulosa cell gene expression in cattle. Saskatoon, SK, Canada: University of Saskatchewan; 2013.

[93] Bassil S, Wyns C, Toussaint-Demylle D, Nisolle M, Gordts S, Donnez J. The relationship between ovarian vascularity and the duration of stimulation in in-vitro fertilization. Human Reproduction. 1997;12:1240-5.

[94] Oliveira ME, Feliciano MA, D'Amato CC, Oliveira LG, Bicudo SD, Fonseca JF, Vicente WR, Visco E, Bartlewski PM. Correlations between ovarian follicular blood flow and superovulatory responses in ewes. Anim Reprod Sci. 2014;144:30-7.

[95] Fatima LA, Binelli M, Baruselli PS, Bonfim Neto AP, Papa PC. Angiogenic and steroidogenic responses of the corpus luteum after superovulatory and stimulatory treatments using eCG and FSH. Anim Reprod. 2012;9:273-80.

[96] Honnens A, Niemann H, Herzog K, Paul V, Meyer HH, Bollwein H. Relationships between ovarian blood flow and ovarian response to eCG-treatment of dairy cows. Anim Reprod Sci. 2009;113:1-10.

[97] Bhal PS, Pugh ND, Gregory L, O'Brien S, Shaw RW. Perifollicular vascularity as a potential variable affecting outcome in stimulated intrauterine insemination treatment cycles: a study using transvaginal power Doppler. Human Reproduction 2001;16:1682-9.

[98] Arora A, Gainder S, Dhaliwal L, Suri V. Clinical significance of ovarian stromal blood flow in assessment of ovarian response in stimulated cycle for in vitro fertilization. International Journal of Reproduction, Contraception, Obstetrics and Gynecology. 2015:1380-3.

[99] Souza SS, Alves BG, Alves KA, Santos JDR, Diogenes YP, Bhat MH, Melo LM, Freitas VJF, Teixeira DIA. Relationship of Doppler velocimetry parameters with antral follicular population and oocyte quality in Canindé goats. Small Ruminant Research. 2016;141:39-44.

[100] Thatcher WW, Drost M, Savio JD, Macmillan KL, Entwistle KW, Schmitt EJ, De la Sota RL, Morris GR. New clinical uses of GnRH and its analogues in cattle. Anim Reprod Sci. 1993;33:27-49.

[101] Paul V, Prakash BS. Efficacy of the Ovsynch protocol for synchronization of ovulation and fixed-time artificial insemination in Murrah buffaloes (Bubalus bubalis). Theriogenology. 2005;64:1049-60.

[102] Perry GA, Smith MF, Lucy MC, Green JA, Parks TE, MacNeil MD, Roberts AJ, Geary TW. Relationship between follicle size at insemination and pregnancy success. Proc Natl Acad Sci U S A. 2005;102:5268-73.

[103] Dadarwal D, Mapletoft RJ, Adams GP, Pfeifer LF, Creelman C, Singh J. Effect of progesterone concentration and duration of proestrus on fertility in beef cattle after fixed-time artificial insemination. Theriogenology. 2013;79:859-66.

[104] Niswender GD, Juengel JL, Silva PJ, Rollyson MK, McIntush EW. Mechanisms controlling the function and life span of the corpus luteum. Physiol Rev. 2000;80:1-29.

[105] Powers RW, Chen L, Russell PT, Larsen WJ. Gonadotropin-stimulated regulation of blood-follicle barrier is mediated by nitric oxide. American Journal of Physiology-Endocrinology And Metabolism. 1995;269:E290-E8.

[106] Siddiqui MA, Ferreira JC, Gastal EL, Beg MA, Cooper DA, Ginther OJ. Temporal relationships of the LH surge and ovulation to echotexture and power Doppler signals of blood flow in the wall of the preovulatory follicle in heifers. Reprod Fertil Dev. 2010;22:1110-7.

[107] Brogliatti GM, Adams GP. Ultrasound-guided transvaginal oocyte collection in prepubertal calves. Theriogenology. 1996;45:1163-76.

[108] Neglia G, Gasparrini B, di Brienza VC, Di Palo R, Campanile G, Presicce GA, Zicarelli L. Bovine and buffalo in vitro embryo production using oocytes derived from abattoir ovaries or collected by transvaginal follicle aspiration. Theriogenology. 2003;59:1123-30.

[109] Palomino JM, McCorkell RB, Woodbury MR, Cervantes MP, Adams GP. Ovarian superstimulation and oocyte collection in wood bison (Bison bison athabascae) during the ovulatory season. Theriogenology. 2014;81:250-6.

[110] Cook NL, Squires EL, Ray BS, Jasko DJ. Transvaginal ultrasound-guided follicular aspiration of equine oocytes. Equine Veterinary Journal. 1993;25:71-4.

[111] Nargund G, Bourne T, Doyle P, Parsons J, Cheng W, Campbell S, Collins W. Associations between ultrasound indices of follicular blood flow, oocyte recovery and preimplantation embryo quality. Human Reproduction. 1996;11:109-13.

[112] Manjunatha BM, Ravindra JP, Gupta PS, Devaraj M, Nandi S. Effect of breeding season on in vivo oocyte recovery and embryo production in non-descriptive Indian river buffaloes (Bubalus bubalis). Anim Reprod Sci. 2009;111:376-83.

[113] Rodriguez C, Anel L, Alvarez M, Anel E, Boixo JC, Chamorro CA, de Paz P. Ovum Pick-up in Sheep: a Comparison between Different Aspiration Devices for Optimal Oocyte Retrieval. Reprod Dom Anim. 2006;41:106-13.

[114] Siddiqui MA, Gastal EL, Gastal MO, Almamun M, Beg MA, Ginther OJ. Relationship of vascular perfusion of the wall of the preovulatory follicle to in vitro fertilisation and embryo development in heifers. Reproduction. 2009;137:689-97.

[115] Ginther OJ, Gastal EL, Gastal MO, Siddiqui MA, Beg MA. Relationships of follicle versus oocyte maturity to ultrasound morphology, blood flow, and hormone concentrations of the preovulatory follicle in mares. Biol Reprod. 2007;77:202-8.

[116] Dias FC, Dadarwal D, Adams GP, Mrigank H, Mapletoft RJ, Singh J. Length of the follicular growing phase and oocyte competence in beef heifers. Theriogenology. 2013;79:1177-83 e1.

[117] Garcia Guerra A, Tribulo A, Yapura J, Singh J, Mapletoft RJ. Lengthening the superstimulatory treatment protocol increases ovarian response and number of transferable embryos in beef cows. Theriogenology. 2012;78:353-60.

[118] Gandolfi F, Luciano AM, Modina S, Ponzini A, Pocar P, Armstrong DT, Lauria A. The in vitro developmental competence of bovine oocytes can be related to the morphology of the ovary. Theriogenology. 1997;48:1153-60.

[119] Vassena R, Adams GP, Mapletoft RJ, Pierson RA, Singh J. Ultrasound image characteristics of ovarian follicles in relation to oocyte competence and follicular status in cattle. Anim Reprod Sci. 2003;76:25-41.

[120] Lozano DH, Frydman N, Levaillant JM, Fay S, Frydman R, Fanchin R. The 3D vascular status of the follicle after HCG administration is qualitatively rather than quantitatively associated with its reproductive competence. Hum Reprod. 2007;22:1095-9.

[121] Pinaffi FLV, Santos ÉS, Silva MGd, Maturana Filho M, Madureira EH, Silva LA. Follicle and corpus luteum size and vascularity as predictors of fertility at the time of artificial insemination and embryo transfer in beef cattle. Pesquisa Veterinária Brasileira. 2015;35:470-6.

[122] Alila HW, Dowd JP, Corradino RA, Harris WV, Hansel W. Control of progesterone production in small and large bovine luteal cells separated by flow cytometry. J Reprod and Fert. 1988;82:645-55.

[123] Robinson RS, Woad KJ. Luteal Angiogenesis. 2017:1-21.

[124] Dickson SE, Fraser HM. Inhibition of early luteal angiogenesis by gonadotropin-releasing hormone antagonist treatment in the primate. J Clin Endocrinol Metab. 2000;85:2339-44.

[125] Fraser HM, Dickson SE, Lunn SF, Wulff C, Morris KD, Carroll VA, Bicknell R. Suppression of luteal angiogenesis in the primate after neutralization of vascular endothelial growth factor. Endocrinology. 2000;141:995-1000.

[126] Yamashita H, Kamada D, Shirasuna K, Matsui M, Shimizu T, Kida K, Berisha B, Schams D, Miyamoto A. Effect of local neutralization of basic fibroblast growth factor or vascular endothelial growth factor by a specific antibody on the development of the corpus luteum in the cow. Mol Reprod Dev. 2008;75:1449-56.

[127] Kastelic JP, Bergfelt DR, Ginther OJ. Relationship between ultrasonic assessment of the corpus luteum and plasma progesterone concentration in heifers. Theriogenology. 1990;33:1269-78.

[128] Luttgenau J, Beindorff N, Ulbrich SE, Kastelic JP, Bollwein H. Low plasma progesterone concentrations are accompanied by reduced luteal blood flow and increased size of the dominant follicle in dairy cows. Theriogenology. 2011;76:12-22.

[129] Miyamoto A, Shirasuna K, Wijayagunawardane MP, Watanabe S, Hayashi M, Yamamoto D, Matsui M, Acosta TJ. Blood flow: a key regulatory component of corpus luteum function in the cow. Domest Anim Endocrinol. 2005;29:329-39.

[130] Singh J, Pierson RA, Adams GP. Ultrasound image attributes of the bovine corpus luteum: structural and functional correlates. Journal of Reproduction and Fertility. 1997;109:35-44.

[131] Thijssen JM, Herzog K, Weijers G, Brockhan-Luedemann M, Starke A, Niemann H, Bollwein H, de Korte CL. Ultrasound image analysis offers the opportunity to predict plasma progesterone concentrations in the estrous cycle in cows: a feasibility study. Anim Reprod Sci. 2011;127:7-15.

[132] Miyazaki T, Tanaka M, Miyakoshi K, Minegishi K, Kasai K, Yoshimura Y. Power and colour Doppler ultrasonography for the evaluation of the vasculature of the human corpus luteum. Human Reproduction. 1998;13:2836-41.

[133] Gordon JD, Shifren JL, Foulk RA, Taylor RN, Jaffe RB. Angiogenesis in the Human Female Reproductive Tract. Obstetrical & Gynecological Survey. 1995;50:688-97.

[134] Russo M, Vecchio D, Neglia G, Pacelli C, Prandi A, Gasparrini B, Zicarelli L, D'Occhio MJ, Campanile G. Corpus luteum function and pregnancy outcome in buffaloes during the transition period from breeding to non-breeding season. Reprod Domest Anim. 2010;45:988-91.

[135] Beindorff N, Honnens A, Penno Y, Paul V, Bollwein H. Effects of human chorionic gonadotropin on luteal blood flow and progesterone secretion in cows and in vitro-microdialyzed corpora lutea. Theriogenology. 2009;72:528-34.

[136] Brito LFC, Satrapa R, Marson EP, Kastelic JP. Efficacy of PGF2alpha to synchronize estrus in water buffalo cows (*Bubalus bubalis*) is dependent upon plasma progesterone concentration, corpus luteum size and ovarian follicular status before treatment. Animal Reproduction Science. 2002;73:23-35.

[137] Okuda K, Miyamoto Y, Skarzynski DJ. Regulation of endometrial prostaglandin F2$\alpha$ synthesis during luteolysis and early pregnancy in cattle. Domest Anim Endocrinol. 2002;23:255-64.

[138] Ginther OJ, Silva LA, Araujo RR, Beg MA. Temporal associations among pulses of 13,14-dihydro-15-keto-PGF2alpha, luteal blood flow, and luteolysis in cattle. Biol Reprod. 2007;76:506-13.

[139] Shirasuna K, Watanabe S, Asahi T, Wijayagunawardane MP, Sasahara K, Jiang C, Matsui M, Sasaki M, Shimizu T, Davis JS, Miyamoto A. Prostaglandin F2alpha increases endothelial nitric oxide synthase in the periphery of the bovine corpus luteum: the possible regulation of blood flow at an early stage of luteolysis. Reproduction. 2008;135:527-39.

[140] Kerbler TL, Buhr MM, Jordan LT, Leslie KE, Walton JS. Relationship between maternal plasma progesterone concentration and interferon-tau synthesis by the conceptus in cattle. Theriogenology. 1997;47:703-14.

[141] Campanile G, Neglia G, D'Occhio MJ. Embryonic and fetal mortality in river buffalo (Bubalus bubalis). Theriogenology. 2016;86:207-13.

[142] Herzog K, Brockhan-Ludemann M, Kaske M, Beindorff N, Paul V, Niemann H, Bollwein H. Luteal blood flow is a more appropriate indicator for luteal function during the bovine estrous cycle than luteal size. Theriogenology. 2010;73:691-7.

[143] Herzog K, Voss C, Kastelic JP, Beindorff N, Paul V, Niemann H, Bollwein H. Luteal blood flow increases during the first three weeks of pregnancy in lactating dairy cows. Theriogenology. 2011;75:549-54.

[144] Pugliesi G, Silva JCB, Nishimura T, Miyai D, Silva LA, Binelli M. Use of color-Doppler ultrasonography to improve selection of higher fertility beef recipient cows for embryo transfer. Anim Reprod. 2016;13:454.

[145] Neglia G, Vecchio D, Russo M, Di Palo R, Pacelli C, Comin A, Gasparrini B, Campanile G. Efficacy of PGF(2alpha) on pre-ovulatory follicle and corpus luteum blood flow. Reprod Domest Anim. 2012;47:26-31.

[146] Guimaraes CR, Oliveira ME, Rossi JR, Fernandes CA, Viana JH, Palhao MP. Corpus luteum blood flow evaluation on Day 21 to improve the management of embryo recipient herds. Theriogenology. 2015;84:237-41.

[147] Rodrigues AS, Silva MAA, Brandao TO, Santos ES, Maggitti Junior LDP, Flores ER, da Silva JBR, Bittencourt RF, Chalhoub M, Ribeiro Filho AL. Morphological evaluation of the corpus luteum and use of doppler ultrasound as pregnancy prediction tool for 20 days post TAI in crossbred cows. Anim Reprod. 2016;13:428.

[148] Siqueira LG, Areas VS, Ghetti AM, Fonseca JF, Palhao MP, Fernandes CA, Viana JH. Color Doppler flow imaging for the early detection of nonpregnant cattle at 20 days after timed artificial insemination. J Dairy Sci. 2013;96:6461-72.

[149] Jarvela IY, Sladkevicius P, Kelly S, Ojha K, Campbell S, Nargund G. Quantification of ovarian power doppler signal with Three-Dimensional ultrasonography to predict response during in vitro fertilization. Obstetrics & Gynecology. 2003;102:816-22.

[150] Kupesic S, Kurjak A, Bjelos D, Vujisic S. Three-dimensional ultrasonographic ovarian measurements and in vitro fertilization outcome are related to age. Fertil Steril. 2003;79:190-7.

[151] Merce LT, Bau S, Barco MJ, Troyano J, Gay R, Sotos F, Villa A. Assessment of the ovarian volume, number and volume of follicles and ovarian vascularity by three-dimensional ultrasonography and power Doppler angiography on the HCG day to predict the outcome in IVF/ICSI cycles. Hum Reprod. 2006;21:1218-26.

[152] Vlaisavljevic V, Reljic M, Gavric Lovrec V, Zazula D, Sergent N. Measurement of perifollicular blood flow of the dominant preovulatory follicle using three-dimensional power Doppler. Ultrasound Obstet Gynecol. 2003;22:520-6.

[153] Fleischer AC. Recent advances in the sonographic assessment of vascularity and blood flow in gynecologic conditions. Am J Obstet Gynecol. 2005;193:294-301.

[154] Gomez B, Alvarez P, Bajo JM, Engels V, Martinez A, De la Fuente J. Corpus luteum morphology and vascularization assessed by transvaginal two-dimensional and three-dimensional ultrasound. Donald School Journal of Ultrasound in Obstetrics and Gynecology. 2007;1:42-9.

[155] Mickelsen WD, Wright Jr RW, Menino AR, Zamora CS, Paisley LG. Superovulation, fertilization and embryo recovery in gonadotropin treated prepubertal calves. Theriogenology. 1978;10:167-74.

[156] Testart J, Kann G, Saumande J, Thibier M. Oestradiol-17β, progesterone, FSH and LH in prepubertal calves induced to superovulate. J Reprod and Fert. 1977;51:329-36.

[157] Maclellan LJ, Whyte TR, Murray A, Fitzpatrick LA, Earl CR, Aspden WJ, Kinder JE, Grotjan HE, Walsh J, Trigg TE, D'Occhio MJ. Superstimulation of ovarian follicular growth with FSH, oocyte recovery, and embryo production from Zebu (*Bos indicus*) calves: effects of treatment with a GnRH agonist or antagonist. Theriogenology. 1998;49:1317-29.

[158] Brannstrom M, Zackrisson U, Hagstrom H, Josefsson B, Hellberg P, Granberg S, Collins WP, Bourne T. Preovulatory changes of blood flow in different regions of the human follicle. Fertil Steril. 1998;69:435-42.

[159] Scully S, Evans AC, Duffy P, Crowe MA. Characterization of follicle and CL development in beef heifers using high resolution three-dimensional ultrasonography. Theriogenology. 2014;81:407-18.

[160] Silva LA, Gastal EL, Gastal MO, Beg MA, Ginther OJ. Relationship between vascularity of the preovulatory follicle and establishment of pregnancy in mares. Anim Reprod. 2006;3:339-46.

[161] Coulam CB, Goodman C, Rinehart JS. Colour Doppler indices of follicular blood flow as predictors of pregnancy after in-vitro fertilization and embryo transfer. Human Reproduction. 1999;14:1979-82.

[162] Borini A, Maccoloni A, Tallarini A, Bonu MA, Sciajno R, Flamigni C. Perifollicular vascularity and its relationship with oocyte maturity and IVF outcome. Ann N Y Acad Sci. 2001;943:64-7.

[163] Monteleone P, Giovanni Artini P, Simi G, Casarosa E, Cela V, Genazzani AR. Follicular fluid VEGF levels directly correlate with perifollicular blood flow in normoresponder patients undergoing IVF. J Assist Reprod Genet. 2008;25:183-6.

[164] Utt MD, Johnson III GL, Beal WE. The evaluation of corpus luteum blood flow using color-flow Doppler ultrasound for early pregnancy diagnosis in bovine embryo recipients. Theriogenology. 2009;71:707-15.

[165] Revelli A, Martiny G, Piane LD, Benedetto C, Rinaudo P, Tur-Kaspa I. A critical review of bi-dimensional and threedimensional ultrasound techniques to monitor follicle growth: do they help improving IVF outcome? Reprod Biol Endocrinol. 2014;12:107-14.

[166] Baerwald A, Dauk S, Kanthan R, Singh J. Use of ultrasound biomicroscopy to image human ovaries in vitro. Ultrasound Obstet Gynecol. 2009;34:201-7.

[167] Perry GA, Smith MF, Roberts AJ, MacNeil MD, Geary TW. Relationship between size of the ovulatory follicle and pregnancy success in beef heifers. J Anim Sci. 2007;85:684-9.

[168] Grazul-Bilska AT, Navanukraw C, Johnson ML, Vonnahme KA, Ford SP, Reynolds LP, Redmer DA. Vascularity and expression of angiogenic factors in bovine dominant follicles of the first follicular wave. J Anim Sci. 2007;85:1914-22.

[169] Adams GP, Evans ACO, Rawlings NC. Follicular waves and circulating gonadotrophins in 8-month-old prepubertal heifers. J Reprod and Fert. 1994;100:27-33.

[170] Gandolfi F, Milanesi E, Pocar P, Luciano AM, Brevini TAL, Acocella F, Lauria A, Armstrong DT. Comparative analysis of calf and cow oocytes during in vitro maturation. Molecular Reproduction and Development. 1998;49:168-75.

[171] Duby RT, Damiani P, Looney CR, Fissore RA, Robl JM. Prepuberal calves as oocyte donors: promises and problems. Theriogenology. 1996;45:121-30.

[172] Landry DA, Bellefleur AM, Labrecque R, Grand FX, Vigneault C, Blondin P, Sirard MA. Effect of cow age on the in vitro developmental competence of oocytes obtained after FSH stimulation and coasting treatments. Theriogenology. 2016;86:1240-6.

[173] Dadarwal D, Honparkhe M, Dias FC, Alce T, Lessard C, Singh J. Effect of superstimulation protocols on nuclear maturation and distribution of lipid droplets in bovine oocytes. Reprod Fertil Dev. 2015;27:1137-46.

[174] Dadarwal D, Dias FC, Adams GP, Singh J. Effect of follicular aging on ATP content and mitochondria distribution in bovine oocytes. Theriogenology. 2017;89:348-58.

[175] Smith MF, McIntush EW, Smith GW. Mechanisms associated with corpus luteum development. J Anim Sci. 1994;72:1857-72.

[176] O'Hara L, Scully S, Maillo V, Kelly AK, Duffy P, Carter F, Forde N, Rizos D, Lonergan P. Effect of follicular aspiration just before ovulation on corpus luteum characteristics, circulating progesterone concentrations and uterine receptivity in single-ovulating and superstimulated heifers. Reproduction. 2012;143:673-82.

[177] D'Occhio MJ, Jillella D, Lindsey BR. Factors that influence follicle recruitment, growth and ovulation during ovarian superstimulation in heifers: opportunities to increase ovulation rate and embryo receovery by delaying the exposure of follicles to LH. Theriogenology. 1999;51:9-35.

[178] Spilman CH, Seidel GE, Jr., Larson LL, Foote RH. *In vitro* progesterone synthesis by corpora lutea induced in prepubertal cattle. J Anim Sci. 1972;34:1025-30.

[179] Spilman CH, Seidel GE, Larson LL, Vukman GR, Foote RH. Progesterone, 2Oβ-Hydroxypregn-4en-3-one, and Luteinizing Hormone Levels in Superovulated Prepuberal and Postpuberal Cattle. Biology of Reproduction. 1973;9:116-24.

[180] Lonergan P, Fair T. Maturation of Oocytes in Vitro. Annu Rev Anim Biosci. 2016;4:255-68.

[181] Basini G, Grasselli F. Nitric oxide in follicle development and oocyte competence. Reproduction. 2015;150:R1-9.

[182] Einspanier R, Schonfelder M, Muller K, Stojkovic M, Kosmann M, Wolf E, Schamds D. Expression of the vascular endothelial growth factor and its receptors and effects of VEGF during in vitro maturation of bovine cumulus-oocyte complexes (COC). Molecular Reproduction and Development. 2002;62:29-36.

[183] Mossa F, Jimenez-Krassel F, Scheetz D, Weber-Nielsen M, Evans ACO, Ireland JJ. Anti-Mullerian Hormone (AMH) and fertility management in agricultural species. Reproduction. 2017;154:R1-R11.

[184] Singh J, Dominguez M, Jaiswal R, Adams GP. A simple ultrasound test to predict the superstimulatory response in cattle. Theriogenology. 2004;62:227-43.

[185] Ireland JL, Scheetz D, Jimenez-Krassel F, Themmen AP, Ward F, Lonergan P, Smith GW, Perez GI, Evans AC, Ireland JJ. Antral follicle count reliably predicts number of morphologically healthy oocytes and follicles in ovaries of young adult cattle. Biol Reprod. 2008;79:1219-25.

[186] Batista EO, Guerreiro BM, Freitas BG, Silva JC, Vieira LM, Ferreira RM, Rezende RG, Basso AC, Lopes RN, Renno FP, Souza AH, Baruselli PS. Plasma anti-Mullerian hormone as a predictive endocrine marker to select Bos taurus (Holstein) and Bos indicus (Nelore) calves for in vitro embryo production. Domest Anim Endocrinol. 2016;54:1-9.

[187] Gobikrushanth M, Dutra PA, Bruinje TC, Colazo MG, Butler ST, Ambrose DJ. Repeatability of antral follicle counts and anti-Mullerian hormone and their associations determined at an unknown stage of follicular growth and an expected day of follicular wave emergence in dairy cows. Theriogenology. 2017;92:90-4.

[188] Batista EO, Macedo GG, Sala RV, Ortolan MD, Sa Filho MF, Del Valle TA, Jesus EF, Lopes RN, Renno FP, Baruselli PS. Plasma antimullerian hormone as a predictor of ovarian antral follicular population in Bos indicus (Nelore) and Bos taurus (Holstein) heifers. Reprod Domest Anim. 2014;49:448-52.

[189] Elmashad AI. Impact of laparoscopic ovarian drilling on anti-Mullerian hormone levels and ovarian stromal blood flow using three-dimensional power Doppler in women with anovulatory polycystic ovary syndrome. Fertil Steril. 2011;95:2342-6, 6 e1.

[190] Ozdemir O, Sari ME, Kalkan D, Koc EM, Ozdemir S, Atalay CR. Comprasion of ovarian stromal blood flow measured by color Doppler ultrasonography in polycystic ovary syndrome patients and healthy women with ultrasonographic evidence of polycystic. Gynecol Endocrinol. 2015;31:322-6.

[191] Aerts JM, Oste M, Bols PE. Development and practical applications of a method for repeated transvaginal, ultrasound-guided biopsy collection of the bovine ovary. Theriogenology. 2005;64:947-57.

# CHAPTER 7: APPENDIX A

The following Appendix was created to enable the user to build surfaces in Imaris using colour Doppler ultrasound video clips. The details in this Appendix are highlights of important steps. Please refer to the more detailed document for additional instructions (jaswant.singh@usask.ca, or s.caunce@usask.ca).

A supplemental video is also attached to this thesis: S Caunce - supplemental video.mpg

Setting the geometry in Imaris

Step 1:n Fiji (ImageJ)

After setting your scale in Fiji using the built in scale for the ultrasound machine

Sample:
1mm = 9.44pixels
Therefore 1 pixels = 0.106mm

In Fiji go to Image -> Properties
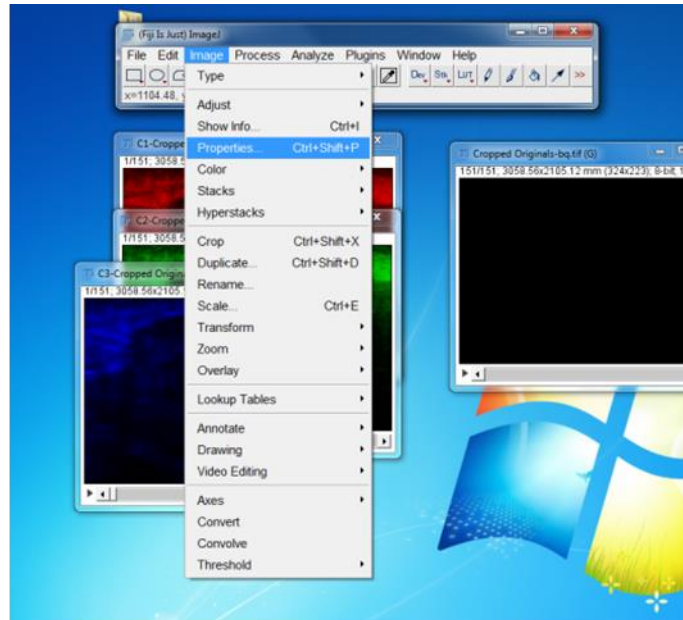


The voxel depth should equal the pixel height and width

Remember these values, as you need to change the Geometry settings in the Imaris software to match its dimensions. 0.106 in this example

Each ultrasound machine will be different (ie using MyLab5 in these instructors will be different than using MyLab alpha)

This will also depend on the depth you used on the ultrasound machine when you recorded.
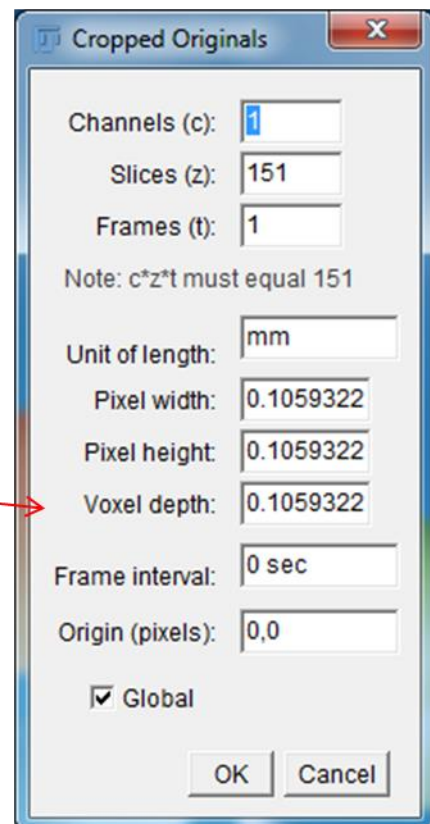
Step 2 for setting the voxel size in Imaris

After you have opened your TIFF files in Imaris
ClickEdit -> Image Properties
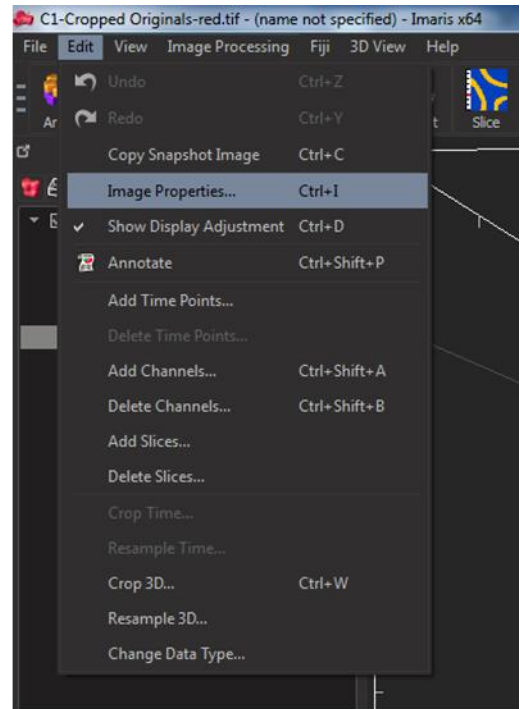


Click Geometry
Change the X, Y, Z voxel size to match that which was in Fiji
- in this example, the voxels are default to 0.00100 and need to be changed to 0.106)
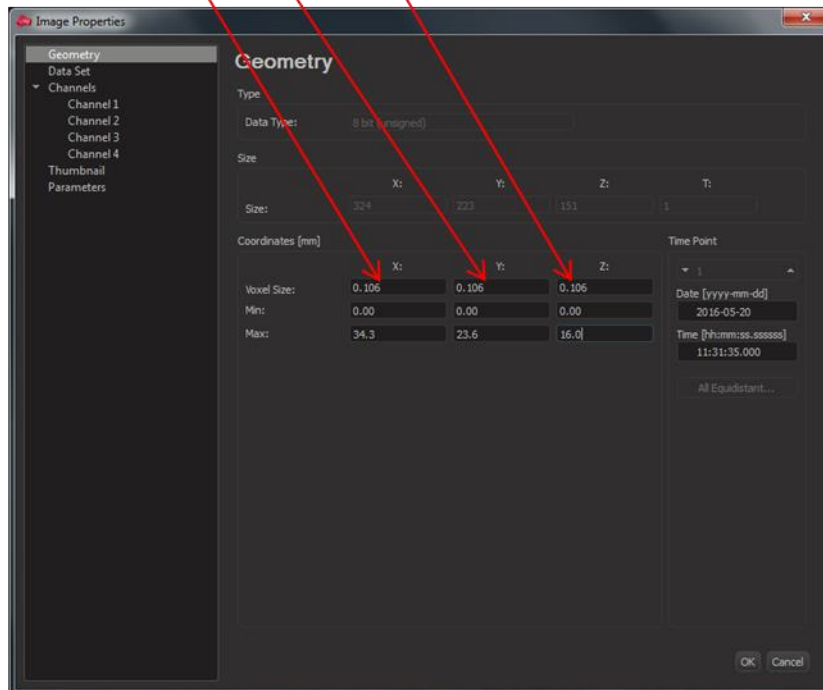
If you have a KNOWN dimension of your Z axis, you can change it here.

In this example the Z axis was calculated as 0.75 of 0.106 = 0.08

Therefore you create a voxel that is 0.106x0.106x0.08
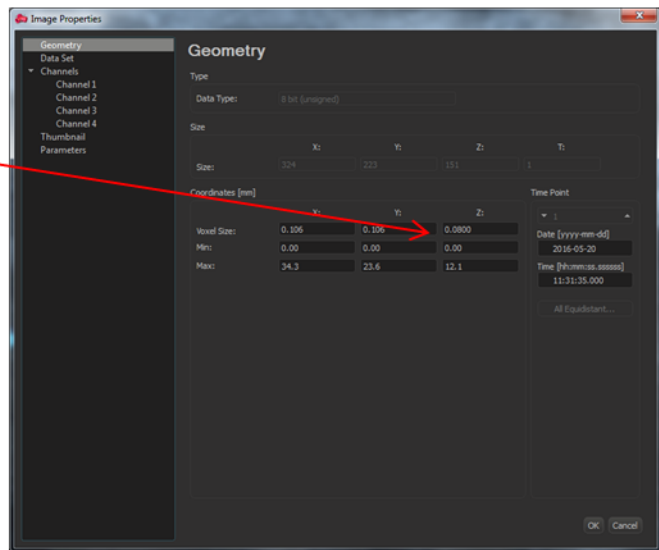


Your Frame scale will now need to be adjusted to fit your scale bar

Here it is changed to Tick marks at 1mm

You will know you missed these steps when you go to measure a follicle of 10mm, and it shows up as 0.1mm
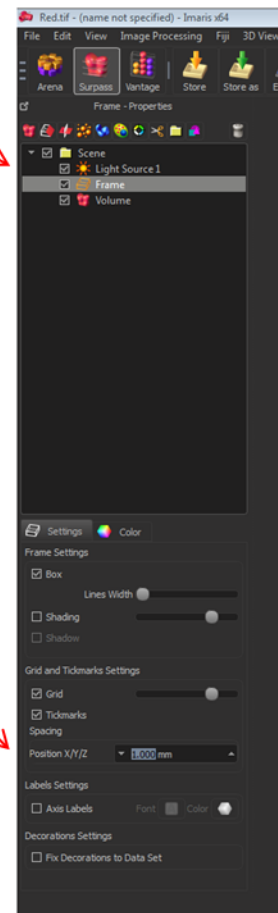
## Creating a TIFF stack to isolate coloured regions in ultrasound images using Fiji

while in RGB colour

You can adjust your colour threshold to select the colour Doppler areas on your image
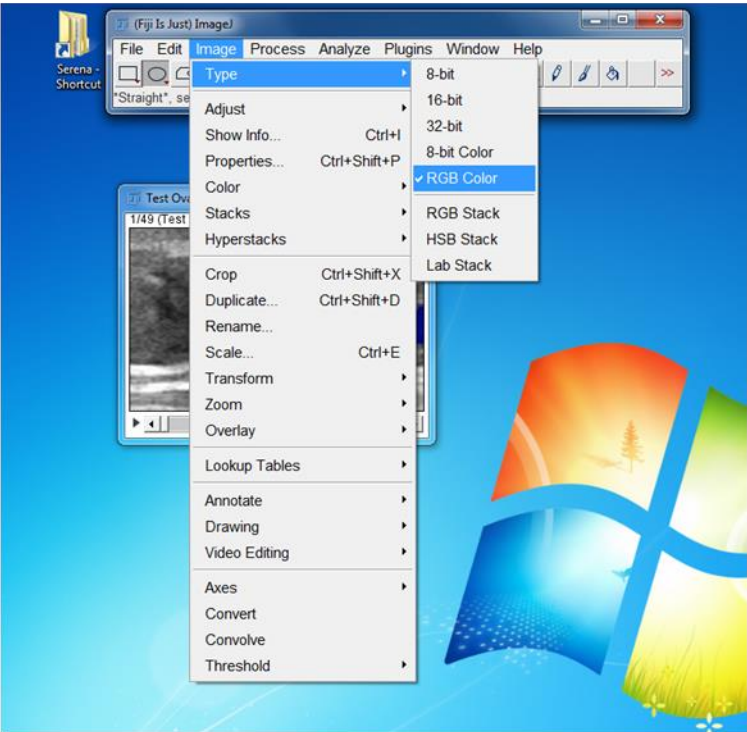


Click "Image"
-> Adjust
-> Color Threshold
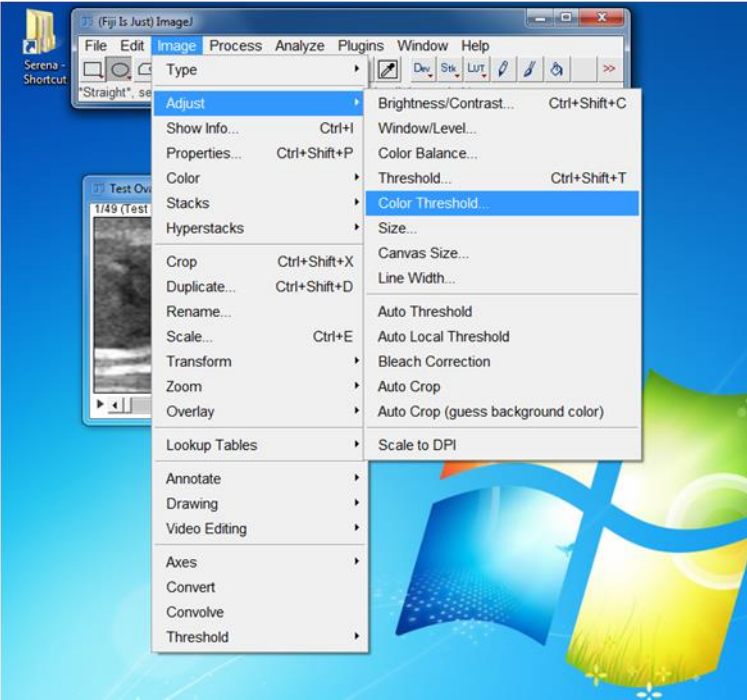
Brightness and Saturation sliders need to be adjusted to select just the colour and not white areas in the image
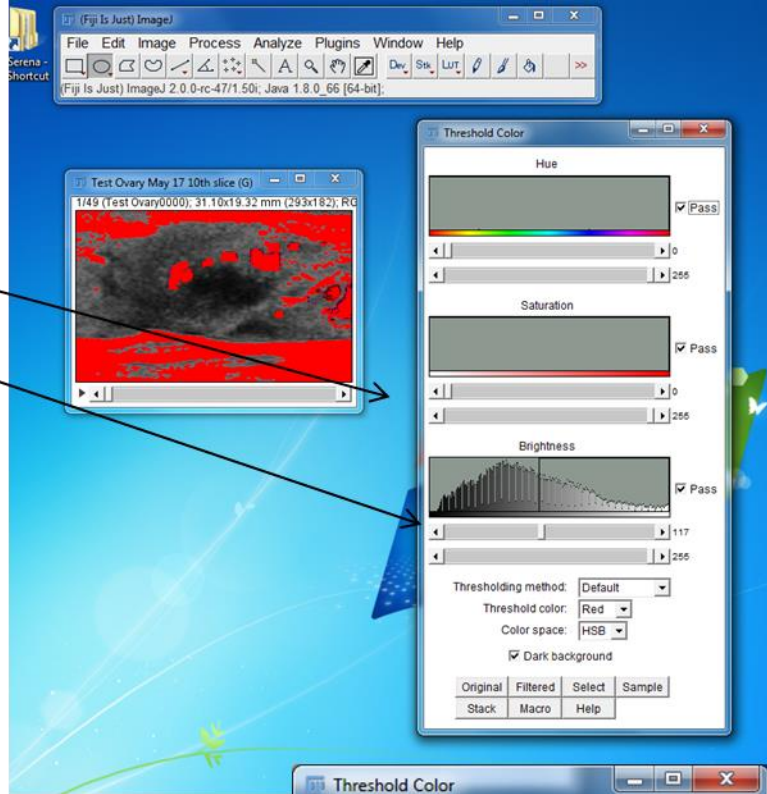


In this example

Saturation has been set to 65
Brightness to 110

Click "Stack" to apply these settings to each image in your sequence



99
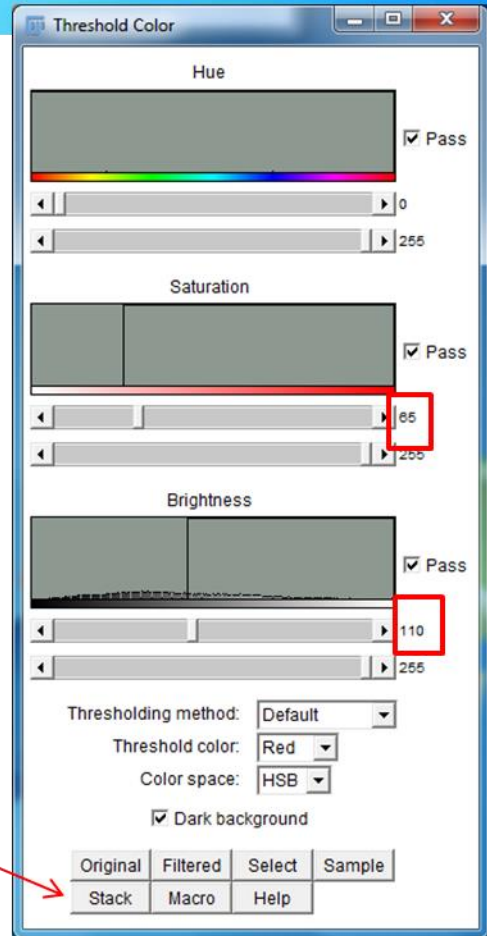
Now Switch it to B&W

Click Stack to apply to all images
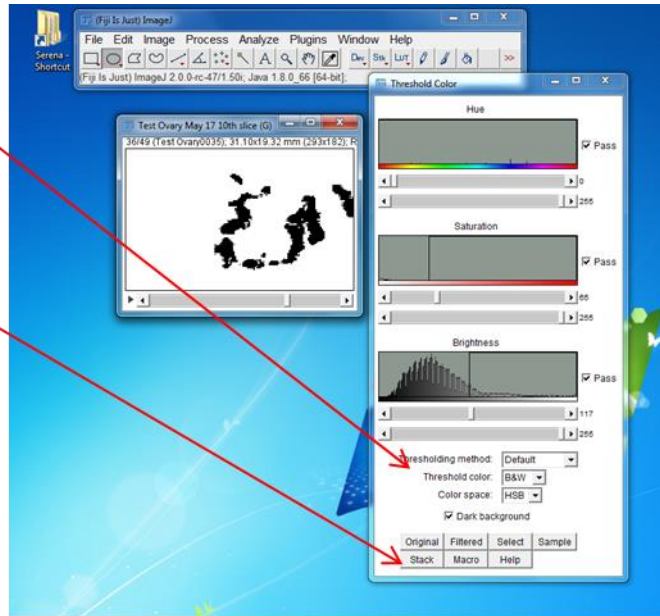


Change to 8 bit

Image -> Type -> 8 bit

Imaris is programmed to work in 8-bit, so all files must be converted



100
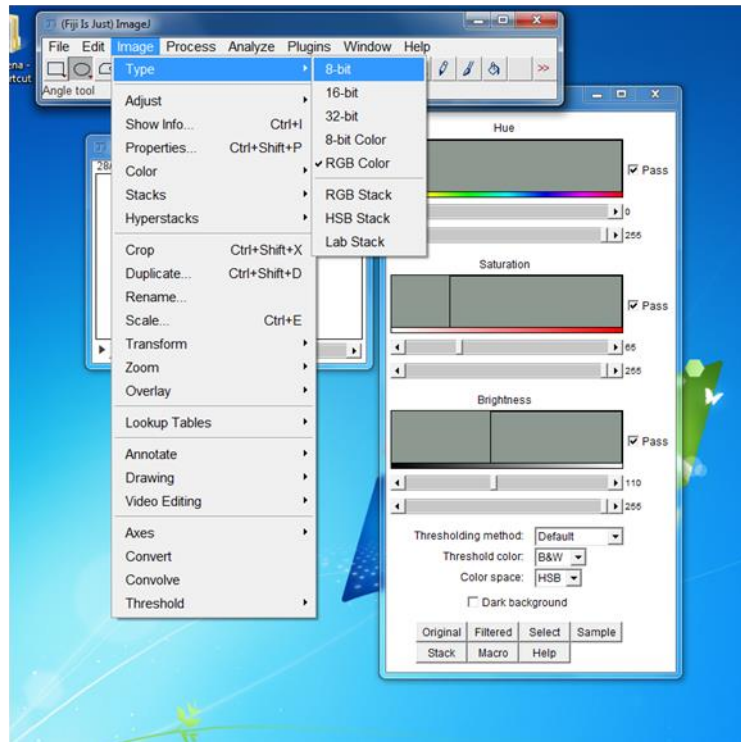
Once in 8-bit
Click Image ->
Adjust -> Threshold
Click Black
Background (of binary
masks)
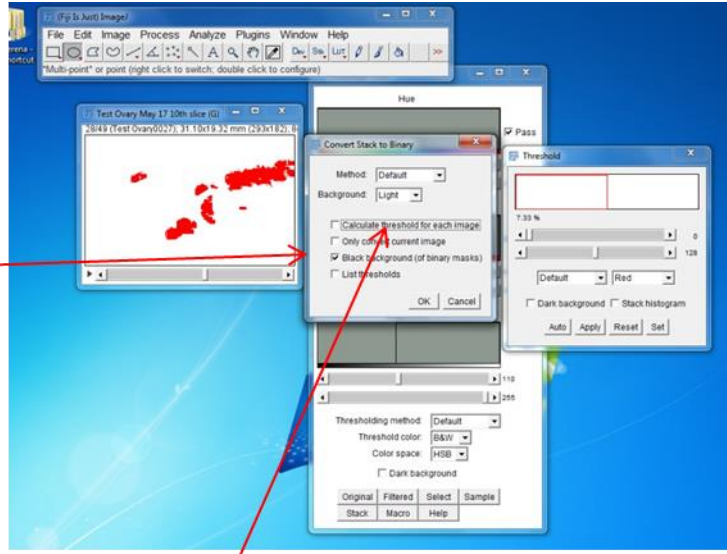


This one should be unchecked prior to clicking Apply

*You should end up with a **White on Black** image

This is a **Key point** to importing it into Imaris
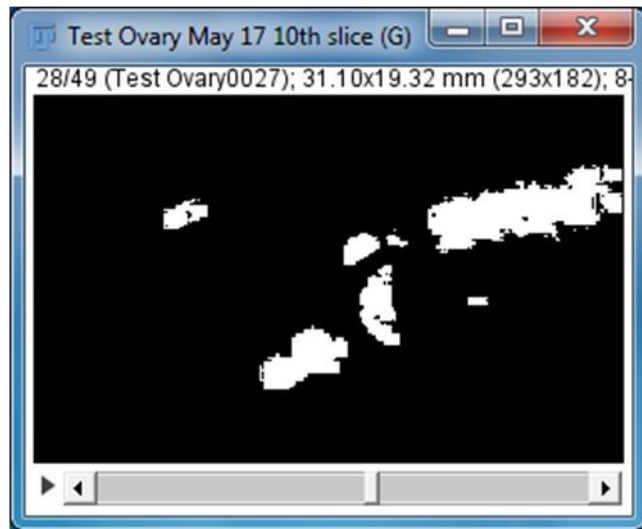


Click Save As TIFF
This file will be imported into Imaris for masking of coloured regions

## Calibration for Z dimension

The following instructions are for changing the Z axis dimension
*Remember to do this before building surfaces*

Using the X and Y diameters of a follicle the Z diameter is calculated

$$Z_{Estimated} = (X + Y)/2$$

It is **important** to note that Imaris is a 3 dimensional software, and while you are looking at an image that appears in 2D on your screen, Imaris does not know to click ONLY within that plane.

Therefore, you have to change the location of your ABCD points of measurement to be within the plane you are working in. Otherwise you will get an overestimation of your measurement.

Use the measurement tool to measure the X and Y of the follicle
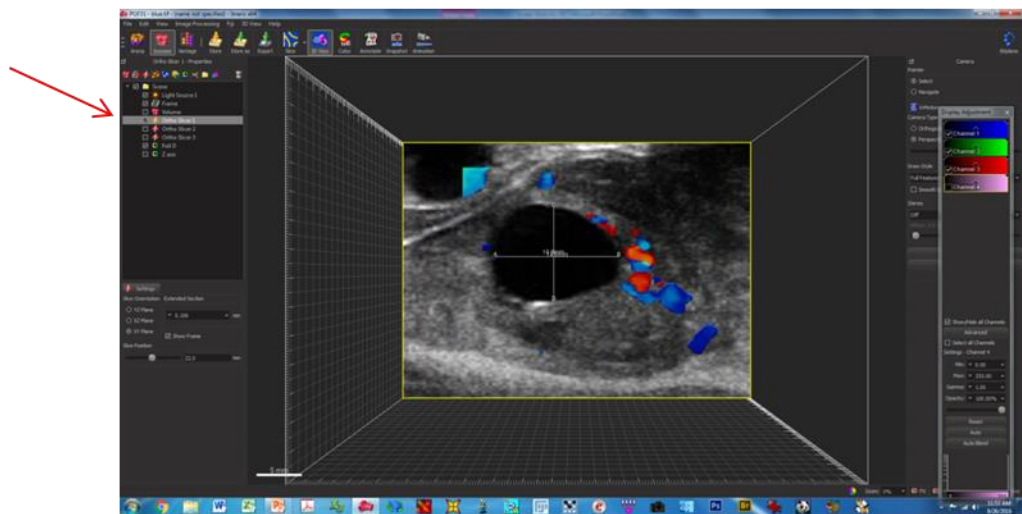


This follicle's diameter measurements have already been adjusted to the XY plane that you see on the screen. To double check, use the Navigation tool

Use the Orthogonal views at a cross point at A
(Repeat for B C D)

Use the slice coordinates
XY, XZ, YZ
NOW change the X, Y, Z values to match. Where YZ denotes the X value, XZ denotes
the Y value, and XY denotes the Z value

This is the tedious part. If you find a short-cut, that would be better, than do that! But
be mindful that without this adjustment you overestimate your measurements.

Click the
OrthoSlice button
three times to get
all three planes
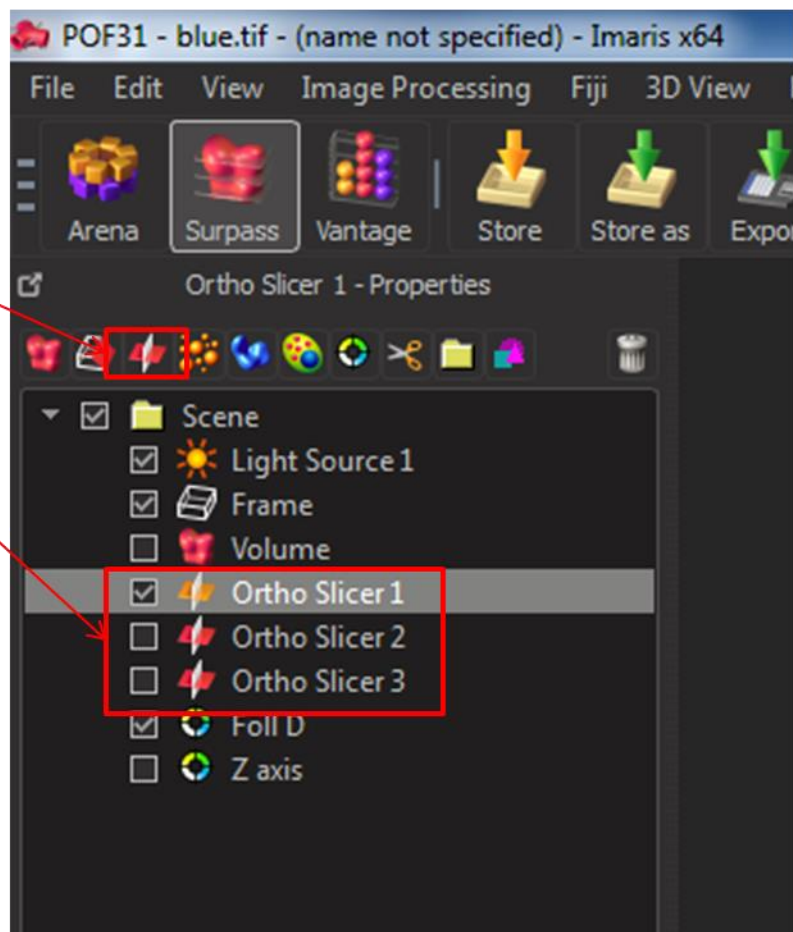
Using an example:
In this screen, the measurement tool was used to draw the X diameter and Y diameter

See that X = 15.8mm
Y = 13.6
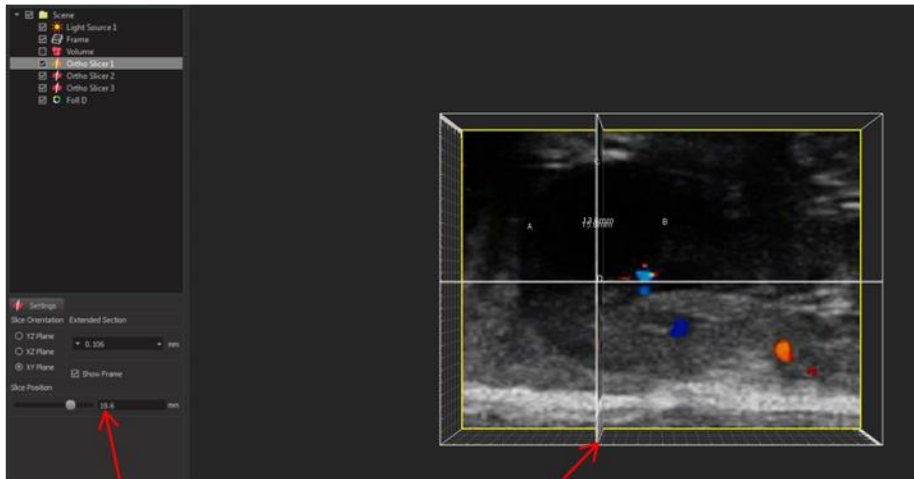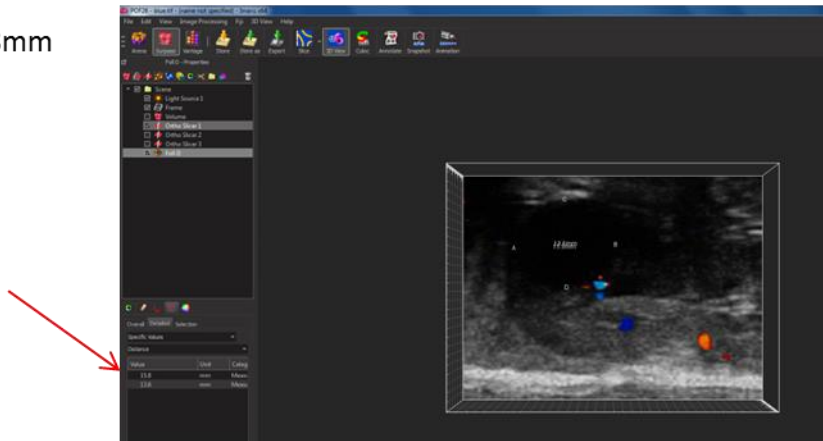




All three orthogonal slices are crossing at the value D here

Take note of the XY, YZ, XZ distance when all three planes are lined up at the point you want to add the marker D
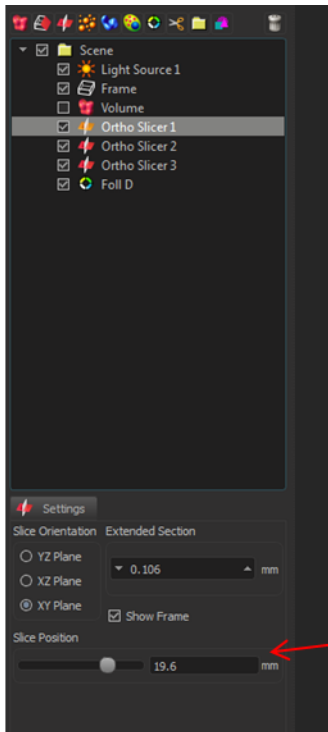
Use these values
The XY plane will be the Z value

Once you have noted all your ABCD points, you need to change them in the Measurement Tool.

With just the measurement highlighted, click on A
And change the values to match the cross point for all three planes
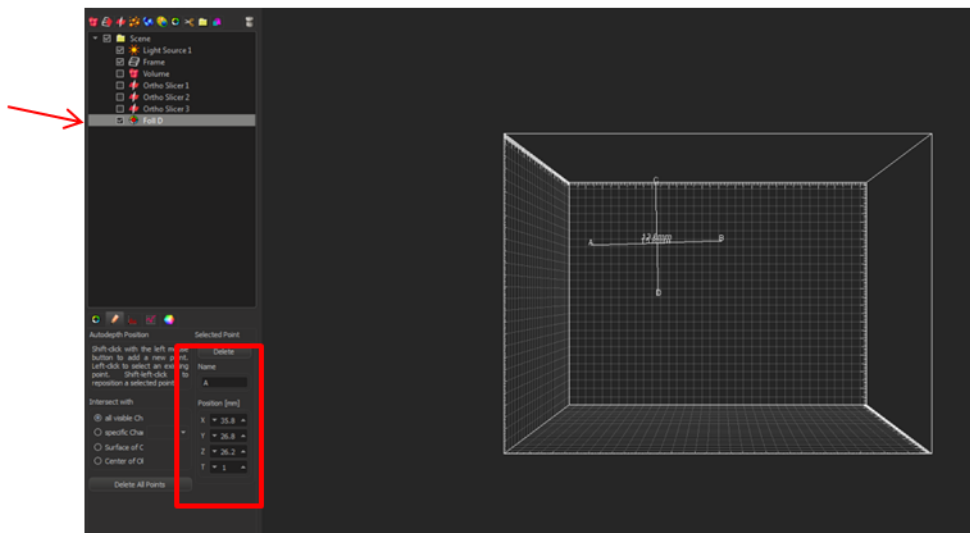
Now we can see that Imaris has the correct plane for our measurement (you can verify this by using the Navgiate tool on the right)

X = 12.4
Y = 10.4

Compare these to those previous values from before, and you will see the previous measurement was an over-estimation of the diameter of the follicle.
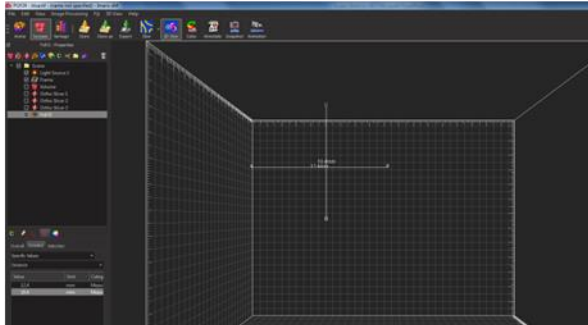


Rotate your Frame 90 degrees using the Navigate

Click the Fit button at the bottom right to make sure it's close to square

Use another measurement tool to get the current Z diameter

Navigate
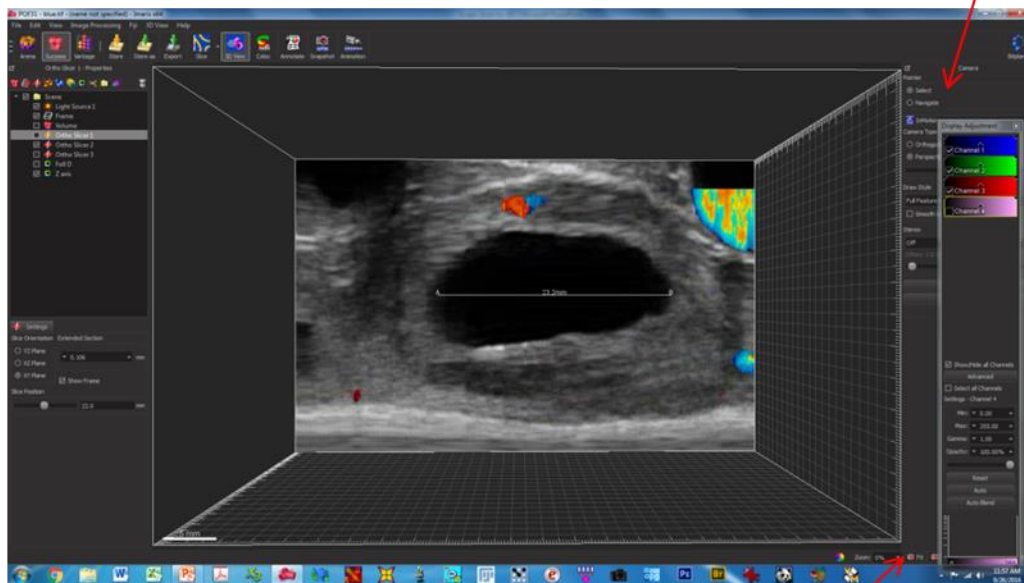


Fit button

If we say Z = X+Y/2

Then here Z = 11.4mm

Again, using the Ortho Slicer 1,2,3 to gain information on the points A and B for our new measurement which is the length of the follicle in the Z direction
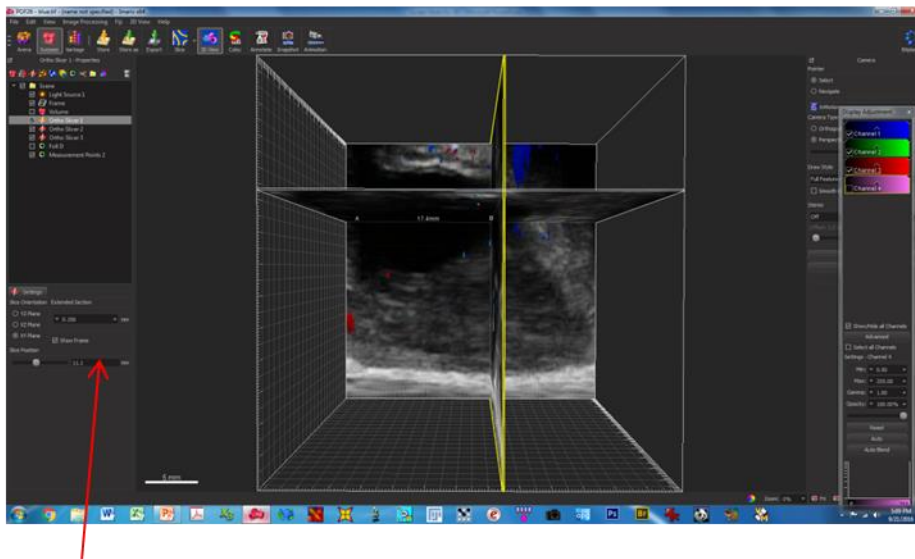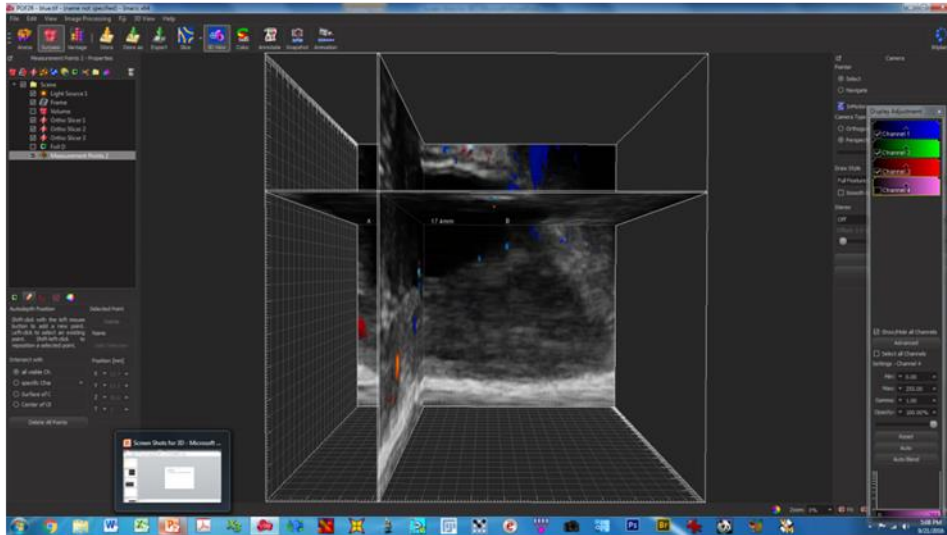




Again take note of these                                          B =

A =                                                                      XY = 11.1

XY = 24.6; YZ = 12.7; XZ = 18.6

Again, click on A
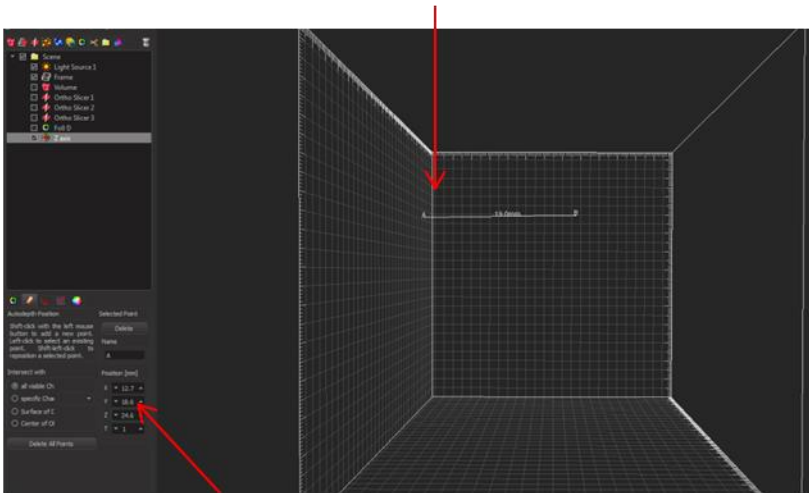


Change these values to match there corresponding orthogonal view

X = 12.7 = YZ value
Y = 18.6 = XZ value
Z = 24.6 = XY value

In this example, Z dimension is 13.5 which is longer than 11.4
Therefore we adjust our Z voxel size

Use the equation of cross multiplication to get the distance for the Z direction

$$Z_{Estimated}/Z_{measured} = Z_{voxel}/0.106$$

So $Z_{voxel} = Z_{Estimated}/Z_{measured} \times 0.106$

Go to Geometry
to adjust
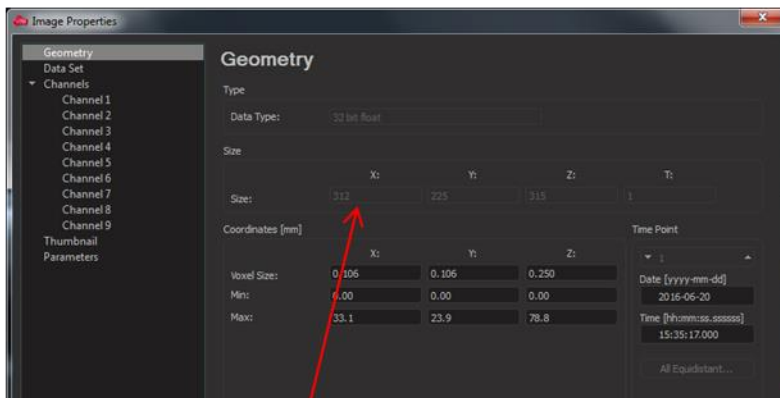


Enter in Z voxel size

## Distance Transformation: Enlargement of Surfaces

Prior to distance transformation, save your work, as Imaris can crash during this point.

To Save click File Export
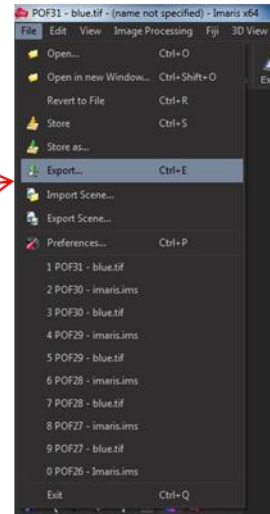
## How to Enlarge a Surface

Edit -> Change Data Type
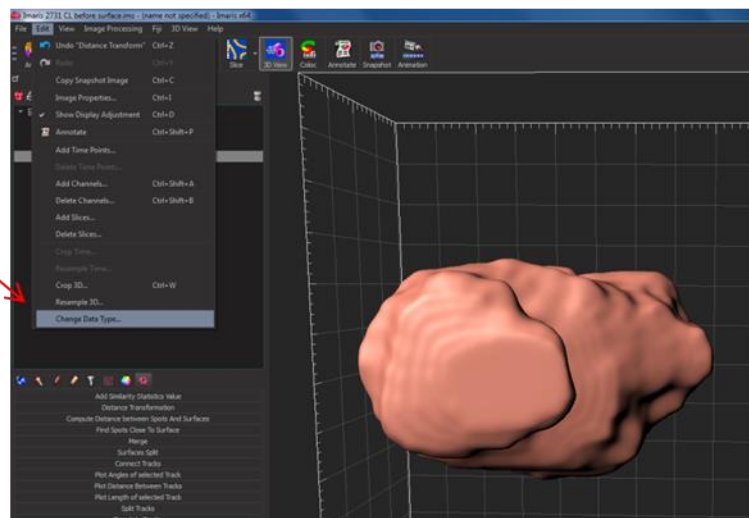
Change to 32 bit float
**Key step to make Distance Transformation** work in the Imaris 8.1.2 version that is corrected in Imaris 8.2
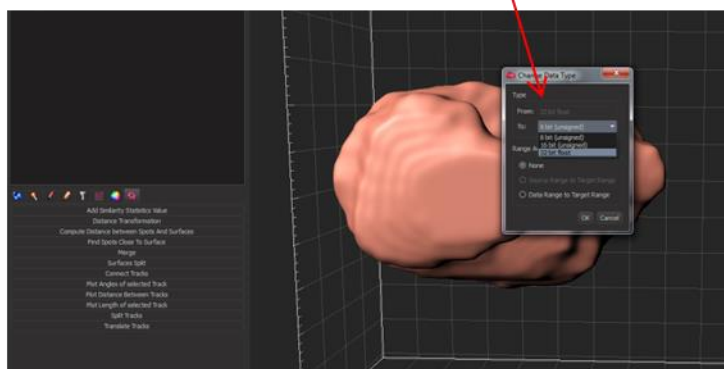
Click on the Surface

Then Tool tab

Then Distance
Transformation
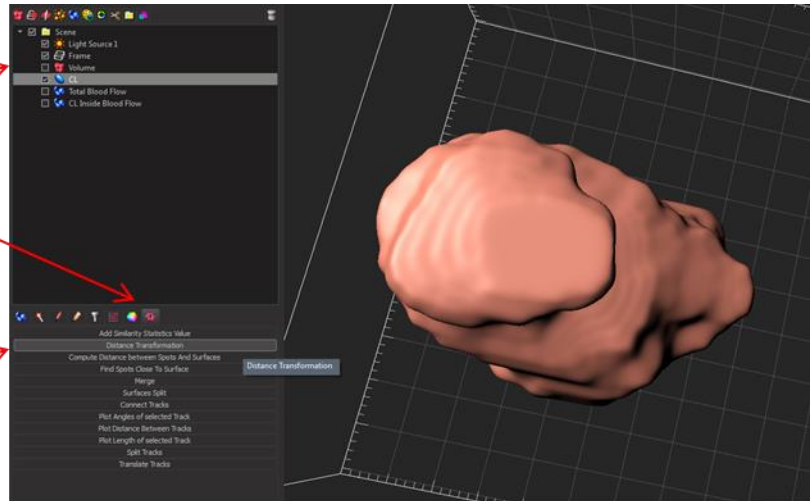


Imaris will take time to think, then this
prompt will appear.

Select Outside of Surface if you wish to
enlarge the surface
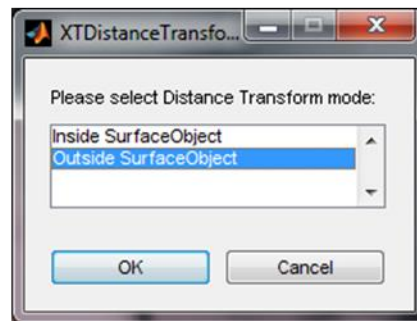


This creates a new channel labeled Distance To...
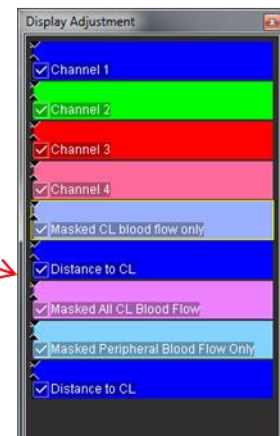
Now, create a new surface, click the blue Surface button
And click the blue Next button
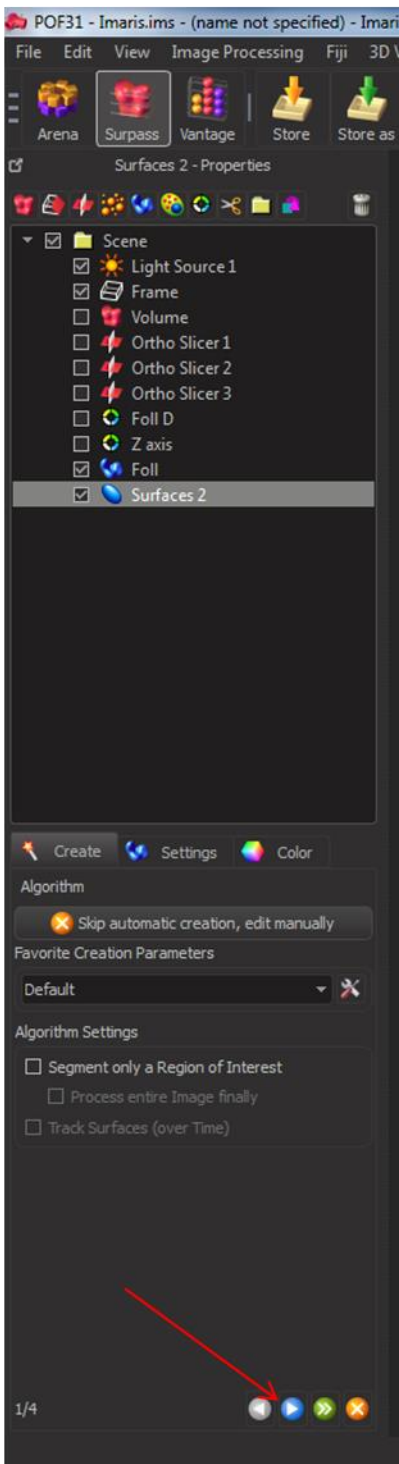


In the second step, click the Distance Channel, here Channel 6
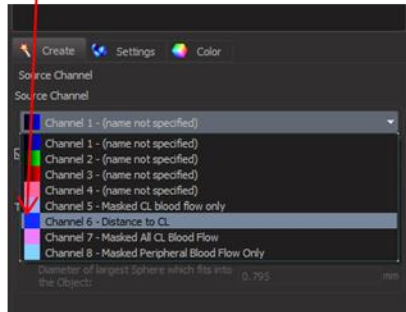


UNCHECK smooth, which is also **Key** in this surface creation of distance transformation
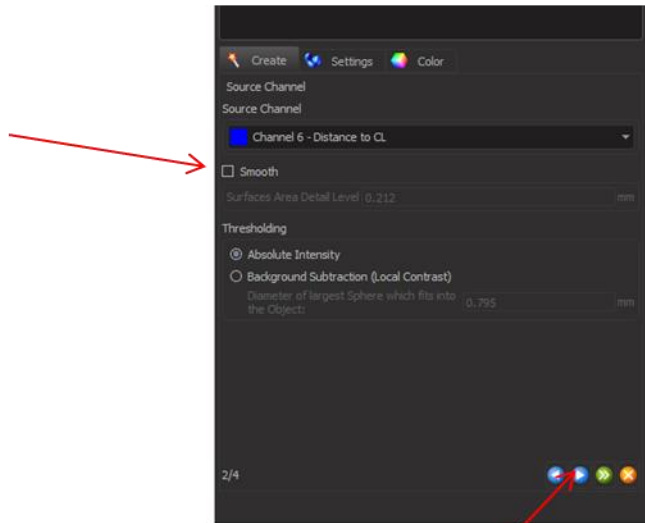


Click Next again

Turn off the lower threshold limit by clicking the power button

Highlight the Power button of the upper threshold

To increase the CL surface to 1.5mm larger, Imaris is working in um here, so type in 1500

Then click the green button to finish

You now have the **Peripheral volume** of all distances that are 1.5mm from the edge of your follicle or CL
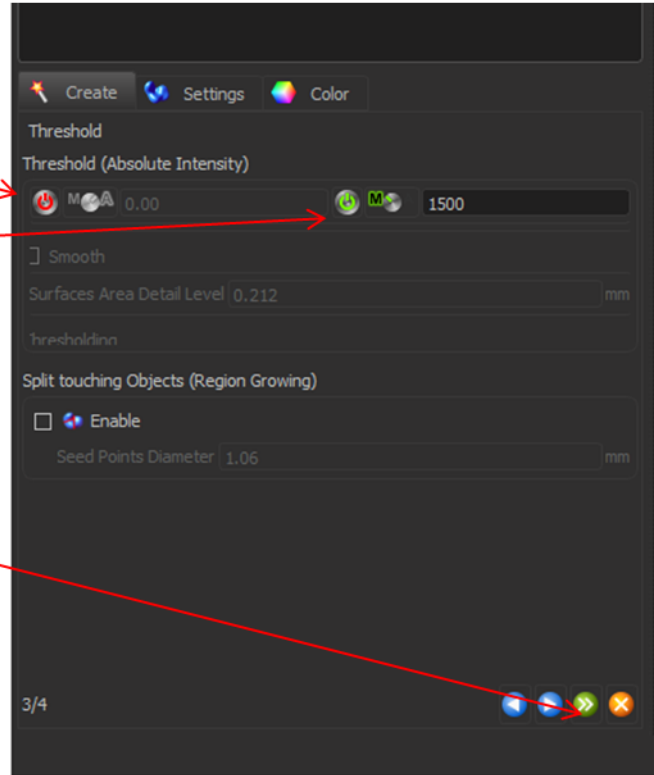
Next, you can create a surface that is inclusive of the Enlarged CL and the CL volume.

You need to create a Mask of the Channel

To Do this, Select the surface of your Follicle (or CL)

Select the Pencil

Click Mask Selection
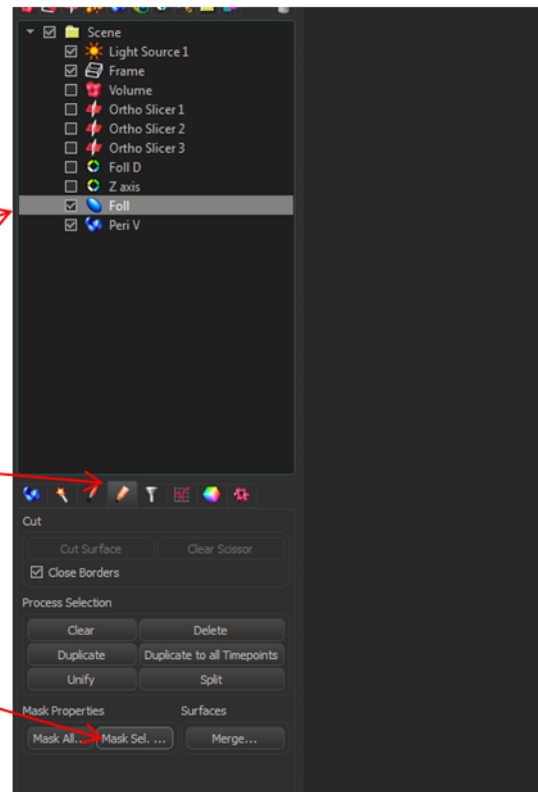
Set the Voxels **inside** to be something larger than 0.00
1 was used in this image analysis

Select the
Channel
Distance
to…
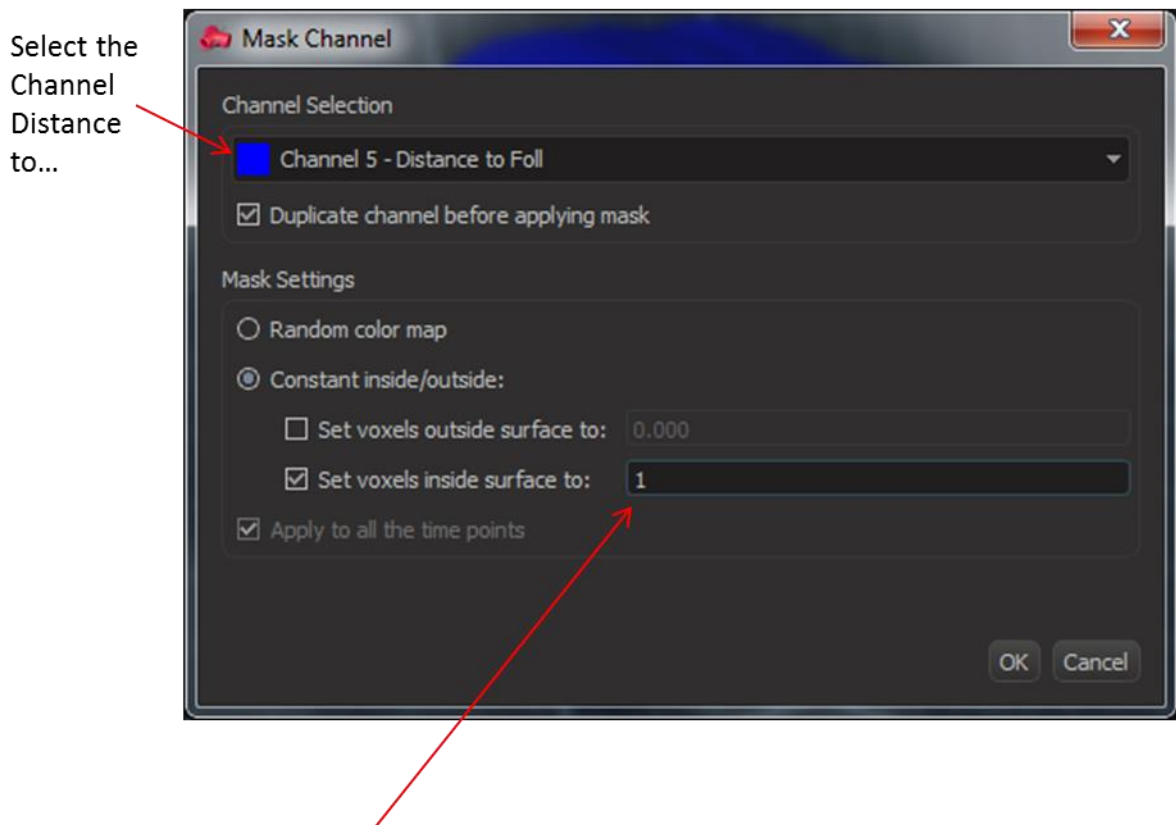
Change to something other than 0.00

To create a surface that is the Enlarged CL, the steps are similar to creating the surface for the Peripheral CL, except that it will no longer create an inner surface

Select the New Channel that was created from your masking for the Enlarged CL (refer to previous steps)

## Determining Volume of Blood Flow

Masked Channels of the Surfaces need to be generated

For the Total BF to the CL (within 1.5mm of the CL surface) use the Enlarged CL Surface
Click the Pencil (Edit) Tab and click Mask All – This will get the peripheral AND intra-luteal blood flow or Total blood flow
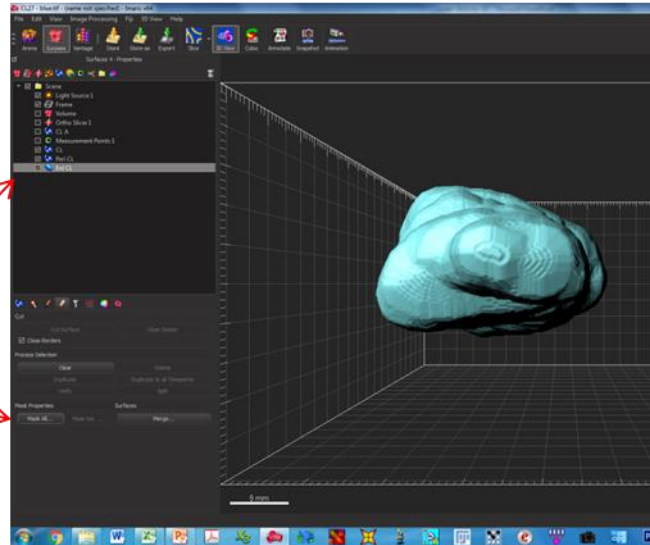
Select the Channel for just blood flow (here Channel 4)
This corresponds to the BW tiff stack that was imported

Set the Outside Voxels to 0.00
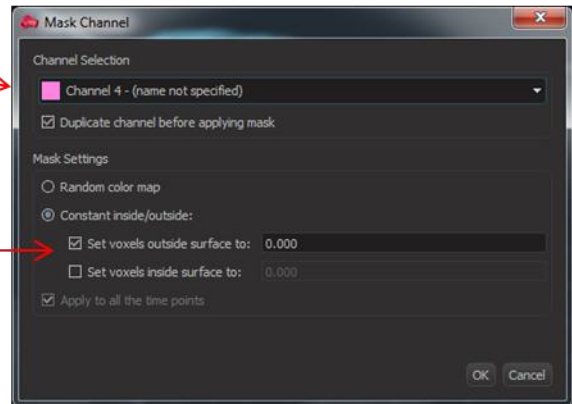
Next, create a Mask of the new channel that was created, but use the CL Surface – This will then give you JUST the peripheral blood flow

Click Mask Selection
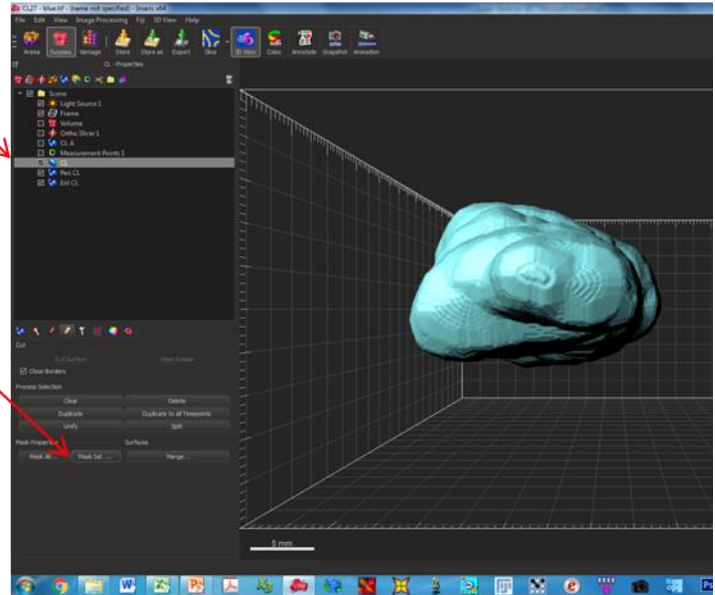


Use the new channel (here Ch 7)

This time, set the voxels **INSIDE** the surface to 0.00

This allows you to generate the volume of blood flow that is just in the periphery of the CL
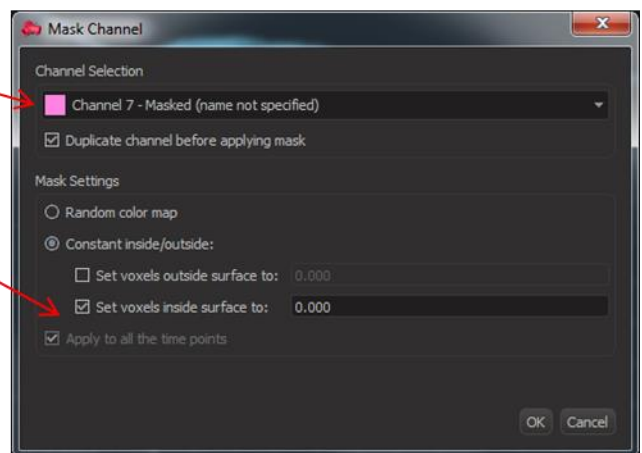


The last blood flow mask is again on the initial BF channel, (Channel 4 in this example) – This will give you Intra-luteal blood flow only

But you are using the CL surface and setting voxels OUTSIDE to 0.00
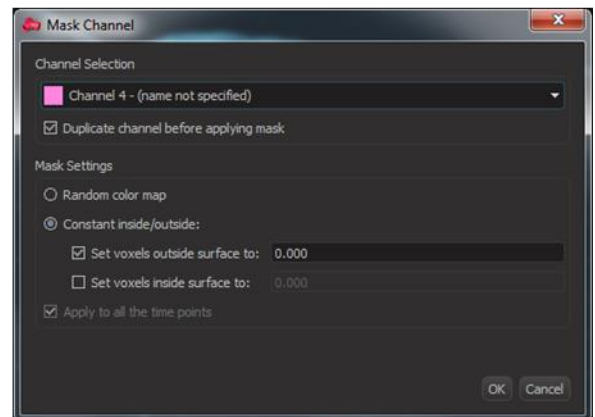
Next, build surfaces
based on these
channels

## Demonstration of building surfaces for blood flow

Settings used in this analysis